PAULA JUDITH PEREZ ESPITIA

DESENVOLVIMENTO E AVALIAÇÃO DE EMBALAGENS ATIVAS ANTIMICROBIANAS A BASE DE METIL CELULOSE E POLPA DE AÇAÍ

Tese apresentada à Universidade Federal de Viçosa, como parte das exigências do Programa de Pós-Graduação em Ciência e Tecnologia de Alimentos, para obtenção do título de *Doctor Scientiae*.

VIÇOSA
MINAS GERAIS – BRASIL
2013

Ficha catalográfica preparada pela Seção de Catalogação e Classificação da Biblioteca Central da UFV

T
P438d
2013

Perez Espitia, Paula Judith, 1985-
Desenvolvimento e avaliação de embalagens ativas antimicrobianas a base de metil celulose e polpa de açaí / Paula Judith Perez Espitia . – Viçosa, MG, 2013.
xv, 156f. : il. (algumas color.) ; 29cm.

Texto em inglês e português
Orientador: Nilda de Fátima Ferreira Soares
Tese (doutorado) - Universidade Federal de Viçosa.
Inclui bibliografia.

1. Alimentos - Embalagens. 2. Embalagens flexíveis. 3. Nanotecnologia. 4. Materiais nanoestruturados. 5. Açaí. 6. Essências e óleos essenciais. 7. Micro-organismos patogênicos. 8. Alimentos - Conservação. I. Universidade Federal de Viçosa. Departamento de Tecnologia de Alimentos. Programa de Pós-Graduação em Ciência e Tecnologia de Alimentos. II. Título.

CDD 22. ed. 664.09

PAULA JUDITH PEREZ ESPITIA

DESENVOLVIMENTO E AVALIAÇÃO DE EMBALAGENS ATIVAS ANTIMICROBIANAS A BASE DE METIL CELULOSE E POLPA DE AÇAÍ

Tese apresentada à Universidade Federal de Viçosa, como parte das exigências do Programa de Pós-Graduação em Ciência e Tecnologia de Alimentos, para obtenção do título de *Doctor Scientiae*.

APROVADA: 9 de março de 2013.

Profª. Jane Sélia dos Reis Coimbra
(Coorientadora)

Prof. Nélio José de Andrade
(Coorientador)

Prof. Reinaldo Francisco Teófilo

Profª. Nathália Ramos de Melo

Profª. Nilda de Fátima Ferreira Soares
(Orientadora)

A Deus, com imensa gratidão, pelo privilégio
desta maravilhosa oportunidade.

Aos meus sobrinhos queridos, Charlyze e Oliver,
por me fazerem lembrar da esperança que temos
na pureza da infânica e que acabamos esquecendo
quando já somos mais velhos.
Dedico

Hay un momento en que todos los obstáculos se derrumban, todos los conflictos se apartan, y a uno se le ocurren cosas que no había soñado, y entonces no hay en la vida nada mejor que escribir.
Gabriel García Márquez

AGRADECIMENTOS

Agradeço a Deus e aos meus Anjos por me protegerem sempre no meu caminhar.

À Universidade Federal de Viçosa, ao Departamento de Tecnologia de Alimentos e ao Programa de Pós-Graduação em Ciência e Tecnologia de Alimentos pela oportunidade de realização deste estudo.

À Coordenação de Aperfeiçoamento de Pessoal de Nível Superior (CAPES) pela concessão da bolsa de estudos mediante o programa PEC-PG.

À professora Nilda de Fátima Ferreira Soares por ter disposição e muita paciência para me orientar.

À professora Jane Sélia dos Reis Coimbra pelo aconselhamento, atenção, paciência, amizade e incentivo.

Ao professor Nélio José de Andrade pelas valiosas sugestões e críticas a este trabalho, pelo exemplo de dedicação e profissionalismo.

Ao professor Reinaldo Francisco Teófilo pela paciência e valiosos conhecimentos compartilhados, fundamentais para o desenvolvimento de grande parte deste trabalho.

À professora Nathália Ramos de Melo por participar da minha banca de defesa de tese.

Ao professor Sukarno O. Ferreira pela grande ajuda com as análises de microscopia de força atômica.

Aos professores Frederico B. de Sousa (UNIFEI) e Rubén D. Sinisterra (UFMG) por disponibilizarem os equipamentos do Laboratório de Química de Inclusão e Encapsulamento Molecular, e pela ajuda no desenvolvimento da parte inicial deste trabalho.

Aos funcionários do DTA pela contribuição no momento oportuno.

Aos meus colegas da Pós-graduação pela ótima convivência.

Aos colegas do Laboratório de Embalagens pela acolhida, e pelo espaço para reflexão e aprendizado.

À Rejane A. Batista, minha irmã brasileira, pela amizade incondicional e conselhos sempre em horas oportunas.

À Debora M. Vitor, Mariana Lamas, Taíla Veloso, Hiasmyne Medeiros, Caio Otoni e Germanna Wilk pela valiosa amizade e convivência agradável.

Ao Eber Medeiros pela amizade e profisionalismo no Laboratório de Embalagens.

Ao professor Roberto Avena Bustillos pela amizade, conselhos e orientação durante o período de pesquisa na Califórnia.

À pesquisadora Tara McHugh pela disposição em me receber como parte da sua equipe na Unidade de Alimentos Processados do Departamento de Agricultura dos Estados Unidos (Processed Foods Research Unit, USDA, ARS).

Aos colegas de laboratório no USDA pela acolhida e amizade nesse curto tempo de pesquisa e aprendizado, em especial à Greta Peretto, Diana Valenzuela Medina, Cristina Bilbao, Bor-Sen Chiou, Wen-Xian Du, Rebecca Milczarek e Carl Olsen.

À Tina G. Williams e Delilah Wood pela grande ajuda com as análises no microscópio eletrônico de varredura por emissão de campo.

Aos meus pais queridos, Evelys e Angel, que, com tanto amor, me ajudaram com palavras de carinho e motivação.

Aos meus irmãos Luz Angela e Carlos Andres pelo carinho e amizade.

Ao meu namorado Nicholas pela ajuda incondicional na realização deste trabalho, pelo amor, estímulo e companheirismo em todos os momentos.

Às colegas de república Janaína e Rafaela pela companhia e amizade.

Certamente, estes parágrafos não contêm os nomes de todos que fizeram parte desta importante fase da minha vida. Portanto, desde já, peço desculpas àqueles que não estão presentes nestas palavras, mas podem estar certos de que fazem parte do meu pensamento e da minha gratidão.

Muito obrigada!

BIOGRAFIA

Paula Judith Pérez Espitia, filha de Angel Gregório Pérez Sierra e Evelys Espitia Camacho, nasceu em Cereté, Córdoba, Colômbia, no dia 15 de janeiro de 1985.

Engenheira de Alimentos pela Universidad de Córdoba, Montería, Colômbia. Iniciou em março de 2007 o mestrado em Ciência e Tecnologia de Alimentos do Departamento de Tecnologia de Alimentos da Universidade Federal de Viçosa, Brasil, concluindo-o em fevereiro de 2009.

Em março de 2009, iniciou o doutorado no Programa de Pós-Graduação em Ciência e Tecnologia de Alimentos, pela mesma instituição, concluindo-o em março de 2013.

SUMÁRIO

Página

RESUMO

ESPITIA, Paula Judith Perez, D.Sc., Universidade Federal de Viçosa, Março de 2013. **Desenvolvimento e avaliação de embalagens ativas antimicrobianas a base de metil celulose e polpa de açaí.** Orientadora: Nilda de Fátima Ferreira Soares. Coorientadores: Jane Selia dos Reis Coimbra e Nélio José de Andrade.

Os biopolímeros têm atraído grande interesse na área de embalagens em virtude de sua biodegradabilidade, grande disponibilidade na natureza, baixo custo e facilidade de processamento. Estas características permitem a sua aplicação no desenvolvimento de novos filmes biodegradáveis e comestíveis. Este trabalho foi dividido em duas partes. A primeira parte objetivou o estudo e otimização das condições de sonicação (potência, tempo e a presença de um agente dispersante) de nanopartículas de óxido de zinco (nanoZnO), bem como a avaliação da sua atividade antimicrobiana em diferentes concentrações (1 %, 5 % e 10 % m/m). Além disso, objetivou desenvolver filmes nanocompósitos de metil celulose (MC) incorporados com pediocina e nanoZnO, e avaliar suas propriedades antimicrobianas e físico-mecânicas, utilizando a metodologia de superfície de resposta (MSR) com o delineamento composto central (DCC). Os resultados indicaram que a presença do agente dispersante teve efeito significativo sobre o tamanho das nanoZnO, e a condição ótima de dispersão foi alcançada utilizando-se 200 W de potência durante 45 minutos de sonicação. Nas condições testadas, a dispersão de nanoZnO apresentou atividade antimicrobiana contra *Escherichia coli, Salmonella* Choleraesuis*, Staphylococcus aureus*, *Saccharomyces cerevisiae* e *Aspergillus niger*. Quanto aos nanocompósitos desenvolvidos, observou-se que a incorporação de nanoZnO e pediocina afetou as propriedades de cristalinidade, deformação na ruptura, cor, superfície e estabilidade térmica dos filmes. Os filmes nanocompósitos

apresentaram atividade antimicrobiana contra *Staphylococcus aureus* e *Listeria monocytogenes*. O alongamento na ruptura e os parâmetros colorimétricos L*, b*, opacidade, índice de amarelamento e índice de branco dos filmes foram escolhidos para otimização simultânea pela função de desejabilidade. A otimização foi realizada a fim de se obter filmes com boas propriedades mecânicas e colorimétricas, e o melhor resultado foi alcançado incorporando-se 20 % (m/m) de nanoZnO e 15 % (m/m) de pediocina. A segunda parte deste trabalho objetivou desenvolver e avaliar filmes comestíveis de açaí incorporados com polifenóis obtidos de casca de maçã (ASP) e óleo essencial de tomilho (TEO), bem como a sua combinação, para conservação de alimentos. As concentrações ótimas destes antimicrobianos nos filmes de açaí foram determinadas utilizando-se a MSR com DCC. A incorporação de ASP e TEO resultou em interação contra *L. monocytogenes*. A adição de ASP melhorou as propriedades mecânicas. Entretanto, a incorporação do TEO diminuiu a resistência mecânica do filme. Os antimicrobianos não influenciaram a permeabilidade ao vapor de água dos filmes. Os filmes de açaí apresentaram tendência à luminosidade e ao vermelho. A incorporação de ASP resultou na melhoria da estabilidade térmica dos filmes. A presença de agregados foi observada na superfície de todos os filmes comestíveis de açaí. A atividade antimicrobiana, módulo de elasticidade e os parâmetros colorimétricos L*, a* e b* foram utilizados como critérios de avaliação na função de desejabilidade, usada para a análise de otimização multiresposta. De acordo com o perfil de desejabilidade, os filmes de açaí com as características desejadas foram obtidos incorporando-se 6,07 % (m/m) de ASP e 3,1 % (m/m) de TEO.

ABSTRACT

ESPITIA, Paula Judith Perez, D.Sc., Universidade Federal de Viçosa, March, 2013. **Development and evaluation of antimicrobial active packaging based on methyl cellulose and açaí puree.** Advisor: Nilda de Fátima Ferreira Soares. Co-advisers: Jane Selia dos Reis Coimbra and Nélio José de Andrade.

Biopolymers have attracted the interest for the development of new packaging because of their biodegradability, wide availability in nature, low cost and easy of processing. These characteristics allow the use of biopolymers to elaborate biodegradable edible films. This study was divided into two parts. The first part aimed to study and optimize the sonication conditions of ZnO nanoparticles (nanoZnO), including power, time and the presence of a dispersing agent, as well as to evaluate the antimicrobial activity of NanoZnO at different concentrations (1 %, 5 % and 10 % w/w). Furthermore, this work aimed to develop nanocomposite films of methyl cellulose (MC) incorporated with pediocin and nanoZnO. Antimicrobial and physical-mechanical properties were evaluated using response surface methodology (RSM) with central composite design (CCD). The results indicated that the presence of dispersant had a significant effect on nanoZnO size and the optimal dispersion condition was achieved by sonication at 200 W for 45 min. NanoZnO dispersion had antimicrobial activity against *Escherichia coli, Salmonella* Choleraesuis*, Staphylococcus aureus, Saccharomyces cerevisiae* and *Aspergillus niger*. Moreoer, the incorporation of nanoZnO and pediocin affected the crystallinity, elongation at break, color, thermal stability and surface of MC nanocomposite films. Nanocomposite films exhibited antimicrobial activity against *S. aureus* and *Listeria monocytogenes*. Elongation at break and the colorimetric parameters L*, b*, opacity, yellowness and whiteness index of developed films were selected to

perform the optimization by desirability function. The optimization was performed to obtain films with good mechanical and colorimetric properties. The optimization showed that films with desired characteristics can be obtained by incorporating 20 % (w/w) nanoZnO and 15 % (w/w) pediocin. The second part of this study aimed to develop and evaluate açaí edible films incorporated with apple skin polyphenol (ASP) and thyme essential oil (TEO), as well as their combination for food preservation. The optimal concentrations of these antimicrobials in açaí films were determined using RSM with CCD. The incorporation of ASP and TEO resulted in interaction against *L. monocytogenes*. Addition of ASP resulted in improved mechanical properties, while the incorporation of TEO decreased the mechanical strength of films. Antimicrobials had no influence on water vapor permeability of films. Açaí films tended to lightness and redness. Incorporation of ASP resulted in improved thermal stability of films. The presence of aggregates was observed on the surface of all açaí edible films. Antimicrobial activity, elastic modulus and colorimetric parameters L*, a* and b* were used in the evaluation criteria of desirability function, used for the multi-response optimization analysis. According to the desirability profile, açaí film with desired characteristics is obtained by incorporating 6.07 % (w/w) ASP and 3.1 % (w/w) TEO.

INTRODUÇÃO GERAL

O consumo mundial de plásticos tem aumentado cada vez mais, agravando o problema da contaminação devido ao acúmulo de resíduos não biodegradáveis. Dessa forma, o aumento do uso de embalagens plásticas traz uma série de preocupações quanto à contaminação ambiental. Tais preocupações têm resultado no interesse crescente pela pesquisa de biopolímeros biodegradáveis. O biopolímero metil celulose é considerado uma alternativa atraente, devido a sua capacidade de permitir o desenvolvimento de produtos biodegradáveis, sua grande disponibilidade na natureza, baixo custo e facilidade de processamento (RIMDUSIT et al., 2008).

Outros biopolímeros têm sido estudados em relação às suas propriedades para produzir filmes comestíveis e serem utilizados como embalagem de alimentos (AZEREDO et al., 2009). Os filmes comestíveis podem ser preparados a partir de biopolímeros naturais tais como proteínas (gelatina, proteínas de soro de leite, caseína, zeína, etc.) e polissacarídeos (amido, derivados de celulose, alginatos, pectina, etc.). A pectina tem sido usada em combinação com frutas para a elaboração de filmes comestíveis. Assim, maçã (MILD et al., 2011) e tomate (DU et al., 2008), dentre outros, podem ser utilizados como ingrediente principal para a elaboração destes filmes comestíveis. Entretanto, atualmente não existem estudos utilizando a polpa de açaí como matriz polimérica para o desenvolvimento de filmes comestíveis visando o seu uso como embalagens de alimentos.

O açaí (*Euterpe oleracea*) é uma fruta tropical típica do Brasil que tem recebido grande atenção devido à sua atividade biológica. Trata-se de um fruto bacáceo redondo, de palma, de cor roxa quando maduro, com um diâmetro médio de 2 cm (SCHRECKINGER et al., 2010).

Recentemente, os filmes biodegradáveis e comestíveis têm sido usados para o desenvolvimento de embalagens antimicrobianas. A embalagem antimicrobiana é um tipo de embalagem ativa, que interage com o produto ou *headspace* para reduzir, inibir ou retardar o crescimento de micro-organismos que podem estar presentes na superfície dos alimentos (SOARES et al., 2009). No entanto, a principal desvantagem dos filmes comestíveis e biodegradáveis quanto ao seu uso como embalagem de alimento são suas limitadas propriedades mecânicas e de barreiras (TUNÇ & DUMAN, 2011). Neste contexto, pesquisas têm indicado que as propriedades dos materias de embalagem podem ser melhoradas aplicando-se a nanotecnologia na criação de novos materiais. Estes novos materiais são conhecidos como nanocompósitos, considerados compostos híbridos, onde o material de enchimento (*filler*) incorporado na matriz polimérica tem pelo menos uma dimensão de tamanho nanométrico (ESPITIA et al., 2012).

O principal objetivo deste trabalho foi desenvolver embalagens antimicrobianas a partir de metil celulose (MC) ou açaí. Os filmes desenvolvidos com MC foram incorporados com nanopartículas de óxido de zinco (nanoZnO) e pediocina. O uso de nanoZnO nos filmes de açaí foi inviável devido a alta reação oxidante produzida. Alternativamente, foram utilizados como compostos antimicrobianos naturais para incorporação nos filmes comestíveis de açaí, o óleo essencial de tomilho (TEO) e polifenóis de casca de maçã (ASP). Desta forma, o presente trabalho foi dividido em duas partes: a primeira parte consistiu no estudo da dispersão das nanoZnO, sua atividade antimicrobiana *in vitro* e desenvolvimento de filmes de MC incorporados com nanoZnO e pediocina. A segunda parte deste trabalho abrangeu o desenvolvimento de filmes comestíveis de açaí incorporados com TEO e ASP de forma individual, bem como o estudo da otimização da concentração destes antimicrobianos nos filmes de açaí. Este trabalho é apresentado na forma de artigos científicos, respeitando a formatação da revista na qual foi submetido cada artigo, de acordo com as normas para apresentação de tese atualizadas em 2011 pela Pró-Reitoria de Pós-Graduação da Universidade Federal de Viçosa (PPG / UFV).

REFERÊNCIAS BIBLIOGRAFICAS

AZEREDO, H. M. C.; MATTOSO, L. H. C.; WOOD, D.; WILLIAMS, T. G.; AVENA-BUSTILLOS, R. J.; MCHUGH, T. H. Nanocomposite edible films from mango puree reinforced with cellulose nanofibers. **Journal of Food Science**, 74, 5, N31-N35, 2009.

DU, W. X.; OLSEN, C. W.; AVENA-BUSTILLOS, R. J.; MCHUGH, T. H.; LEVIN, C. E.; FRIEDMAN, M. Antibacterial activity against *E. coli* O157:H7, physical properties, and storage stability of novel carvacrol-containing edible tomato films. **Journal of Food Science**, 73, 7, M378-M383, 2008.

ESPITIA, P.; SOARES, N. D. F.; COIMBRA, J. S. D. R.; ANDRADE, N. J.; CRUZ, R. S.; MEDEIROS, E. A. A. Zinc oxide nanoparticles: Synthesis, antimicrobial activity and food packaging applications. **Food and Bioprocess Technology**, 5, 5, 1447-1464, 2012.

MILD, R. M.; JOENS, L. A.; FRIEDMAN, M.; OLSEN, C. W.; MCHUGH, T. H.; LAW, B.; RAVISHANKAR, S. Antimicrobial edible apple films inactivate antibiotic resistant and susceptible *Campylobacter jejuni* strains on chicken breast. **Journal of Food Science**, 76, 3, M163-M168, 2011.

RIMDUSIT, S.; JINGJID, S.; DAMRONGSAKKUL, S.; TIPTIPAKORN, S.; TAKEICHI, T. Biodegradability and property characterizations of methyl cellulose: Effect of nanocompositing and chemical crosslinking. **Carbohydrate Polymers**, 72, 3, 444-455, 2008.

SCHRECKINGER, M. E.; LOTTON, J.; LILA, M. A.; MEJIA, E. G. D. Berries from South America: A comprehensive review on chemistry, health potential, and commercialization. **Journal of Medicinal Food**, 13, 2, 233-246, 2010.

SOARES, N. F. F.; PIRES, A. C. S.; CAMILLOTO, G. P.; SANTIAGO-SILVA, P.; ESPITIA, P. J. P.; SILVA, W. A. Recent patents on active packaging for food application. **Recent Patents on Food, Nutrition & Agriculture**, Sharjah, 1, 1, 171-178, 2009.

TUNÇ, S.; DUMAN, O. Preparation of active antimicrobial methyl cellulose/carvacrol/montmorillonite nanocomposite films and investigation of carvacrol release. **LWT - Food Science and Technology**, 44, 2, 465-472, 2011.

PRIMEIRA PARTE

Hay una fuerza motriz más poderosa que el vapor, la electricidad y la energía atómica, la voluntad.
Albert Einstein

ARTIGO CIENTÍFICO 1

NANOPARTÍCULAS DE ZnO: ATIVIDADE ANTIMICROBIANA E APLICAÇÃO EM EMBALAGENS PARA ALIMENTOS

Resumo

O óxido de zinco (ZnO) é um composto inorgânico e está listado como material GRAS (*generally recognized as safe*) pela FDA, podendo portanto, ser utilizado como aditivo alimentar. O advento da nanotecnologia tem permitido o desenvolvimento de novos materiais com propriedades antimicrobianas. Assim, o ZnO em tamanho nanométrico apresenta-se como um antimicrobiano com potencial aplicação na área da conservação de alimentos. As nanopartículas de ZnO têm sido incorporadas em matrizes poliméricas, a fim de proporcionar atividade antimicrobiana ao material de embalagem. Esta revisão apresenta o estado da arte sobre a atividade antimicrobiana de nanopartículas de ZnO e sua aplicação em matrizes poliméricas. Aspectos de segurança também são discutidos.

Palavras-chave: Atividade antimicrobiana, embalagens ativas, nanopartículas, óxido de zinco, segurança.

Zinc Oxide Nanoparticles: Antimicrobial Activity and Food Packaging Applications

Abstract

Zinc oxide (ZnO) is an inorganic compound, currently listed as GRAS (*generally recognized as safe*) material by FDA and used as food additive. The advent of nanotechnology has lead the development of materials with new properties for use as antimicrobial agents. Thus, ZnO in nanoscale has shown antimicrobial properties and potential applications in food preservation. ZnO nanoparticles have been incorporated in polymeric matrices in order to provide antimicrobial activity to the packaging. This review presents the antimicrobial activity of ZnO nanoparticles, as well as the effect of their incorporation in polymeric matrices. Aspects of safety are also discussed.

Keyword: Zinc oxide, nanoparticle, synthesis, antimicrobial activity, application, active packaging, safety.

1. INTRODUCTION

Foodborne diseases are a global public health issue. In the U.S. alone, the CDC (Center for Disease Control and Prevention) estimated 76 million foodborne illnesses, 325,000 hospitalizations and 5,000 deaths each year in 1999, resulting in medical expenses and productivity loss of approximately $152 billion USD (TAUXE et al., 2010; SCHARF, 2010).

Moreover, the CDC has estimated 47.8 million foodborne illnesses, 127,839 hospitalizations and 3,037 deaths for 2011 (CDC, 2011), and although the full extent of cost by unsafe food and their effects is still unknown for this year, the impact on global health, trade and economy is likely to be profound.

The demand for new technologies to control foodborne pathogens has increased significantly in recent years. As such, food packaging plays an important role in providing safety and maintaining quality of food. Food packaging with new functions is known as active packaging, developed as a

result of consumer demand for safety and more natural products with a longer shelf life, better cost-benefits and convenience (AHVENAINEN, 2003).

According to regulations 1935/2004/EC and 450/2009/EC of the European Union, active packaging is defined as active materials in contact with food, with the ability to change the composition of the food or the atmosphere around it (RESTUCCIA et al. 2010).

Antimicrobial packaging is a type of active packaging which aims to extend the shelf life of foods by reducing microbial growth on the product surface (APPENDINI & HOTCHKISS, 2002). This type of packaging interacts with the product or the headspace inside to reduce, inhibit or retard the growth of microorganisms that may be present on food surfaces (SOARES et al., 2009).

In this way, the incorporation of antimicrobials into packaging materials allows the gradual diffusion of target bactericidal or bacteriostatic compounds into a food matrix, which eliminates the need for additional high concentrations of antimicrobials directly on the food product.

Organic compounds, such as essential oils, organic acids, enzymes like lysozyme and bacteriocins such as nisin and pediocin, have been widely studied for their antimicrobial properties and tested for their potential application in polymeric matrixes as antimicrobial packaging.

However, organic compounds present some disadvantages. These include sensitivity to intense processing conditions that are present in many industrial processes (such as high temperatures and pressures) and the development of microorganism resistance (YAMAMOTO et al., 2001; ZHANG et al., 2007).

The advent of nanotechnology, which involves the manufacture and use of materials with size of up to about 100 nm in one or more dimensions (BRADLEY et al., 2011), has brought great opportunities for the development of materials with new properties for use as antimicrobial agents. Thus, the interest in inorganic compounds at nanosize has been steadily increasing over the last decade.

Inorganic compounds at nanosize present strong antibacterial activity at low concentrations due to their high surface area to volume ratio and unique chemical and physical properties (RAI et al., 2009). They are also more

stable in extreme conditions, such as high temperature and pressures (SAWAI, 2003), some are considered non-toxic, and even contain mineral elements essential to the human body (ROSELLI et al., 2003).

Most antibacterial inorganic materials are metallic nanoparticles and metal oxide nanoparticles such as silver, copper, titanium oxide, and zinc oxide (ZnO).

Research on ZnO as an antimicrobial agent started in the early 1950s. However, the real move toward the use of ZnO as an antimicrobial was in 1995, when Sawai and his colleagues found that MgO, CaO and ZnO powders had antimicrobial activities against some bacteria strains (SAWAI et al., 1997; SAWAI et al., 1998; SAWAI, 2003).

Currently, ZnO is one of the five zinc compounds that are listed as a Generally Recognized as Safe (GRAS) material by the U.S. Food and Drug Administration (21CFR182.8991) (FDA, 2011).

The current investigation presents a review of research works that address ZnO nanoparticles antimicrobial activity and applications on polymeric matrixes. Also, safety aspects regarding the use of ZnO nanoparticles are discussed.

2. STRUCTURE AND MECHANISMS OF ANTIMICROBIAL ACTIVITY

ZnO is currently listed by FDA as GRAS material (FDA, 2011), and food industries use ZnO as a supplement of zinc element, which is an essential micronutrient and serves important and critical roles in growth, development, and well-being in humans and animals (SHI et al., 2008).

Özgür et al. (2005) pointed out that ZnO is not a newly discovered material. Reports of ZnO physical characterization go back to 1935. ZnO can present three crystal structures, Wurtzite, zincblende and rocksalt (Figure 2). At ambient conditions, the thermodynamically stable phase is the Wurtzite structure, in which every zinc atom is tetrahedrally coordinated with four oxygen atoms.

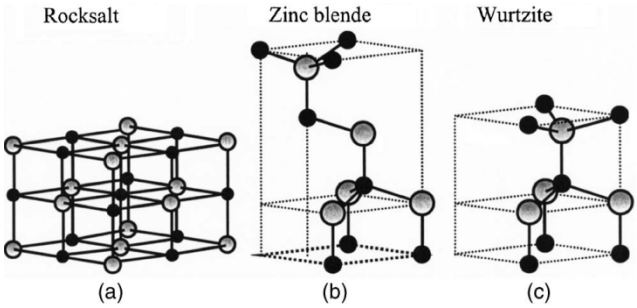

Figure 2. ZnO crystal structures: cubic rocksalt (a), cubic zincblende (b) and hexagonal Wurtzite (c). The shaded gray and black spheres denote zinc and oxygen atoms, respectively. (ÖZGÜR et al., 2005.)

The exact mechanism of action of ZnO nanoparticles is still unknown. However, the antimicrobial activity of these nanoparticles is attributed to several mechanisms (Figure 3), including the release of antimicrobial ions (KASEMETS et al., 2009), interaction of nanoparticles with microorganisms, subsequently damaging the integrity of bacterial cell (ZHANG et al., 2008), and the formation of reactive oxygen species (ROS) by the effect of light radiation (JALAL et al., 2010).

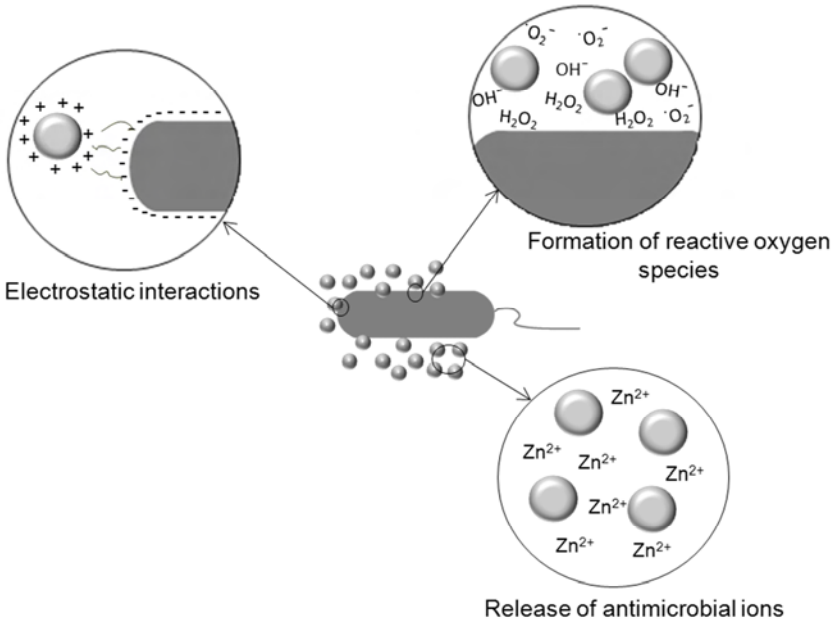

Figure 4. Different mechanisms of antimicrobial activity of ZnO nanoparticles (grey spheres)

The release of Zn^{2+} antimicrobials ions has been suggested as a reasonable hypothesis about the toxicity of ZnO against *S. cerevisiae* (KASEMETS et al.,

2009). According to this author, the toxicity of ZnO nanoparticles could result from the solubility of Zn^{2+} ions in the medium containing the microorganisms. However, low concentrations of solubilized Zn^{2+} can trigger a relatively high tolerance by the microorganism.

In addition, there are differences in metabolic processes of Zn^{2+} ions, which depend on characteristics intrinsic to each microorganism. This could be one of the possible reasons for the observed differences in toxicity thresholds of ZnO nanoparticles in various microorganisms. Thus, while metals and metallic oxides are known to be toxic at relatively high concentrations, ZnO has shown no toxicity at low concentrations, since the zinc element is an essential cofactor in a variety of cellular processes (PADMAVATHY & VIJAYARAGHAVAN, 2008).

On the other hand, interactions of ZnO with the bacterial cell membranes and the generation of damage on bacterial surface have been suggested as responsible for the antimicrobial activity of this metal oxide. In this way, Zhang et al. (2008) indicated that part of the antibacterial activity of ZnO results from the direct contact of nanoparticles with bacterial membrane and from the production of ROS close to the bacterial membrane.

Thus, the inactivation of bacteria by ZnO involves mainly direct interaction between ZnO nanoparticles and the surface of cells, affecting the permeability of the membrane, allowing the internalization of nanoparticles and inducing oxidative stress in bacterial cells, resulting in the inhibition of cell growth.

However, unlike the previous mechanisms, several researchers have indicated the occurrence of ROS as the main mechanism responsible for the antimicrobial activity of ZnO nanoparticles.

The generation of ROS such as hydroxyl radical ($^{\bullet}OH$), hydrogen peroxide (H_2O_2) and superoxide ($O_2^{\bullet -}$), is the result of ZnO nanoparticles activation by visible light and UV. Since ZnO is a semiconductor material, the incident radiation with photon energy higher than the value of its band gap (~ 3.3 eV) causes the movement of electrons from the valence band (*vb*) to the conduction band (*cb*) of the nanoparticle. The result of this process is the

formation of a positive area, known as an electron hole (h^+) in the valence band and a free electron (e^-) in the conduction band (SEVEN et al., 2004).

The electron hole (h^+) reacts with H_2O molecules (from the suspension of ZnO) separating them into $^{\bullet}OH$ and H^+. In addition, O_2 molecules dissolved in the medium are transformed into superoxide anion radicals ($O_2^{\cdot -}$), which in turn react with H^+ to generate ($HO_2^{\bullet}$). Subsequently, this species collides with electrons producing hydrogen peroxide anions (HO_2^-). Thus, the hydrogen peroxide anion reacts with hydrogen ions to produce H_2O_2 molecules (PADMAVATHY & VIJAYARAGHAVAN, 2008; GORDON et al., 2011).

Moreover, the mechanism of action based on the generation of ROS on the ZnO nanoparticles surface seems contradictory, since some studies have shown the antimicrobial activity of ZnO nanoparticles even in dark conditions (ADAMS et al., 2006; ZHANG et al., 2007; HIROTA et al., 2010).

On the other hand, the mechanism of action of ZnO on fungi has not been clearly determined. For example, a study of ZnO activity against the fungi *P. expansum* and *B. cinerea* showed inhibition of conidial development, by distorting of conidiophores of *P. expansum*, while the fungal hyphae of *B. cinerea* were deformed (HE et al., 2011). Hence, the results of this study suggest that the ZnO has a mechanism of action in fungi different from those reported previously for bacteria. Therefore, further studies are needed to clarify the mechanism of action of ZnO in this type of microorganisms.

3. ZnO APPLICATIONS ON FOOD PACKAGING

Food packaging materials developed with nanotechnology are the largest category of current nanotechnology applications for the food sector. The use of nanotechnology can extend and improve packaging functions, which traditionally have been containment, protection, preservation, marketing and communication, leading to a new kind of active food packaging.

In polymer science, composites are made of a polymeric matrix, known as continuous phase, and a discontinuous phase known as filler (AJAYAN et al. 2003; ARORA & PADUA, 2010). Recent advances have allowed the application of nanotechnology in the development of new kinds of materials.

Consequently, nanocomposite materials have been developed as a result of fillers (with at least one dimension in the nanometer scale) incorporated in the polymeric matrices (ARORA & PADUA, 2010).

The development of nanocomposites represents an alternative to conventional technologies used to improve the properties of polymers, since nanocomposites have improved barrier and mechanical properties, as well as heat resistance when compared with the original polymers or conventional composites (SORRENTINO et al., 2007).

In recent years, researchers have shown interest in the study of noble metals and metal oxides, such as silver (Ag), titanium dioxide (TiO_2), zinc oxide (ZnO) and copper oxide I and II (Cu_2O, CuO), due to their stability at high temperatures and antimicrobial activity (SIMONCIC & TOMSIC, 2010).

In this way, the incorporation of ZnO nanoparticles in polymeric matrices can offer advantages, such as providing safer and more affordable food packaging solutions compared to silver nanoparticles. This is due to the wide use of ZnO as Zn supplements in the food industry, with ZnO decomposing into Zn^{2+} ions after going into the human body (SHI et al., 2008).

The main applications of ZnO nanoparticles for food packaging materials include providing antimicrobial activity, since the presence of ZnO nanoparticles in the polymeric matrix allows the packaging to interact with the food and have a dynamic role in their preservation. In addition, ZnO nanoparticles allow for the improvement of packaging properties, such as mechanical strength, barrier properties and stability.

4. PERFORMANCE CHARACTERIZATION

The characterization of nanocomposites involves two main processes: structural analysis and property measurements (Table 5). Structural analysis is carried out using a variety of microscopic and spectroscopic techniques, while property characterization is more diverse and depends on individual applications (KOO, 2006).

Although the techniques presented in table 5 have been used to characterize ZnO nanocomposites, those related to structural analysis are widely used for ZnO nanoparticle characterization before incorporation in polymeric matrices.

Table 5. Characterization techniques of ZnO nanoparticles

ANALYSIS	TECHNIQUE	FACTORS STUDIED
Structural analysis	X-ray diffraction (XRD)	Structural characterization
	Scanning electron microscopy (SEM)	Morphology characterization. Dispersion quality in the polymeric matrix
	Transmission electron microscope (TEM)	
	Atomic force microscopy (AFM)	Surface morphology and topography characterization
	Ultraviolet–visible spectroscopy	Transmission optical spectra
	Fourier transform infrared spectroscopy (FTIR)	Chemical changes in polymers after nanoparticles incorporation Photostability measurements
Property measurements	Mechanical properties	Measurement of mechanical performance. Standard method: ASTM D882
	Barrier properties	Measurement of water vapor permeability. Standard method: ASTM E398; E96/E96M Measurement of oxygen permeability. Standard method: ASTM D 3985
	Differential scanning calorimetry (DSC)	Measurement of sample enthalpy under controlled increase or decrease in temperature
	Thermogravimetric analysis (TGA)	Measurement of weight variation of sample as a function of temperature/time, in a controlled temperature programming

The X-ray diffraction (XRD) technique uses the scattered intensity of an X-ray beam on the sample, revealing information about the crystallographic structure, chemical composition, and physical properties of the material studied (NETO, 2003). This technique is nondestructive and does not require elaborated sample preparation, which partially explains its wide usage in materials characterization (KOO, 2006). XRD is one of the most commonly used techniques to characterize the crystal structure of ZnO.

Although some structural features can be revealed by XRD, direct imaging of individual nanoparticles is only possible using microscopy techniques, such as scanning electron microscopy (SEM), transmission electron microscope (TEM) or atomic force microscopy (AFM).

As a result, researchers use more than one type of structural analysis to characterize the developed nanocomposites. For example, Applerot et al. (2009) used AFM and SEM to study the surface morphology of the deposited ZnO on glass. Similarly, Lepot et al. (2011) used two techniques, SEM and TEM, to evaluate the dispersion quality, as well as the morphology of ZnO nanoparticles incorporated in biaxially oriented polypropylene (BOPP) films. In addition, to characterize the performance of polymer nanocomposites intended for food packaging applications, some mechanical properties, such as Young's modulus (MPa), tensile strength (MPa) and elongation at break (%) have been studied. Barrier properties such as oxygen permeability have also been determined. The thermal capacity has been studied by means of thermoanalytical techniques, such as differential scanning calorimetry (DSC) and thermogravimetric analysis (TGA).

Thermogravimetry studies the weight variation of sample (loss or gain) as a function of temperature and/or time while the sample is subjected to a controlled temperature programming. This technique is widely used in polymer science, since it enables the determination of the temperature range in which the sample acquires chemical, fixed, defined and constant composition, and also the temperature in which sample start to decompose (MATOS & MACHADO, 2003). On the other hand, differential scanning calorimetry (DSC) is another widely used thermoanalytical technique. DSC consists of the direct measurement of heat changes, represented by enthalpy (ΔH) that occurs in the sample during a controlled increase or decrease in temperature, making possible the study of materials in their native state (MATOS & MACHADO, 2003).

5. ASPECTS OF SAFETY

Food safety and quality, as well as the potential impact on consumers, are key issues related to food packaging developed with nanotechnology.

Recently, interest has grown in safety issues regarding the use of nanoparticles in food packaging. Researchers are especially concerned with the possibility of nanoparticles migrating from the packaging material into the food, and whether this migration would have a negative impact on the safety or quality of the packaged product (BRADLEY et al., 2011).

According to Chaudry et al. (2008), nanoparticles have much larger surface area to volume ratios, thus they may exhibit substantially different physicochemical and biological properties compared to conventionally sized particles.

An important factor to be considered in toxicity tests is the diversity of the exposure routes. In the case of nanocomposite materials intended for food packaging applications, the main route of exposure to be evaluated is by ingestion.

For the final consumers of food packaged in nanocomposite materials, the first concern is to verify the migration of nanoparticles from the packaging into the food. If this migration happens, the next step would be to study the effect of the ingestion of these nanoparticles inside the body from the mouth to the gastrointestinal tract, through *in vitro* as well as *in vivo* exposure tests (SILVESTRE et al 2011).

Currently, there is a great need for further studies. These must include toxicological studies based on data obtained from migration tests to understand how nanoparticles, as well as released ions may act within the body, their biotransformation and elimination routes, and their absorption by various organs.

6. FINAL CONSIDERATIONS AND FUTURE PROSPECTS

In addition to being a compound with many applications in everyday life, ZnO is also a promising antimicrobial agent due to its activity against a wide range of microorganisms and high resistance to severe processing conditions. Moreover, the use of ZnO nanoparticle in biodegradable polymeric matrices

is an alternative for material performance improvements, enhancing mechanical, thermal and barrier properties.

However, additional research is needed to understand ZnO nanoparticle toxicity when used as an antimicrobial, applied directly or incorporated in packaging material.

Therefore, some issues still need to be addressed, such as the exact mechanism of action of ZnO nanoparticles on bacteria and fungi, the migration of nanoparticles from the packaging material to food, and their toxicological effects and routes of biotransformation and elimination.

7. REFERENCES

ADAMS, L. K., LYON, D. Y., ALVAREZ, P. J. J. Comparative eco-toxicity of nanoscale TiO_2, SiO_2, and ZnO water suspensions. **Water Research.** v. 40, p. 3527–3532. 2006.

AHVENAINEN, R. **Novel food packaging techniques.** Boca Raton: CRC Press LLC, 2003. 590p.

AJAYAN, P. M., SCHADLER, L. S., BRAUN. P. V. **Nanocomposite Science and Technology.** Weinheim: WILEY-VCH, 2003. 230p.

APPENDINI, P., HOTCHKISS, J. H. Review of antimicrobial food packaging. **Innovative Food Science & Emerging Technologies.** v. 3, p. 113-126. 2002.

APPLEROT, G., PERKAS, N., AMIRIAN, G., GIRSHEVITZ, O., GEDANKEN, A. Coating of glass with ZnO via ultrasonic irradiation and a study of its antibacterial properties. **Applied Surface Science**. v. 256S, p. S3–S8. 2009.

ARORA, A., PADUA, G. W. Review: Nanocomposites in food packaging. **Journal of Food Science.** v. 75(1), p. R43–R49. 2010.

BRADLEY, E. L., CASTLE, L., CHAUDHRY, Q. Applications of nanomaterials in food packaging with a consideration of opportunities for developing countries. **Trends in Food Science & Technology.** v. 12 (11), p. 604-610. 2011.

Center for Disease Control and Prevention (CDC). **Data & Statistics**. <http://www.cdc.gov/Features/dsFoodborneEstimates/>. Retrieved: 06.05.2011.

Food and Drug Administration (FDA). **Substances Generally Recognized as Safe.** <http://www.fda.gov/Food/FoodIngredientsPackaging/GenerallyRecognizedasSafeGRAS/default.htm>. Retrieved: 28.03.2011.

GORDON, T., PERLSTEIN, B., HOUBARA, O., FELNER, I., BANIN, E., MARGEL, S. Synthesis and characterization of zinc/iron oxide composite nanoparticles and their antibacterial properties. **Colloids and Surfaces A: Physicochemical and Engineering Aspects.** v. 374, p. 1–8. 2011.

HE, L., LIU, Y., MUSTAPHA, A., LIN, M. Antifungal activity of zinc oxide nanoparticles against *Botrytis cinerea* and *Penicillium expansum*. **Microbiological Research.** v. 166, p. 207—215. 2011.

HIROTA, K., SUGIMOTO, M., KATO, M., TSUKAGOSHI, K., TANIGAWA, T., SUGIMOTO, H. Preparation of zinc oxide ceramics with a sustainable antibacterial activity under dark conditions. **Ceramics International.** v. 36, p. 497-506. 2010.

JALAL, R., GOHARSHADIA, E. K., ABARESHIA, M., MOOSAVIC, YOUSEFID, A., NANCARROW, P. ZnO nanofluids: Green synthesis, characterization, and antibacterial activity. **Materials Chemistry and Physics.** v. 121, p. 198–201. 2010.

KASEMETS, K., IVASK, A., DUBOURGUIER, H. C., KAHRU, A. Toxicity of nanoparticles of ZnO, CuO and TiO_2 to yeast *Saccharomyces cerevisiae*. **Toxicology in Vitro.** v. 23, p. 1116–1122. 2009.

KOO, J. H. **Polymer nanocomposites: Processing, characterization, and application.** New York: McGraw-Hill. 2006. 272p.

LEPOT, N., VAN BAEL, M. K., VAN DEN RUL, H., D'HAEN, J., PEETERS, R. FRANCO, D., MULLENS, J. Influence of incorporation of ZnO nanoparticles and biaxial orientation on mechanical and oxygen barrier properties of polypropylene films for food packaging applications. **Journal of Applied Polymer Science.** v. 120, p. 1616–1623. 2011.

MATOS, J. R., MACHADO, L. D. B. **Análise térmica - Termogravimetria.** In: CANEVAROLO Jr., S. V. Técnicas de caracterização de polímeros. São Paulo: Artliber. p. 209-228. 2003.

NETO, R.B. **Raio X.** In: CANEVAROLO Jr., S. V. Técnicas de caracterização de polímeros. São Paulo: Artliber. p. 41-60. 2003.

ÖZGÜR, Ü., ALIVOV, Y. I., LIU, C., TEKE, A., RESHCHIKOV, M. A., DOĞAN, S., AVRUTIN, V., CHO, S.-J., MORKOÇ, H. A comprehensive review of ZnO materials and devices. **Journal of Applied Physics.** v. 98, p. 041301-1 - 041301-103. 2005.

PADMAVATHY, N., VIJAYARAGHAVAN, R. Enhanced bioactivity of ZnO nanoparticles—an antimicrobial study. **Science and Technology of Advanced Materials.** v. 9, p. 1-7. 2008.

RAI, M., YADAV, A., GADE, A. Silver nanoparticles as a new generation of antimicrobials. **Biotechnology Advances.** v. 27, p. 76-83. 2009.

RESTUCCIA, D., SPIZZIRRI, U. G., PARISI, O.I., CIRILLO, G., CURCIO, M., IEMMA, F., PUOCI, F., VINCI, G., PICCI, P. New EU regulation aspects and global market of active and intelligent packaging for food industry applications. **Food Control.** v. 21, p. 1425–1435. 2010.

ROSELLI, M., FINAMORE, A., GARAGUSO, I., BRITTI, M. S., MENGHERI, E. Zinc oxide protects cultured enterocytes from the damage induced by *Escherichia coli*. **Journal of Nutrition.** v. 133, p. 4077–4082. 2003.

SAWAI, J., KOJIMA, H., ISHIZU, N., ITOH, M., IGARASHI, H., SAWAKI, T., SHIMIZU, M. Bactericidal action of magnesium oxide powder. **Journal of Inorganic Biochemistry.** v. 67 (1), p. 443-443. 1997.

SAWAI, J., SHOJI, S., IGARASHI, H., HASHIMOTO, A., KOKUGAN, T., SHIMIZU, M., KOJIMA, H. Hydrogen peroxide as an antibacterial factor in zinc oxide powder slurry. **Journal of Fermentation and Bioengineering.** v. 86 (5), p. 521-522. 1998.

SAWAI, J. Quantitative evaluation of antibacterial activities of metallic oxide powders (ZnO, MgO and CaO) by conductimetric assay. **Journal of Microbiological Methods.** v. 54, p.177–182. 2003.

SCHARF, R. L. **Health-related costs from foodborne illness in the United States.** <http://www.producesafetyproject.org/media?id=0009>. Retrieved: 10.05.2011.

SEVEN, O., DINDAR, B., AYDEMIR, S., METIN, D., OZINEL, M. A., ICLI, S. Solar photocatalytic disinfection of a group of bacteria and fungi aqueous suspensions with TiO_2, ZnO and Sahara desert dust. **Journal of Photochemistry and Photobiology A: Chemistry**. v. 165, p. 103–107. 2004.

SHI, L., ZHOU, J., GUNASEKARAN, S. Low temperature fabrication of ZnO–whey protein isolate nanocomposites. **Materials Letters.** v. 62, p. 4383–4385. 2008.

SILVESTRE, C., DURACCIO, D., CIMMINO, S. Food Packaging based on Polymer Nanomaterials. **Progress in Polymer Science**. 2011. doi:10.1016/j.progpolymsci.2011.02.003.

SIMONCIC, B., TOMSIC, B. Structures of Novel Antimicrobial Agents for Textiles - A Review. **Textile Research Journal.** v. 80 (16), p. 1721-1737. 2010.

SOARES, N. F. F., SILVA, C. A. S., SANTIAGO-SILVA, P., ESPITIA, P. J. P., GONÇALVES, M. P. J. C., LOPEZ, M. J. G., MILTZ, J., CERQUEIRA, M. A., VICENTE, A. A., TEIXEIRA, J., SILVA, W. A., BOTREL, D. A. **Active and intelligent packaging for milk and milk products.** In: COIMBRA, J. S. R., TEIXEIRA, J. A. (Eds.) Engineering aspects of milk and dairy products. New York: CRC Press Taylor & Francis Group. Chapter 7. p. 155-174. 2009.

SORRENTINO, A., GORRASI, G., VITTORIA, V. Potential perspectives of bionanocomposites for food packaging applications. **Trends in Food Science & Technology.** v. 18, p. 84–95. 2007.

TAUXE, R. V., DOYLE, M. P., KUCHENMÜLLER, T., SCHLUNDT, J., STEIN, C. E. Evolving public health approaches to the global challenge of foodborne infections. **International Journal of Food Microbiology.** v. 139, p. S16–S28. 2010.

YAMAMOTO, O. Influence of particle size on the antibacterial activity of zinc oxide. **International Journal of Inorganic Materials**. v. 3, p. 643–646. 2001.

ZHANG, L., JIANG, Y., DING, Y., POVEY, M., YORK, D. Investigation into the antibacterial behaviour of suspensions of ZnO nanoparticles (ZnO nanofluids). **Journal of Nanoparticle Research.** v. 9, p. 479–489. 2007.

ZHANG, L., DING, Y., POVEY, M., YORK, D. ZnO nanofluids – A potential antibacterial agent. **Progress in Natural Science.** v. 18, p. 939–944. 2008.

ARTIGO CIENTÍFICO 2
APLICAÇÕES DA PEDIOCINA EM EMBALAGENS ATIVAS

Resumo

A pediocina é um peptídeo com atividade antimicrobiana contra *Listeria monocytogenes*. Devido à sua atividade antimicrobiana, tem sido aplicada na conservação de alimentos, mediante a adição da sua estirpe produtora tanto diretamente no alimento, quanto a incorporação da pediocina nas embalagens. Este trabalho apresenta as principais características da pediocina. Adicionalmente, discutem-se as aplicações da pediocina em polímeros para conservação de alimentos. Finalmente, são analisadas questões de segurança e as tendências relacionadas ao uso da pediocina.

Palavras-chave: Atividade antimicrobiana, conservação de alimentos, embalagens ativas, pediocina, segurança.

Applications of Pediocin in Active Food Packaging

Abstract

Pediocin is an active peptide with activity against *Listeria monocytogenes*. Due to its antimicrobial activity, pediocin has many applications in food preservation, such as the addition of its producer strain on the food, direct addition into the food, and recently its incorporation into packaging. This review begins with pediocin main characteristics. Moreover, pediocin applications in polymers for food preservation are presented. Finally, safety issues and future trends related to the use of pediocin are discussed.

Keywords: Pediocin, antimicrobial activity, food preservation, active packaging, safety issue.

1. INTRODUCTION

Food is one of the vehicles by which humans can be infected or contaminated by microorganisms that cause foodborne disease. Foodborne diseases are a global public-health issue, and each year food safety becomes an increasingly important international concern. As a result of these concerns, researchers have great interest in natural antimicrobial agents, such as bacteriocins, for food preservation.

Bacteriocins are an interesting alternative to the use of traditional chemical preservatives for the control of foodborne pathogens or spoilage bacteria. Bacteriocins are antimicrobial peptides, ribosomally synthesized by bacteria and have the ability to kill closely related bacteria. However, the bacterium that secretes the peptide is immune to the produced bacteriocin (Cleveland, Montville, Nes, & Chikindas, 2001). Pediocin and nisin are the most studied bacteriocins and are commercially used as natural preservatives (Acuña, Morero, & Bellomio, 2011).

Currently, nisin is the only bacteriocin licensed as a food additive. However, the use of pediocin for food preservation has also been commercially exploited in the form of a food ingredient generated from *Pediococcus*

acidilactici, a pediocin-producing strain (Rodríguez, Martínez, & Kok, 2002), and its use is covered by several US and European patents (El-Ghaish, et al., 2011).

Pediocin and pediocin-like bacteriocins belong to the group IIa bacteriocins and are active against *Listeria* species (Ennahar, Sashihara, Sonomoto, & Ishizaki, 2000). Pediocin has many applications in food preservation due to its activity in controlling *Listeria monocytogenes*, a foodborne pathogen of special concern in the food industry.

L. monocytogenes is a Gram-positive, non-spore-forming, facultative anaerobic rod that grows between -0.4 and 50 ºC (Farber & Peterkin, 1991). According to Scharff (2012), the incidence of *L. monocytogenes* in food products causes 1,591 illnesses, 1,455 hospitalization and 255 deaths annually in the US. Food products, such as bologna sausage, cooked ham, smoked salmon or fermented sausages, are highly susceptible to this microorganism.

Listeriosis, the disease caused by this microorganism, primarily affects older adults, pregnant women, newborns, and adults with weakened immune systems. However, rarely, persons without these risk factors can also be affected (CDC, 2011).

To control *Listeria* growth in food products after processing, pediocin has been incorporated into polymeric materials to create antimicrobial packaging for the preservation of food.

Antimicrobial packaging plays an important role in food preservation because this packaging prolongs food shelf life through the interaction with either the product or the headspace within the packaging. This interaction results in the reduction or inhibition of the growth of microorganisms that might be present on the food surface.

This review highlights the main characteristics of the antimicrobial peptide pediocin. Additionally, pediocin applications in polymeric matrices intended as food packaging are reviewed. Finally, safety issues regarding the use of pediocin and future prospects are discussed.

2. PEDIOCIN AND ITS APPLICATION ON FOOD PACKAGING

Pediocin is a 44-residue peptide composed of both aromatic and aliphatic amino acids and with no posttranslational modifications (Henderson, Chopko, & van Wassenaar, 1992). The structure of pediocin is mainly composed of two regions: a hydrophilic, cationic, N-terminal region, and a hydrophobic/amphiphilic, C-terminal region (Johnsen, Fimland, & Nissen-Meyer, 2005).

The cationic, N-terminal region presents a three-stranded, antiparallel β-sheet supported by a disulfide bond. This disulfide bond consists of two cysteine residues (C_9 and C_{14}) present in the N-terminal region. At the end of the structure, there is a C-terminal tail with two cysteine residues (C_{24} and C_{44}) that folds back onto the central α-helix by a disulfide bond, resulting in a hairpin domain. Additionally, between the N-terminal region and the hairpin domain in the C-terminal region, there is a flexible hinge (located in the amino acid residue W_{18}) that allows the two regions to move relative to one another (Figure 1).

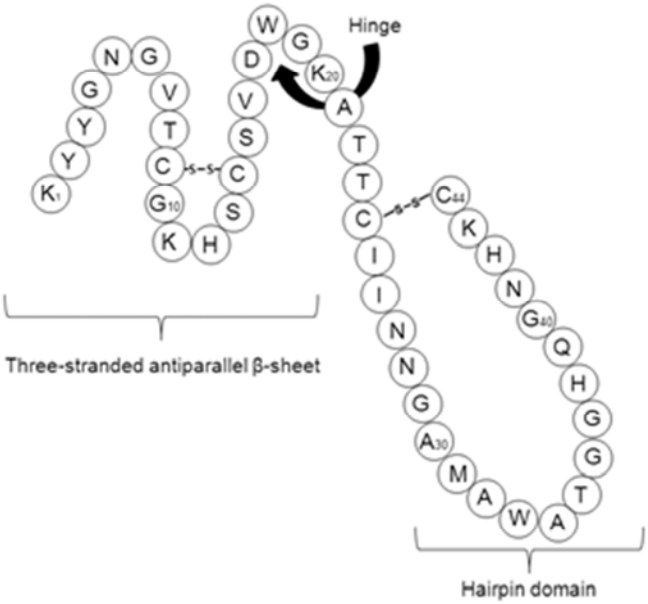

Figure 2. Structure for the amino acids sequence of pediocin PA-1, adapted from Rodríguez et al. (2002).

The antimicrobial activity of pediocin is closely related to its structure and involves the formation of pores in the target membrane, which results in

efflux of small, intracellular substances, depletion of cytoplasmic ATP, dissipation of proton motive force, and ultimately cell death (Montville & Chen, 1998).

Recently, pediocin have been used in food preservation by its incorporation in antimicrobial active packaging. Active packaging is as a packaging system that changes the condition of the package to extend the shelf life, improve food safety or sensory properties while maintaining the quality of the food (Vermeiren, Devlieghere, van Beest, de Kruijf, & Debevere, 1999).

Moreover, antimicrobial packaging is a type of active packaging that aims to extend the shelf life of foods by reducing microbial growth on the product surface (Appendini & Hotchkiss, 2002). This type of packaging interacts with the product or the headspace within the packaging to reduce, inhibit or retard the growth of microorganisms that might be present on food surfaces.

Active packaging with antimicrobial peptides can be developed by three main methods of incorporation: 1) direct peptide incorporation into the polymer; 2) peptide coating on the polymeric surface; and 3) peptide immobilization within the polymer (Espitia, et al., 2012).

The method of direct peptide incorporation in the polymer was used to develop an antimicrobial packaging of whey protein isolates (WPI) and ethanol-soluble corn zein (CZ) films with pediocin (Quintero-Salazar, Vernon-Carter, Guerrero-Legarreta, & Ponce-Alquicira, 2005). The antimicrobial activity of CZ films against *Listeria innocua* progressively increased with pediocin concentration, whereas the antimicrobial activity of WPI films was not affected by pediocin concentration. This result indicates that a high concentration of pediocin in WPI films does not necessarily improve their effectiveness against *L. innocua*.

Additionally, the direct incorporation method has been used for the development of antimicrobial cellulosic packaging with pediocin (Soares, et al., 2007). This packaging presented activity against *L. monocytogenes* in analysis *in vitro* as well as in bologna samples. Moreover, the same method was used for the development of antimicrobial packaging of cellulose base against *L. innocua* or *Salmonella.* These antimicrobial films were more effective at inhibiting the growth of *L. innocua* with a reduction of 2 log cycles

relative to the control, whereas the growth of *Salmonella* sp. presented only a 0.5 log cycle reduction relative to the control (Santiago-Silva, et al., 2009).

However, peptide coating on the polymeric surface is an alternative when the polymer requires extreme processing conditions for packaging development, such as high pressure and temperature, which can result in the inactivation of the antimicrobial agent (Appendini & Hotchkiss, 2002). Generally, the antimicrobial coating is generated by contacting or immersing the polymeric material in the peptide solution.

The coating method has been used to evenly distribute pediocin on the inner surfaces of plastic packaging bags by agitation (Ming, Weber, Ayres, & Sandine, 1997). The antimicrobial packaging completely inhibited the growth of *L. monocytogenes* inoculated in samples of chicken, beef and ham during 12 weeks of storage at 4 ºC.

Both methods of pediocin application, direct peptide incorporation and coating on polymers, result in the migration of the bioactive compound into the food. However, peptide immobilization in the polymer results in a non-migratory active packaging, in which bioactive components are tethered to the packaging (Barish & Goddard, 2011).

Although peptide immobilization presents advantages, such as sustained antimicrobial activity, and benefits with regard to regulatory concerns due to the non-migratory nature of the developed packaging, several drawbacks of this method, such as losses in bioactivity due to structural changes in the peptide, diffusional limitations and loss in molecular mobility, could explain why this method has not yet been used for pediocin immobilization on polymeric surfaces.

3. SAFETY ISSUES

Several studies in recent decades have shown that peptides have certain bioactive properties (Agyei & Danquah, 2011). However, despite their natural origin, peptides selected for use in foods as antimicrobial agents must be thoroughly evaluated for potential cytotoxicity to mammalian cells to ensure food safety and quality as well as the potential impact on consumers.

For the final consumer of food contained in packaging materials with pediocin, one concern is the presence of this peptide in the food product. To evaluate this effect, the migration of the peptide from the packaging into the food must be verified, with ingestion considered as the main route of exposure to be evaluated. If pediocin ingestion occurred, then the next concern to be considered is the effect of this peptide within the body using both *in vitro* and *in vivo* exposure tests.

In vitro analyses have been used to study the toxicity of pediocin toward mammalian cells. Murinda, Rashid, and Roberts (2003) studied the cytotoxicity of pediocin toward transfected human colon (SV40-HC) cells, a type of malignant cell, and monkey kidney (Vero) cells, which are healthy cells. As a result, pediocin selectively affected SV40-HC cell lines more extensively than normal Vero cells, suggesting that this peptide has the potential for use as a therapeutic agent against virally infected or malignant cells.

Additionally, pediocin has shown cytotoxic activity against human colon adenocarcinoma (HT29) cells and human cervical carcinoma (HeLa) cells (Villarante, et al., 2011).

According to Hoskin and Ramamoorthy (2008), there are fundamental differences between the membranes of malignant cells and normal cells that allow certain peptides to selectivity attack malignant or carcinogenic cells without affecting healthy cells. In this way, malignant cells develop more receptors on the surfaces of the cell membrane, and these receptors can be used for attachment and uptake of a variety of biological substances, including bacteriocins.

In addition, *in vitro* analyses have been used to study the effect of pediocin in the gastrointestinal tract. Le Blay, Lacroix, Zihler, and Fliss (2007) studied the inhibition activity of pediocin against 21 common intestinal bacteria. They indicated that pediocin, which is very active against *Listeria* spp. and other foodborne pathogens, did not inhibit major bacterial species of the human intestine, in contrast to nisin A and nisin Z. Moreover, the authors suggest that pediocin has the potential to inhibit *Listeria* within the intestinal microbiota without altering commensal bacteria.

However, Kheadr, et al. (2010) demonstrated the sensitivity of pediocin to digestive enzymes especially pancreatin and, consequently, its loss of activity under gastrointestinal (GIT) conditions. These researchers investigated the physicochemical and biological stability of purified pediocin in GIT conditions using a dynamic gastrointestinal model (known as TIM-1), which simulates the human stomach, duodenum, jejunum and ileum, and the authors observed that the activity of purified pediocin was significantly poor under GIT conditions.

According to these authors, the activity of pediocin in the GIT compartment was slightly reduced after 90 min of gastric digestion, whereas no detectable activity was found in the duodenal, jejunal and ileal compartments during 5 h of digestion. Moreover, HPLC analysis showed partial degradation of pediocin in the duodenal compartment and massive breakdown in the jejunal and ileal compartments.

Therefore, to overcome pediocin sensitivity to digestive enzymes, Kheadr, et al. (2010) have suggested using this peptide in a protected form, such as encapsulation in food-grade material, as an alternative to deliver this peptide in its active form for the treatment of infectious diseases.

However, few studies have been conducted on the *in vivo* behavior of bacteriocins. In this context, Bernbom, et al. (2009) examined the stability of ingested pediocin on the composition of the intestinal microbiota of human microbiota-associated rats. The measurement of pediocin 3 h after dosage resulted in no pediocin detection in fecal samples of dosed rats, probably indicating that degradation or inactivation of pediocin occurs in the intestinal tract. However, another possible explanation for the lack of pediocin activity in fecal samples of dosed animals is that pediocin binds to the surfaces of the producer strain, other bacteria, food molecules or intestinal surfaces.

In addition, pediocin exposure tests have been performed to study its anti-listerial activity *in vivo* using a mouse model (Dabour, Zihler, Kheadr, Lacroix, & Fliss, 2009). In contrast to studies that indicated the inactivation of pediocin as a result of digestive enzymes, Dabour, et al. (2009) showed that repeated doses of purified pediocin in mice were not inactivated but provided up to 2-log reductions in fecal listerial counts compared with the infected control

group and slowed pathogen translocation into the liver and spleen, leading to the disappearance of *L. monocytogenes* infection in these two organs within six days. Moreover, in agreement with results of Le Blay, et al. (2007), pure pediocin produced no major changes in the composition of the intestinal flora in either infected or uninfected animals.

Although both *in vitro* and *in vivo* results are promising due to the evidence of maintenance of the intestinal bacteria under pediocin presence and its cytotoxic activity against malignant cells, further studies are need regarding the activity of pediocin in GIT conditions. Moreover, further research addressing toxicity and translocation tests is needed before the final approval of this bacteriocin as a food preservative.

4. FUTURE TRENDS

Pediocin has shown antimicrobial activity, leading to its application in food preservation by incorporation into packaging materials. Food packaging with pediocin has shown effectiveness in inhibiting pathogenic microorganisms *in vitro* as well as in food products.

In addition, the results of the *in vitro* and *in vivo* studies on the cytotoxicity and safety of pediocin are promising. However, additional studies on the release of this peptide from food packaging are needed to better understand the mechanism of diffusion of this antimicrobial agent.

Finally, in the coming years, the advent of nanotechnology will lead to research into the synergistic effect of pediocin and nanoparticles, such as metals, metal oxides and nanoclays, to improve the antimicrobial activity as well as mechanical and barrier properties of the antimicrobial packaging. Moreover, other forms of pediocin delivery, such as nanoliposomes, could be developed to carry this peptide in its active form to the target site.

ACKNOWLEDGEMENTS

The authors gratefully acknowledge Mr. Nicholas J. Walker for providing language help and writing assistance. Miss Espitia gratefully acknowledges the financial support provided by a doctoral scholarship from Coordenação de Aperfeiçoamento de Pessoal de Nível Superior (CAPES) through PEC-

PG agreement, and Mrs. Soares acknowledges a grant from the Conselho Nacional de Desenvolvimento Científico e Tecnológico (CNPq).

5. REFERENCES

Acuña, L., Morero, R., & Bellomio, A. (2011). Development of wide-spectrum hybrid bacteriocins for food biopreservation. *Food and Bioprocess Technology, 4*, 1029-1049.

Agyei, D., & Danquah, M. K. (2011). Industrial-scale manufacturing of pharmaceutical-grade bioactive peptides. *Biotechnology Advances, 29*, 272-277.

Appendini, P., & Hotchkiss, J. H. (2002). Review of antimicrobial food packaging. *Innovative Food Science & Emerging Technologies, 3*, 113-126.

Barish, J. A., & Goddard, J. M. (2011). Polyethylene Glycol Grafted Polyethylene: A Versatile Platform for Nonmigratory Active Packaging Applications. *Journal of Food Science, 76*, E586-E591.

Bernbom, N., Jelle, B., Brogren, C.-H., Vogensen, F. K., Nørrung, B., & Licht, T. R. (2009). Pediocin PA-1 and a pediocin producing *Lactobacillus plantarum* strain do not change the HMA rat microbiota. *International Journal of Food Microbiology, 130*, 251-257.

CDC. (2011). Listeriosis (*Listeria* infection). In (Vol. 2012). Atlanta, USA: Centers for Disease Control and Prevention.

Cleveland, J., Montville, T. J., Nes, I. F., & Chikindas, M. L. (2001). Bacteriocins: safe, natural antimicrobials for food preservation. *International Journal of Food Microbiology, 71*, 1-20.

Dabour, N., Zihler, A., Kheadr, E., Lacroix, C., & Fliss, I. (2009). *In vivo* study on the effectiveness of pediocin PA-1 and *Pediococcus acidilactici* UL5 at inhibiting *Listeria monocytogenes*. *International Journal of Food Microbiology, 133*, 225-233.

El-Ghaish, S., Ahmadova, A., Hadji-Sfaxi, I., El Mecherfi, K. E., Bazukyan, I., Choiset, Y., Rabesona, H., Sitohy, M., Popov, Y. G., Kuliev, A. A., Mozzi, F., Chobert, J.-M., & Haertlé, T. (2011). Potential use of lactic acid bacteria for reduction of allergenicity and for longer conservation of fermented foods. *Trends in Food Science & Technology, 22*, 509-516.

Ennahar, S., Sashihara, T., Sonomoto, K., & Ishizaki, A. (2000). Class IIa bacteriocins: biosynthesis, structure and activity. *FEMS Microbiology Reviews, 24*, 85-106.

Espitia, P. J. P., Soares, N. d. F. F., Coimbra, J. S. d. R., de Andrade, N. J., Cruz, R. S., & Medeiros, E. A. A. (2012). Bioactive peptides: Synthesis, properties, and applications in the packaging and preservation of food. *Comprehensive Reviews in Food Science and Food Safety, 11*, 187-204.

Farber, J. M., & Peterkin, P. I. (1991). *Listeria monocytogenes*, a food-borne pathogen. *Microbiological Reviews, 55*, 476-511.

Henderson, J. T., Chopko, A. L., & van Wassenaar, P. D. (1992). Purification and primary structure of pediocin PA-1 produced by *Pediococcus acidilactici* PAC-1.0. *Archives of Biochemistry and Biophysics, 295*, 5-12.

Hoskin, D. W., & Ramamoorthy, A. (2008). Studies on anticancer activities of antimicrobial peptides. *Biochimica et Biophysica Acta: Biomembranes, 1778*, 357-375.

Johnsen, L., Fimland, G., & Nissen-Meyer, J. (2005). The C-terminal domain of pediocin-like antimicrobial peptides (class IIa bacteriocins) is involved in specific recognition of the C-terminal part of cognate immunity proteins and in determining the antimicrobial spectrum. *Journal of Biological Chemistry, 280*, 9243-9250.

Kheadr, E., Zihler, A., Dabour, N., Lacroix, C., Le Blay, G., & Fliss, I. (2010). Study of the physicochemical and biological stability of pediocin PA-1 in the upper gastrointestinal tract conditions using a dynamic *in vitro* model. *Journal of Applied Microbiology, 109*, 54-64.

Le Blay, G., Lacroix, C., Zihler, A., & Fliss, I. (2007). *In vitro* inhibition activity of nisin A, nisin Z, pediocin PA-1 and antibiotics against common intestinal bacteria. *Letters in Applied Microbiology, 45*, 252-257.

Ming, X., Weber, G. H., Ayres, J. W., & Sandine, W. E. (1997). Bacteriocins applied to food packaging materials to inhibit *Listeria monocytogenes* on meats. *Journal of Food Science, 62*, 413-415.

Montville, T. J., & Chen, Y. (1998). Mechanistic action of pediocin and nisin: recent progress and unresolved questions. *Applied Microbiology and Biotechnology, 50*, 511-519.

Murinda, S. E., Rashid, K. A., & Roberts, R. F. (2003). *In vitro* assessment of the cytotoxicity of nisin, pediocin, and selected colicins on simian virus 40-transfected human colon and vero monkey kidney cells with trypan blue staining viability assays. *Journal of Food Protection, 66*, 847-853.

Quintero-Salazar, B., Vernon-Carter, E. J., Guerrero-Legarreta, I., & Ponce-Alquicira, E. (2005). Incorporation of the antilisterial bacteriocin-like inhibitory substance from *Pediococcus parvulus* VKMX133 into film-

forming protein matrices with different hydrophobicity. *Journal of Food Science, 70*, M398-M403.

Rodríguez, J. M., Martínez, M. I., & Kok, J. (2002). Pediocin PA-1, a wide-spectrum bacteriocin from lactic acid bacteria. *Critical Reviews in Food Science and Nutrition, 42*, 91-121.

Santiago-Silva, P., Soares, N. F. F., Nóbrega, J. E., Júnior, M. A. W., Barbosa, K. B. F., Volp, A. C. P., Zerdas, E. R. M. A., & Würlitzer, N. J. (2009). Antimicrobial efficiency of film incorporated with pediocin (ALTA® 2351) on preservation of sliced ham. *Food Control, 20*, 85-89.

Scharff, R. L. (2012). Economic burden from health losses due to foodborne illness in the United States. *Journal of Food Protection, 75*, 123-131.

Soares, N. F. F., Espitia, P. J. P., Pacheco, J. J. R., Bolano, D. G., Villadiego, A. M. D., Teheran, J. D., & Melo, N. R. (2007). Desenvolvimento e avaliação de embalagem ativa para conservação de produtos cárneos. In S. B. d. Microbiologia (Ed.), *24º Congresso Brasileiro de Microbiologia*. Brasília.

Vermeiren, L., Devlieghere, F., van Beest, M., de Kruijf, N., & Debevere, J. (1999). Developments in the active packaging of foods. *Trends in Food Science & Technology, 10*, 77-86.

Villarante, K., Elegado, F., Iwatani, S., Zendo, T., Sonomoto, K., & De Guzman, E. (2011). Purification, characterization and *in vitro* cytotoxicity of the bacteriocin from *Pediococcus acidilactici* K2a2-3 against human colon adenocarcinoma (HT29) and human cervical carcinoma (HeLa) cells. *World Journal of Microbiology and Biotechnology, 27*, 975-980.

ARTIGO CIENTÍFICO 3

OTIMIZAÇÃO DA DISPERSÃO DE NANOPARTÍCULAS DE ZnO E ATIVIDADE ANTIMICROBIANA CONTRA MICRO-ORGANISMOS PATOGÊNICOS E DETERIORANTES EM ALIMENTOS

Resumo

Nanopartículas primárias de óxido de zinco (nanoZnO) tendem a aglomerar-se, resultando na perda da sua atividade antimicrobiana. Neste trabalho foram estudados os efeitos das condições de sonicação por probe (potência e tempo de sonicação), e a presença do agente dispersante $Na_4P_2O_7$, sobre o tamanho das nanoZnO. A dispersão de NanoZnO foi otimizada mediante o uso da metodologia de superfície de resposta (RSM) e caracterizada pela técnica de potencial zeta (PZ). A atividade antimicrobiana das NanoZnO foi estudada em diferentes concentrações (1 %, 5 % e 10 % m/m) contra quatro micro-organismos patogênicos e quatro micro-organismos deteriorantes. A presença do agente dispersante teve efeito significativo sobre o tamanho das partículas de ZnO. O tamanho mínimo após sonicação foi de 238 nm. A condição de dispersão ótima foi alcançada utilizando-se 200 W de potência, durante 45 minutos de sonicação, na presença do agente dispersante. Análises de PZ indicaram que a carga de superfície das nanopartículas de ZnO foi alterada pela adição do agente dispersante e por mudanças no pH. Nas condições testadas, a dispersão de nanoZnO não apresentou atividade antimicrobiana contra *Pseudomonas aeruginosa*, *Lactobacillus plantarum* e *Listeria monocytogenes*. No entanto, a atividade antimicrobiana foi positiva contra *Escherichia coli, Salmonella* Choleraesuis*, Staphylococcus aureus, Saccharomyces cerevisiae* e *Aspergillus niger*. De acordo com a atividade antimicrobiana exibida pela dispersão ótima de nanoZnO contra alguns

micro-organismos patogênicos e deteriorantes, contaminantes de alimentos, considera-se que as nanoZnO são um promissor agente antimicrobiano para a conservação de alimentos, com potencial aplicação no desenvolvimento de nanocompósitos ativos para embalagens de alimentos.

Palavras-chave: Atividade antimicrobiana, metodologia de superfície de resposta, nanopartículas de óxido de zinco, otimização, processo de dispersão, potencial zeta.

Optimized Dispersion of ZnO Nanoparticles and Antimicrobial Activity against Foodborne Pathogens and Spoilage Microorganisms

Abstract

Single primary nanoparticles of zinc oxide (nanoZnO) tend to form particle collectives, resulting in loss of antimicrobial activity. This work studied the effects of probe sonication conditions: power, time, and the presence of a dispersing agent ($Na_4P_2O_7$), on the size of nanoZnO particles. NanoZnO dispersion was optimized by response surface methodology (RSM) and characterized by the zeta potential (ZP) technique. NanoZnO antimicrobial activity was investigated at different concentrations (1 %, 5 % and 10 % w/w) against four foodborne pathogens and four spoilage microorganisms. The presence of the dispersing agent had a significant effect on the size of dispersed nanoZnO. Minimum size after sonication was 238 nm. An optimal dispersion condition was achieved at 200 W for 45 min of sonication in the presence of the dispersing agent. Zeta potential analysis indicated that the ZnO nanoparticle surface charge was altered by the addition of the dispersing agent and changes in pH. At tested concentrations and optimal dispersion, nanoZnO had no antimicrobial activity against *Pseudomonas aeruginosa, Lactobacillus plantarum* and *Listeria monocytogenes.* However, it did have antimicrobial activity against *Escherichia coli, Salmonella* Choleraesuis*, Staphylococcus aureus, Saccharomyces cerevisiae* and *Aspergillus niger.* Based on the exhibited antimicrobial activity of optimized nanoZnO against some foodborne pathogens and spoilage microorganisms, nanoZnO is a promising antimicrobial for food preservation with potential application for incorporation in polymers intended as food-contact surfaces.

Keywords: Zinc oxide nanoparticles, optimization, response surface methodology, dispersion process, zeta potential, antimicrobial activity.

1. INTRODUCTION

Foodborne diseases are a global public health issue. In the United States alone, it is estimated that 48 million individuals become ill, 128,000 individuals are hospitalized and 3,000 individuals die of foodborne diseases per year (CDC 2011). Foodborne diseases are an economic concern, costing $77.7 billion in the United States annually (Scharff 2012).

Worldwide, one-third of the food produced for human consumption is lost or wasted, totaling approximately 1.3 billion tons per year (Gustavsson et al. 2011), with spoilage as one of the primary causes. Approximately 25 % of all food produced globally is lost post-harvest or post-slaughter due to microbial spoilage. Contamination by spoilage microorganisms is of great concern to the food industry because the changes they cause in food products result in sensory qualities that are unacceptable to consumers, including oxidation, color modification, off-flavors and off-odors (Gram et al. 2002).

Because of these concerns, researchers are interested in new technologies to obtain alternative compounds with antimicrobial properties for food preservation. In this way, nanotechnology provides tremendous opportunities for the development of materials with new properties for use as antimicrobial agents.

These novel and enhanced material properties are the results of the increase in relative surface area that occurs as particle size decreases down to the nanoscale. Nanosize materials are also more biologically active compared to the same material in the macro or micro scale (Ren et al. 2009).

Recently, the use of inorganic materials with antimicrobial activity for biocontrol has attracted considerable attention as a new antibacterial methodology (Pal et al. 2007; Stoimenov et al. 2002).

Nanosized inorganic compounds display strong antibacterial activity at low concentrations and unique chemical and physical properties (Rai et al. 2009). A key advantage of inorganic nanoparticles is their stability under extreme conditions, such as high temperatures and pressures (Sawai 2003) and some inorganic nanoparticles are considered non-toxic because they contain minerals essential to the human body (Roselli et al. 2003).

Most antibacterial inorganic materials are metallic nanoparticles and metal oxide nanoparticles such as silver, copper, titanium oxide, and zinc oxide (ZnO) (Bradley et al. 2011; Chaudhry et al. 2008; Cioffi et al. 2005).

Among them, ZnO has emerged as a potential antimicrobial alternative, first due to studies in 1995 wherein Sawai and colleagues found that ZnO powder had antimicrobial activity against some bacteria strains (Sawai 2003; Sawai et al. 1998; Sawai et al. 1997).

Currently, ZnO has many applications in daily life, such as in drug delivery, cosmetics, and medical devices. Moreover, ZnO is one of the five zinc compounds listed as a Generally Recognized as Safe (GRAS) material by the U.S. Food and Drug Administration (21CFR182.8991) (FDA 2011). The food industry uses ZnO as a zinc supplement, which is an essential micronutrient and serves important and critical roles in growth, development, and well-being in humans and animals (Shi et al. 2008).

Methods of commercial production of ZnO nanoparticles include mechanochemical processing (MCP) and physical vapor synthesis (PVS) (Casey 2006). Both synthesis methods allow the production of nanosized ZnO, in which separated nanoparticles can be obtained. However, after synthesis, nanoparticles that initially appear as single primary particles tend to form particle collectives (Schilde et al. 2011). Hence, although the primary particles have sizes ranging from 5 to 50 nm, most commercially available nanoparticles are in the form of large agglomerates and/or aggregates (Mandzy et al. 2005).

Several applications of synthesized nanoparticles require dispersion in liquids (Müller et al. 2004). The dispersion process is critical and challenging when the primary particle size is in the nanometer scale. Suspensions of nanoparticles in liquids must present separately dispersed primary particles, or at least collectives of these materials with nanoscale aggregate sizes, because their biological or reactive characteristics strongly depend on their size.

Although previous publications have shown dispersion of ZnO nanoparticles (Chung et al. 2009; Rhodes et al. 2009; Ying et al. 2009) and some have presented the antibacterial activity of ZnO nanoparticles (Stanković et al.

2013), to the best of our knowledge none has used the central composite design and statistical approach of response surface methodology (RSM) to optimize the dispersion process.

The central composite design (CCD) has been used extensively to find the operating parameters to optimize a specific process (Zhang et al. 2009). This statistical design has emerged as an alternative to evaluating the effects of several variables and their interactions using the univariate approach, which results in a large number of experiments that are often costly and time consuming.

The CCD and RSM evaluation efficiently provides information on how the response of interest is influenced by several variables, with the main objective being to simultaneously optimize the levels of these variables to attain the best system performance (Bezerra et al. 2008). Thus, the CCD in conjunction with the RSM allows a simultaneous investigation of the main effect of the experimental variables and the effect of their interaction on the desired response, through a small number of experiments (Teófilo and Ferreira 2006).

Therefore, the statistical approach of RSM and the CCD were applied to optimize the dispersion conditions for ZnO nanoparticles in solution. Dispersed ZnO nanoparticles were characterized by size measurement and zeta potential technique. Moreover, after the dispersion conditions were satisfactorily optimized, the antimicrobial activity of ZnO nanoparticles at different concentrations (1 %, 5 % and 10 % w/w) was investigated against four foodborne pathogens (*Salmonella* Choleraesuis*, Escherichia coli*, *Staphylococcus aureus* and *Listeria monocytogenes*) and against four food-spoilage microorganisms (*Pseudomonas aeruginosa, Lactobacillus plantarum, Aspergillus niger* and *Saccharomyces cerevisiae*).

2. MATERIALS AND METHODS

2.1 Materials

In the experiments, zinc oxide (ZnO) nanoparticles purchased from Sigma-Aldrich Co. with primary particle diameters of up to 100 nm were used to

prepare ZnO nanofluids. Sodium pyrophosphate ($Na_4P_2O_7$) at 0.1 M was used as dispersing agent.

2.2 Preparation of ZnO Nanofluids

For all experiments, the dispersion process was performed using a probe sonicator (DES500 Unique, Brazil) equipped with a 4 mm diameter probe. For nanofluid preparation, ZnO nanoparticles (2.5 mg) were dispersed in 10 mL of deionized water (Millipore Milli-Q system) and combined with sodium pyrophosphate solution (0.07 g). To represent the dispersion results clearly, a measurement of average particle size was used to characterize the dispersion process.

2.3 Experimental Design

A two-level full factorial design, 2^3, was carried out aiming to investigate the effects of the independent variables on the response, y_{size} (size of ZnO nanoparticles). The variables investigated were the power of sonication, time of sonication and the presence of the dispersing agent ($Na_4P_2O_7$). Table 1 illustrates the factors under investigation and the levels of each factor used in the experimental design. The experiments were performed in a random order and in duplicate. The response measured was the size of the ZnO nanoparticles.

Table 1. Factors and levels (coded and decoded) used in the full factorial design

Factors	Levels	
	(-)	(+)
Time / min	20	50
Power / W	200	400
Dispersant agent ($Na_4P_2O_7$)	Absent	Present

To study the effects of time and power of probe sonication over an extensive range, a central composite design (CCD) was then applied. Treatment effects upon response were assessed by response surface methodology (RSM). A statistical model was built for the dispersion process and it was validated

using the analysis of variance (ANOVA). The optimized condition was chosen to obtain optimized size of ZnO nanoparticles.

All calculations and graphs in this work were performed using electronic worksheets from Microsoft® Excel 2003 according to Teófilo and Ferreira (2006).

2.4 Characterization of ZnO Nanofluid

Measurement of the median particle size of the experiment from full factorial design, CCD, as well as the ZnO nanofluid obtained at optimal dispersion conditions was performed by dynamic light scattering using the Nanophox DLS (Sympatec GmbH, Germany). Nanophox operation is based on photon cross-correlation spectroscopy (PCCS), which allows the measurement of nanoparticle size in opaque suspensions in the size range between 1 nm and a few mm. The temperature of the instrument was maintained at 25 ℃ throughout the experiment, the laser intensity was 29 %, and samples were diluted in deionized water (Millipore Milli-Q system) to obtain a count rate above 500 kcps. Each measurement was performed in triplicate.

2.5 Zeta Potential Analysis

The zeta (ζ) potential measurements were carried out in a Malvern Zetasizer Nano Series ZS (Malvern Instruments, UK) with a 633 nm red laser, through the Malvern Standard M3 technique (using Doppler electrophoresis as the basic principle of operation) using a capillary cell (DPS1060). The average of the ζ potential values was calculated by three independent measurements, each one obtained as the mean of up to 100 counts. Values of ζ potential were measured as a function of the pH to evaluate the colloidal stability, and these measurements were recorded using different concentrations of HCl or NaOH.

2.6 Transmission Electron Microscopy (TEM)

A drop of ZnO nanofluid was deposited on a copper grid. After drying, the grid was transferred to a transmission electron microscope (TEM, Zeiss EM

109) to observe dispersed nanoparticles. TEM analysis was done at the Center for Microscopy and Microanalysis at the Federal University of Viçosa.

2.7 Bacterial Cultures and the Antibacterial Activity Assay

For the antibacterial experiments, three Gram-negative bacteria (*Pseudomonas aeruginosa* ATCC 15442*, Salmonella* Choleraesuis ATCC 10708 and *Escherichia coli* ATCC 11229), as well as three Gram-positive bacteria (*Staphylococcus aureus* ATCC 6538*, Listeria monocytogenes* ATCC 15313 *and Lactobacillus plantarum* ATCC 8014), were used.

To test the antimicrobial activity of ZnO, nanoparticles were dispersed in solution using the optimal conditions at different concentrations: 1 %, 5 % and 10 % w/w. The antimicrobial activity was determined by the agar well diffusion method in accordance with the method developed by the Clinical and Laboratory Standards Institute (CLSI 2003), with some modifications.

The Gram-positive and Gram-negative bacteria, stored at -80 ℃, were grown twice in Tryptic Soy Broth and incubated for 24 h at 35 ℃. *L. plantarum* was grown in MRS broth (Difco Laboratories) and incubated under the same conditions. Then, the bacteria were streaked on non-selective culture media, Tryptic Soy Agar (TSA; Acumedia), and incubated for 24 h at 35 ℃ to isolate bacterial colonies. The isolated colonies were selected from the TSA Petri dish and suspended in saline solution (0.85 %). The bacterial suspension was adjusted to match the turbidity of the McFarland standard solution 0.5, resulting in an inoculum containing approximately $1x10^8$ UFC/mL.

Bacterial inocula of *P. aeruginosa, S.* Choleraesuis*, E. coli, L. monocytogenes* and *S. aureus* were subcultured in Mueller Hinton Agar (MHA; Difco Laboratories), while a bacterial inoculum of *L. plantarum* was subcultured in MRS agar (Difco Laboratories).

Next, wells for each concentration of ZnO nanoparticle solution were prepared by removing a portion of agar from the culture-media surface. The wells (0.8 cm in diameter) were filled with 0.1 mL of each ZnO nanoparticles solutions. One well was filled with deionized water containing sodium pyrophosphate as a negative control. Then, the Petri dishes inoculated with

the microorganism and containing ZnO nanoparticle solutions were incubated for 24 h at 34±1 ℃.

The antibacterial activity was determined by measuring the inhibition zone around each well (cm). All samples were tested in triplicate, and the experiment was repeated three times.

2.8 Fungi and Antifungal Activity Assay

Aspergillus niger, previously isolated from fruits with symptoms of black mold disease, and *Saccharomyces cerevisiae* (ATCC 9080) were used to test the antifungal activity of ZnO nanoparticles at concentrations of 1 %, 5 % and 10 % w/w.

The inoculum of *S. cerevisiae* was prepared in accordance with the Clinical and Laboratory Standards Institute (CLSI 2002), with some modifications. *S. cerevisiae* was grown twice in Sabouraud broth (Difco Laboratories) and incubated at 25 ℃ for 48 h. Then, *S. cerevisiae* was streaked on Potato Dextrose Agar (PDA; Difco Laboratories) and incubated for 48 h at 25 ℃ to isolate yeast colonies. The isolated colonies were selected from the PDA Petri dish and suspended in saline solution (0.85 %). The yeast suspension was adjusted to match the turbidity of the McFarland standard solution 0.5, resulting in an inoculum containing approximately $1x10^6$ cells/mL.

The inoculum of *S. cerevisiae* was subcultured in PDA, and wells were prepared for each concentration of ZnO nanoparticle solution by removing a portion of agar from the culture-media surface. The wells (0.8 cm in diameter) were filled with 0.1 mL of each ZnO nanoparticle solutions. The Petri dishes with *S. cerevisiae* and the ZnO nanoparticle solutions were incubated for 48 h at 25 ℃. Antifungal activity was determined by measuring the inhibition zone around each well (cm).

The inoculum of *A. niger* was prepared after incubation at 25 ℃ for 72 h. The concentration of *A. niger* inoculum was determined in the Neubauer-counting chamber, resulting in a concentration of approximately $1x10^6$ spores/mL.

An *A. niger* inoculum was subcultured in PDA, and wells for each concentration of ZnO nanoparticle solution were prepared as previously described. The wells were filled with 0.1 mL of each of ZnO nanoparticle

solutions. The Petri dishes containing *A. niger* and ZnO nanoparticle solutions were incubated for 96 h at 25 ℃. Measure ments of the inhibition zone (cm) were carried out at 24 h intervals for 96 h. All samples were tested in triplicate, and the experiment was repeated three times.

3. RESULTS AND DISCUSSION

3.1 Evaluation of the Factors Affecting ZnO Dispersion

Because little information is available on the dispersion of ZnO nanoparticles in solution, a full factorial design was initially performed to investigate the influence of the variables—time, power of sonication and the presence of the dispersing agent sodium pyrophosphate—on the size of ZnO nanoparticles (Table 2).

Table 2. Factor coded (in brackets) and decoded levels used in the full factorial design and the mean responses obtained

Assay	Time (min)	Power (W)	Dispersing agent	Nanoparticle size (nm)
7	20 (-1)	400 (+1)	Present (+1)	268
2	50 (+1)	200 (-1)	Absent (-1)	407
5	20 (-1)	200 (-1)	Present (+1)	292
3	20 (-1)	400 (+1)	Absent (-1)	506
1	20 (-1)	200 (-1)	Absent (-1)	423
8	50 (+1)	400 (+1)	Present (+1)	280
4	50 (+1)	400 (+1)	Absent (-1)	418
6	50 (+1)	200 (-1)	Present (+1)	259

The size of the ZnO nanoparticles ranged from 259 nm to 506 nm. The smallest size was obtained when the dispersion conditions were 50 min, 200 W and the presence of sodium pyrophosphate. However, the largest size of ZnO nanoparticles was obtained when the dispersion conditions were 20 min, 400 W and in the absence of sodium pyrophosphate.

The statistical analysis showed the effects of the studied factors on the response for the different conditions tested (Table 3). From these results, only the presence of sodium pyrophosphate had a significant effect on the size of ZnO nanoparticles. The negative effect of sodium pyrophosphate indicates that the presence of the dispersing agent results in decreased size of ZnO nanoparticles.

Table 3. Effects and their statistical evaluation obtained from the 2^3 full factorial design for particle size of ZnO

Factor	Effect[a]	Std. err.	*t*(14)	*p*
Mean	***356.30***	17.14	20.79	6.3×10^{-12}
T	-30.39	34.27	-0.89	0.39
P	23.50	34.27	0.69	0.50
D.A.	***-163.12***	34.27	-4.76	3.05×10^{-4}
T-P	-13.16	33.36	-0.39	0.70
T- D.A.	20.37	34.27	0.59	0.56
P- D.A.	-25.43	34.27	-0.74	0.47

T, sonication time; P, power of sonication; D.A., presence of dispersing agent. [a] Values in bold and italics are significant at α = 0.05 and 14 degrees of freedom.

When dispersing nanoparticles in solution, the main objective is to increase repulsive forces between particles to suppress or diminish nanoparticle agglomeration. Dispersing machines, such as ultrasonic homogenizers, disc mills, 3-roller mills, kneaders and stirred media mills, have been used to achieve this goal (Schilde et al. 2011). However, the use of chemical substances such as dispersing agents is not as well-studied. These agents stabilize the dispersion and prevent further agglomeration of nanoparticles after the dispersing process that otherwise results in the formation of new aggregates and in greater particles sizes.

According to Michelmore et al. (2003), dispersants increase the stability of suspensions by increasing the repulsion between particles, an effect that is achieved by increasing the electrostatic repulsive forces. This prevents the particles from approaching one another by introducing repulsive interactions.

Our results showed that the presence of sodium pyrophosphate allowed an electrostatic stabilization of ZnO nanoparticles, resulting in an increase in repulsive interactions. The stronger repulsive interactions combined with the input energy from sonication allowed the breakage of the larger agglomerates of ZnO nanoparticles and consequently a reduction in nanoparticle size.

This result is in agreement to the findings of Jiang et al. (2009), who studied the dispersion of TiO_2 for toxicological studies and observed that sodium pyrophosphate was effective in preventing further agglomeration of TiO_2 via probe sonication by suppressing particle–particle agglomeration through enhanced electrostatic repulsive forces.

According to Müller et al. (2004), input energy and time are important parameters for dispersing nanomaterials; however, no significant difference was observed between the amounts of time and the levels of sonication power tested. This finding could have resulted from the narrow range of values of these variables in which the full factorial design was tested. Only two levels for each parameter were tested: the time was 20 or 50 min and power of sonication was 200 or 400 W.

3.2 Optimization of ZnO Nanofluid Dispersion Conditions by CCD

Although the duration and the power of sonication did not initially have a significant effect on the size of ZnO nanoparticles under the tested conditions, given the results of the full factorial design, a wider range of these conditions was explored to optimize the dispersion of ZnO with the probe sonicator.

Sonication is a commonly used technique to disperse agglomerates in a solvent because it can generate a shear force on agglomerates capable of overcoming the van der Waals forces holding them together (Jiang et al. 2009). The energy transferred in the sonication oscillates the liquid, causing the nucleation and collapse of solvent bubbles, which is effective in fracturing them on the solid surfaces of agglomerates. Thus, during sonication, the breakage of agglomerates is controlled predominantly by the specific energy input resulting from the power, time and dispersion volume (Mandzy et al. 2005).

Because the dispersion volume was held constant to determine the optimal dispersal conditions, the response surface methodology (RSM) was applied using a CCD with two independent variables—time and power of sonication—to examine the effect of various combinations of these variables on the size of ZnO nanoparticles. Sizes below 306 nm were obtained in the dispersion of ZnO nanoparticles at different conditions of time and power of sonication, indicating that probe sonication caused the breakage of ZnO agglomerates. However, although primary particles of purchased ZnO had sizes <100 nm (according to the supplier), the minimum size of ZnO nanoparticles after sonication was 238 nm (Table 4).

Table 4. Coded, decoded levels and responses for the CCD in the presence of dispersing agent ($Na_4P_2O_7$)

	Runs	x_1	x_2	*ZnO size (nm)*
Factorial points	2	-1	-1	266.58
	9	1	-1	241.58
	11	-1	1	265.45
	3	1	1	238.24
Centre points	1	0	0	250.59
	6	0	0	244.84
	8	0	0	245.63
	12	0	0	241.98
	10	0	0	247.31
Axial points	7	-1.414	0	306.36
$\alpha=2^{1/2} \approx 1.414$	5	1.414	0	246.42
	12	0	-1.414	246.46
	4	0	1.414	259.07

	Experimental Domain				
Variables	-1.414	-1	0	1	1.414
x_1: ***Time / min***	11	18	35.5	53	60
x_2: ***Power / W***	148	200	325	450	502

This result was confirmed with TEM analysis, showing single small ZnO nanoparticles, as well as bigger ZnO nanoparticles, which seem to be particle collectives (Figure 1).

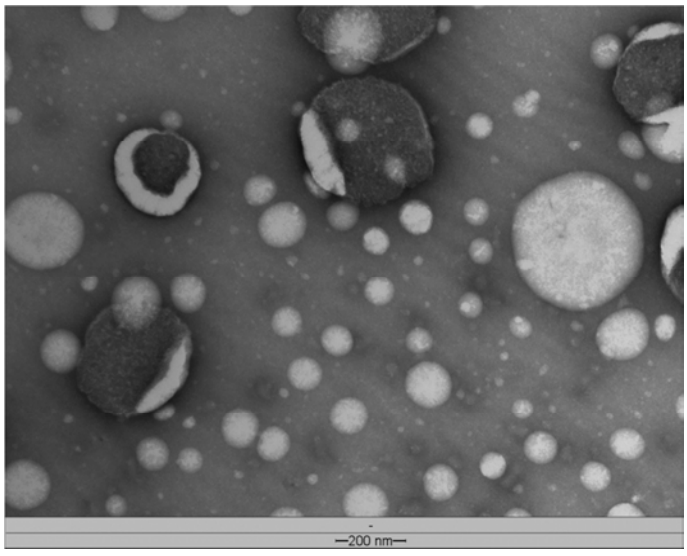

Figure 1. TEM photomicrograph of ZnO nanofluid.

Similar results were reported by Mandzy et al. (2005), who showed that regardless of the small primary size of the tested TiO_2 nanopowders, none of

them was successfully broken into their primary particles within reasonable energy levels and a reasonable time of sonication, up to 2 h.

According to the analysis of regression coefficients of the response function (Table 5), the size of ZnO nanoparticles was influenced only by the linear and quadratic effect of sonication time (p<0.05).

Table 5. Coefficient estimates from CCD and statistical analysis for the ZnO size

	ZnO Size			
	Coefficient[a]	Std. err.	*t* (4)	*p*
Mean	***246.10***	1.42	173.13	9.7×10^{-7}
T	***-17.12***	1.12	15.24	0.00011
P	1.67	1.12	1.49	0.21132
T^2	***12.26***	1.20	10.17	0.00053
P^2	0.44	1.20	0.37	0.73136
T×P	-0.55	1.59	0.35	0.74560

T, sonication time ; P, sonication power.
[a] Values in bold and italics are significant at α=0.05 with 4 degrees of freedom

The ANOVA for the model (Table 6) shows that regression was significant for the size of ZnO and the lack of fit of the regression model was not significant. In addition, the predicted versus observed values indicated a coefficient of determination (R^2) of 0.87 and the residues versus observed values showed a random behavior (results not shown).

Table 6. ANOVA results for the particle size of ZnO

Variation	Size of ZnO				
	SS[af]	df[b]	MS[c]	*F*[d]	*p*[e]
Regression	***3423***	5	684.66	9.49	0.0050
Residues	504.9	7	72.12		
Lack of fit	464.5	3	154.83	15.33	0.0116
Pure Error	40.4	4	10.10		
Total SS	3928	12			

[a] Sum of squares; [b] Degree of freedom; [c] Mean squares; [d] *F* distribution; [e] *p* value; [f] Bold and italic values are significant at α = 0.01.

The linear regression coefficient for sonication time was negative, indicating that a longer time allows for better ZnO dispersion, independent of the sonication power used. This behavior is valid until a critical time is reached,

as observed in the response surface between 40 and 50 min (Figure 2). Beyond this critical point (>55 min), the ZnO nanoparticles presented a reagglomeration behavior, increasing in size.

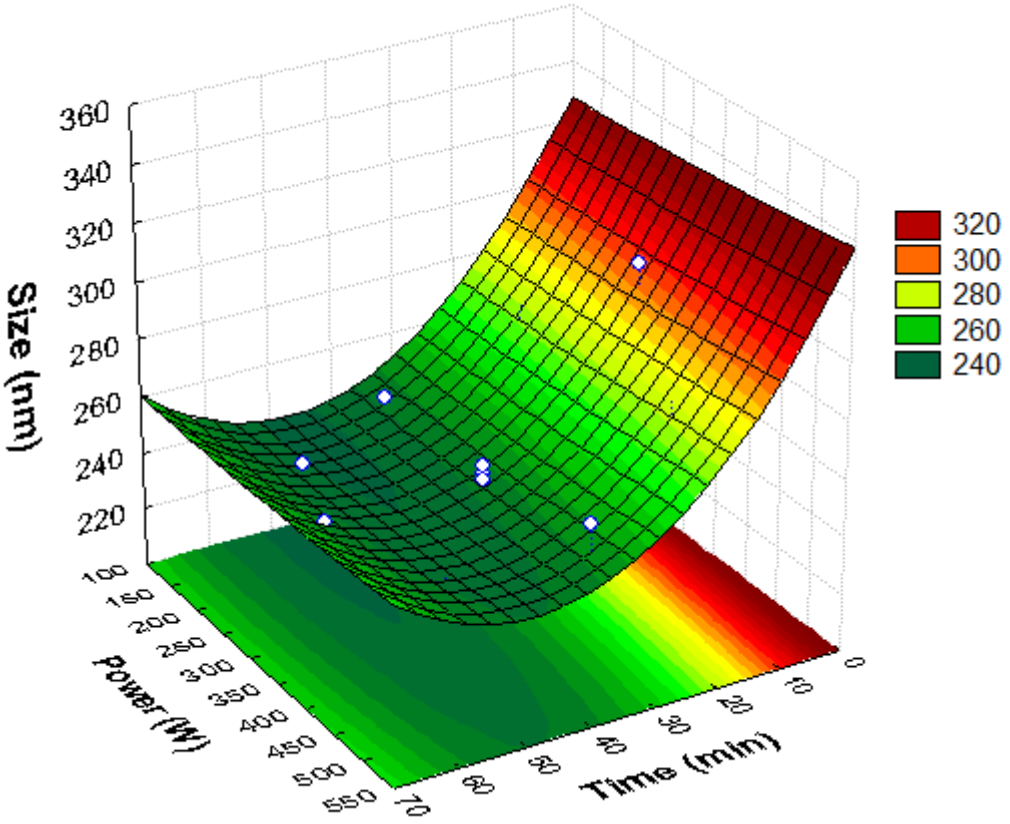

Figure 2. Response surface of ZnO particle size as a function of time and power of sonication.

Moreover, the significant quadratic coefficient for sonication time indicated the ZnO size decreases quadratically as the time increases until 55 min. However, ZnO size increases quadratically with a time longer than 55 min.

The reagglomeration of ZnO nanoparticles is the result of excessively high stress intensity. According to Müller et al. (2004), long times of sonication and high stress intensity should be avoided because energy is wasted and, in particular, because agglomeration becomes favored.

This behavior has been already reported by Mandzy et al. (2005), who dispersed TiO_2 nanoparticles in aqueous solution and observed that after a rapid initial size reduction, continued sonication led to insignificant reduction and even reagglomeration of the particles. Additionally, Jiang et al. (2009) found that for the dispersion of TiO_2 nanoparticles in deionized water, probe

sonication can not only break agglomerates locally but can also promote agglomeration due to enhanced particle–particle interactions. Thus, increasing sonication time resulted in an initial decrease of nanoparticle size followed by an increase in size.

However, the power of sonication did not significantly influence the size reduction of ZnO nanoparticles (p>0.05); in addition, the interaction between time and power of sonication was not significant (p>0.05).

The response surface shows a significant decrease in the size of ZnO nanoparticles with increasing sonication time until the critical point, which is independent of sonication power. Based on these data, an optimal time of sonication is in the range between 40 to 50 min, and the power of choice is close to low values studied because this variable did not have a significant effect on the size of the ZnO nanoparticles. Hence, a possible set of conditions to obtain a minimum size of ZnO is at 200 W for 45 min of sonication in the presence of the dispersing agent.

3.3 Zeta Potential

To study the influence of the dispersing agent ($Na_4P_2O_7$) on the stability of ZnO nanoparticle solutions, values of the zeta potential at different pHs were measured. The adsorption of pyrophosphate ions onto the surface of ZnO nanoparticles changed the zeta (ζ) potential from a positive value (44.1 ± 4.03 mV) to a negative value (-14 ± 2.78 mV) at pH 6.6, while at pH 7.7, the adsorption of pyrophosphate ions resulted in a ζ potential value of -35.9 ± 5.78 mV (Figure 3).

In addition to the change on the surface charge of ZnO nanoparticles due to the presence of sodium pyrophosphate, the surface charge of ZnO nanoparticles is also altered by changing the pH of the solution. At pH values below 6, ZnO nanoparticles had a less negative surface charge, represented by small absolute values of zeta potential. Conversely, at high pH values, a more negative surface charge is observed.

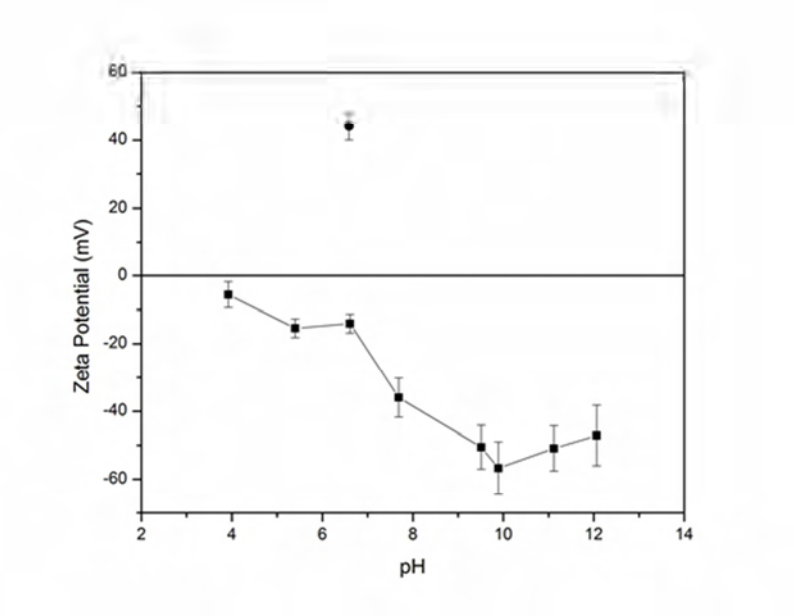

Figure 3. Zeta potential of ZnO nanoparticles as a function of pH in the presence (■) and in the absence (●) of sodium pyrophosphate.

The isoelectric point (IEP) is the pH value at which the nanoparticle carries no electrical charge or the negative and positive charges are equal, and the zeta potential is equal to zero. The IEP of neat ZnO is 9.5 (Wei 2006; Khan et al. 2008). However in this work, the zeta potential measured at different pH values became negative in the presence of sodium pyrophosphate, indicating that the IEP of ZnO nanoparticles corresponds to a pH below 4.

This result is in agreement with the findings of Leong et al. (1993), who previously showed that the use of anionic additives, such as sodium pyrophosphate, lowered the IEP of a zirconia suspension. Huynh and Jenkins (2001) have shown that sodium pyrophosphate and other phosphates were adsorbed at the solid-aqueous solution interface of the pigment dispersion rutile titania, which caused the IEP of the pigment particles to shift to lower pH values.

Moreover, these results showed that above pH 6.6 (approximate neutrality), ZnO nanoparticles presented an absolute value of zeta potential higher than -30 mV, which is an indicator of a stable dispersion. This finding is in agreement with the results in section 3.2, where it was shown that the dispersion of ZnO nanoparticles is highly affected by the addition of sodium pyrophosphate.

Polyphosphate compounds, which are highly negatively charged chemicals, have been used to keep minerals in suspension during industrial processing (Papo et al. 2002). Polyphosphates act as dispersants by altering the surface charges of particles by a significant reduction in the zeta potential of the suspended particles (making ζ value more negative). This process is known as electrostatic stabilization, and it can be achieved by the addition of anionic adsorbates, which act directly on the surface of nanoparticles and change their characteristics.

When sodium pyrophosphate is completely dissociated, it results in sodium cations and pyrophosphate anions (equation 2), and the anions are likely to be attracted by ZnO nanoparticles.

$$Na_4P_2O_7\,(aq) \leftrightarrow 4Na^+\,(aq) + P_2O_7^{4-}(aq) \qquad (2)$$

The attracted anions shift the charge in the electrical double layer surrounding ZnO nanoparticles, which results in the increase of the electrostatic repulsive force and in the increase of the absolute value of the zeta potential, allowing stable dispersion of ZnO nanoparticles (Figure 4).

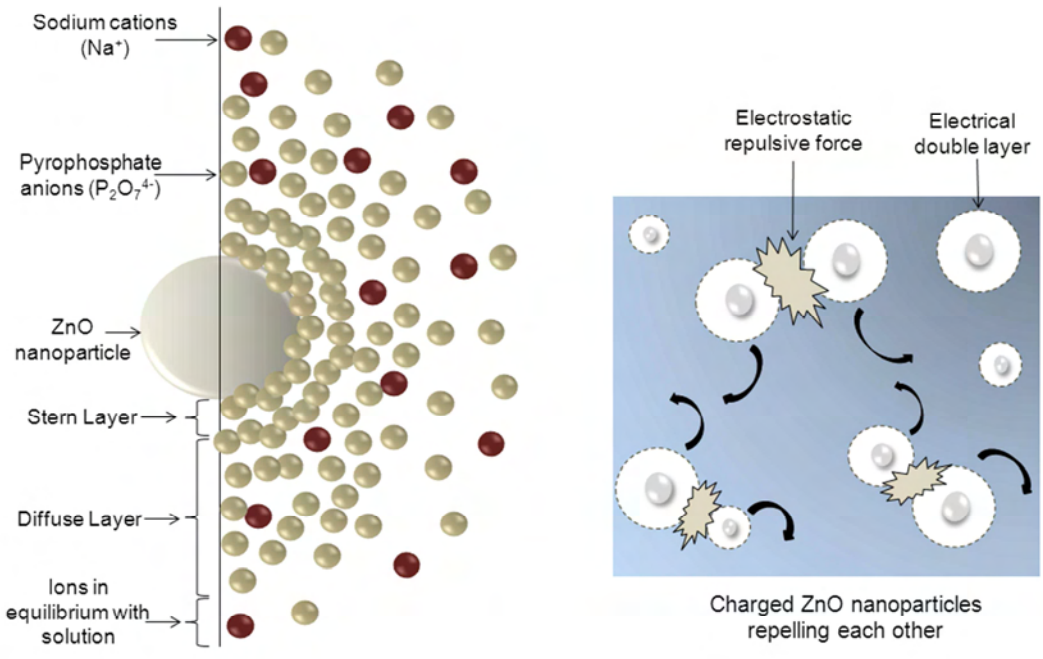

Figure 4. Schematic representation of electrostatic stabilization of ZnO nanoparticles by sodium pyrophosphate

Our results are in agreement with the findings of Jiang et al. (2009), who demonstrated the electrostatic stabilization of TiO_2 nanoparticles as a result of the addition of sodium pyrophosphate. This addition increased the nanoparticle surface charge and, in turn, increased the electrostatic repulsive force between particles.

3.4 Evaluation of Antibacterial Activity

The diameters of the inhibition zones for *E. coli, S.* Choleraesuis, and *S. aureus* increased when the concentration of the ZnO nanoparticles increased (Figure 5).

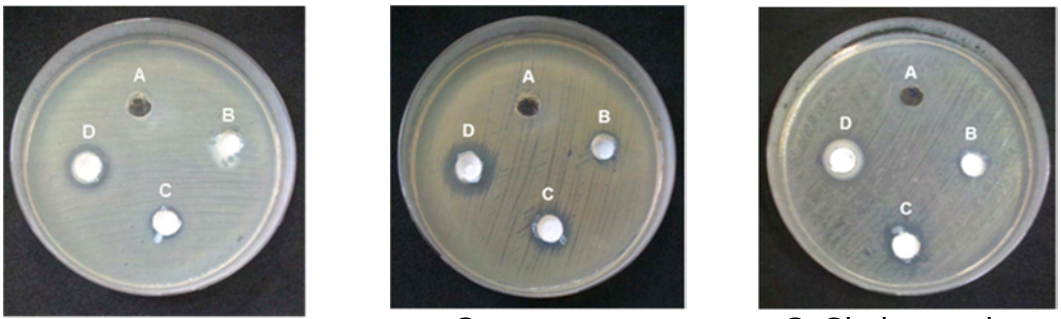

E. coli *S. aureus* *S.* Choleraesuis

Figure 5. Antimicrobial activity of ZnO nanoparticles at 0 % (A), 1 % (B), 5 % (C) and 10 % (D) against foodborne pathogens.

The antimicrobial activity of ZnO nanoparticles at concentrations of 1 % was statistically significant ($p<0.05$) from 5 % and 10 % for *E. coli*. Moreover, the antimicrobial activity of 10 % ZnO nanoparticles solution against *S.* Choleraesuis and *S. aureus* were statistically significant ($p<0.05$) from the other treatments, while 1 % and 5 % ZnO nanoparticle solutions had no statistically significant difference in their antimicrobial activity against these foodborne pathogens (Table 7).

Table 7. Antimicrobial activity of ZnO nanoparticles in solution

Treatment (w/w)	Inhibition zone at specified concentration (cm±standard deviation)*			
	Control	1 %	5 %	10 %
E. coli	0.0±0.0[b]	0.0±0.0[b]	1.5±0.2[a]	1.8±0.3[a]
P. aeruginosa	0.0±0.0	0.0±0.0	0.0±0.0	0.0±0.0
S. Choleraesuis	0.0±0.0[c]	1.0±0.0[b]	1.2±0.1[b]	1.4±0.1[a]
S. aureus	0.0±0.0[c]	1.0±0.1[b]	1.0±0.1[b]	1.5±0.2[a]
L. plantarum	0.0±0.0	0.0±0.0	0.0±0.0	0.0±0.0
L. monocytogenes	0.0±0.0	0.0±0.0	0.0±0.0	0.0±0.0

*Values in the same row bearing the same letter are not significantly different according to Tukey test (p>0.05).Values of inhibition zone include the well diameter (0.8 cm).

However, the ZnO nanoparticles at different concentrations did not display antimicrobial activity against *P. aeruginosa, L. plantarum* or *L. monocytogenes*. Instead, these microorganisms showed a reduction in the density of colonies adjacent to the well filled with 10 % ZnO nanoparticles. Our results are in agreement with previously published works that have shown antimicrobial activity of ZnO nanoparticles against *E. coli* and *S. aureus* (Emami-Karvani and Chehrazi 2011; Adams et al. 2006; Premanathan et al. 2011; Reddy et al. 2007). These works have noted that Gram-positive bacteria have a higher susceptibility to ZnO nanoparticles than Gram-negative bacteria. Conversely, the higher susceptibility of *E. coli* to ZnO nanoparticles compared to that of *S. aureus* has also been reported (Applerot et al. 2009; Yamamoto 2001). However, no differences in the antimicrobial activity of the ZnO nanoparticles against *S. aureus* and *E. coli* were observed at the tested concentrations.

The difference in susceptibility between Gram-positive and Gram-negative bacteria may be due to changes in the interaction mechanisms of ZnO with the bacterial membrane. Gram-positive bacteria have much thicker peptidoglycan cell walls compared with Gram-negative bacteria, which results in a decreased susceptibility to membrane damage induced by ZnO nanoparticles. However, Nair et al. (2009) suggested that if the mechanism of action of ZnO nanoparticles is the generation of reactive oxygen species (ROS), these susceptibility differences are likely related to intracellular events because the membranes of Gram-positive and Gram-negative bacteria are equally permeable to ROS.

Although several theories have been proposed to explain the differences in susceptibility between Gram-negative and Gram-positive bacteria, more studies are necessary to clarify the sensitivities of these two types of microorganisms to ZnO nanoparticles.

The antibacterial activity of ZnO nanoparticles against *P. aeruginosa* has been reported (Jayaseelan et al. 2012; Premanathan et al. 2011); however, no significant growth inhibition was detected.

Several factors can affect the antimicrobial activity of ZnO nanoparticles, among them the size of nanoparticles and thus the surface area (Espitia et al. 2012). In this way, Jones et al. (2008) observed that reduced size of ZnO nanoparticles may have a greater impact on their activity because their efficacy in inhibiting bacterial growth is greater when the particle size is smaller (~8 nm diameter). In this work, the lack of antibacterial activity of ZnO nanoparticles at the tested concentrations against *P. aeruginosa, L. plantarum* and *L. monocytogenes* could have resulted from the larger size of ZnO nanoparticles used (~235 nm).

3.5 Evaluation of Antifungal Activity

The antifungal activity of ZnO nanoparticles against *S. cerevisiae* was also examined. Solutions of 1 %, 5 % and 10 % ZnO nanoparticle concentrations gave inhibition zones of 1.3±0.1 cm, 1.4±0.2 cm and 1.5±0.2 cm in diameter, respectively. The sizes of the inhibition zones were statistically equal among treatments (Figure 7).

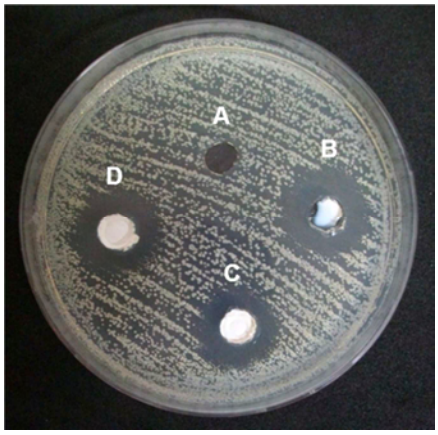

Figure 7. Antifungal activity of ZnO nanoparticles at 0 % (A), 1 % (B), 5 % (C) and 10 % (D) against *S. cerevisiae.*

Our results are in agreement with the findings of Kasemets et al. (2009), who reported the antifungal activity of ZnO nanoparticles (50-70 nm) against *S. cerevisiae*. Kasemets proposed that the release of Zn^{2+} antimicrobials ions in high concentrations caused the toxicity of ZnO against this yeast.

Low concentrations of solubilized Zn^{2+} can trigger a relatively high tolerance in the microorganism. According to Devirgiliis et al. (2004), at low concentrations, labile Zn^{2+} can be rapidly accumulated in dynamic vesicular compartments (vacuoles and zincosomes). These compartments are an important cellular defense system used to buffer against both zinc excess and zinc deficiency. However in this experiment, even the lowest tested concentration (1 % ZnO nanoparticles) demonstrated antifungal activity, which indicates a high susceptibility of this microorganism to ZnO nanoparticles.

Additionally, ZnO nanoparticles at different concentrations showed antifungal activity against *A. niger* for up to three days (Figure 8). However, the antifungal activity was not maintained after four days of incubation.

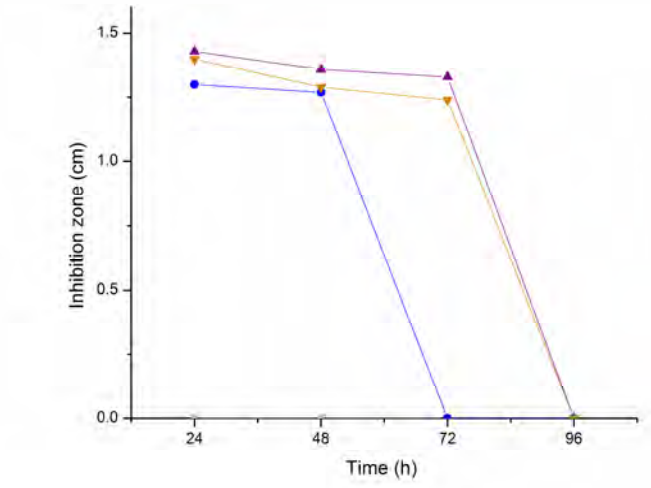

Figure 8. Antifungal activity of ZnO nanoparticles at 0 % (■), 1 % (●), 5 % (▲) and 10 % (▼) against *A. niger.*

In addition, all tested concentrations differed significantly from the control after 24 h and 48 h of incubation. After 72 h of incubation, the 1 % ZnO

nanoparticle solutions lost their antifungal activity, showing mycelia growth and spore production in the areas previously observed as inhibition zones. However, the 5 % and 10 % ZnO nanoparticle solutions maintained their activity against *A. niger*. The inhibition zones of the 5 % ZnO nanoparticle wells were larger than the inhibition zones created around the 10 % ZnO nanoparticle wells, but no significant difference was observed between the treatments.

The antifungal activity of ZnO nanoparticles against other filamentous fungi has been previously reported. He et al. (2011) noted the significant antifungal activity of ZnO nanoparticles (70 nm) against *Botrytis cinerea* and *Penicillium expansum*; both of these fungi cause severe postharvest fruit diseases. Moreover, ZnO nanoparticles have shown antifungal activity against the plant pathogen fungi *Pythium debarynum* and *Sclerotium rolfsii,* causing a significant decrease in the fungal growth that corresponds to increases in the concentration of ZnO nanoparticles (Sharma et al. 2011).

4. CONCLUSION

Using a full factorial design, the influences of time, the power of sonication and the presence of the dispersant agent (sodium pyrophosphate) on the size of ZnO nanoparticles were investigated. The presence of sodium pyrophosphate had a significant effect on the size of the dispersed ZnO nanoparticles. The effects of various combinations of time and power of sonication on the size of ZnO nanoparticles were studied by RSM using a CCD, analyzing time and the power of sonication as two independent variables. As a result, the minimum size of ZnO nanoparticles obtained was 238 nm, produced by 200 W sonication for 45 min in the presence of the dispersing agent.

Additionally, the zeta potential analysis indicated that the charge on the ZnO nanoparticle surface was altered by the addition of sodium pyrophosphate and by pH changes in the solution.

The optimal dispersion of the ZnO nanoparticles at the tested concentrations showed antibacterial activity against *E. coli, S.* Choleraesuis and *S. aureus,* producing a larger inhibition zone when the ZnO nanoparticle concentration

was increased. However, the ZnO nanoparticles did not display antimicrobial activity against *P. aeruginosa, L. plantarum* and *L. monocytogenes*. Optimal dispersions of the ZnO nanoparticles at the tested concentrations showed antifungal activity against *S. cerevisiae*. Additionally, the ZnO nanoparticle solutions at 5 % and 10 % demonstrated antifungal activity against *A. niger* for up to three days.

Therefore, the optimal dispersion of ZnO nanoparticles results in antimicrobial activity against foodborne pathogens and spoilage microorganisms, thus ZnO nanoparticles are considered a promising antimicrobial agent for food preservation with applications for incorporation in biopolymers intended as food contact surfaces.

ACKNOWLEDGEMENTS

The authors gratefully acknowledge Mr. Nicholas J. Walker for providing language help and writing assistance. Financial support for this research was provided by a doctoral scholarship from Coordenação de Aperfeiçoamento de Pessoal de Nível Superior (CAPES) and a grant from Conselho Nacional de Desenvolvimento Científico e Tecnológico (CNPq). Technical support for this research work was provided by INCT–Nanobiofar project. We appreciate the help with the stereoscopic microscope of Gilberto de Oliveira Mendes from the Microbiology Department at Federal University of Viçosa.

5. REFERENCES

Adams LK, Lyon DY, Alvarez PJJ (2006) Comparative eco-toxicity of nanoscale TiO_2, SiO_2, and ZnO water suspensions. Water Res 40 (19):3527-3532. doi:10.1016/j.watres.2006.08.004

Applerot G, Lipovsky A, Dror R, Perkas N, Nitzan Y, Lubart R, Gedanken A (2009) Enhanced antibacterial activity of nanocrystalline ZnO due to increased ROS-mediated cell injury. Adv Funct Mater 19 (6):842-852. doi:10.1002/adfm.200801081

Bezerra MA, Santelli RE, Oliveira EP, Villar LS, Escaleira LA (2008) Response surface methodology (RSM) as a tool for optimization in analytical chemistry. Talanta 76 (5):965-977. doi:10.1016/j.talanta.2008.05.019

Bradley EL, Castle L, Chaudhry Q (2011) Applications of nanomaterials in food packaging with a consideration of opportunities for developing countries. Trends Food Sci Technol 22 (11):604-610. doi:10.1016/j.tifs.2011.01.002

Casey P (2006) Nanoparticle technologies and applications. In: Hannink RHJ, Hill AJ (eds) Nanostructure control of materials. Woodhead Publishing Limited, Cambridge, UK, pp 1-27

CDC (2011) 2011 Estimates of Foodborne Illness in the United States. Center for disease control and prevention. http://www.cdc.gov/Features/dsFoodborneEstimates/. Accessed 6 May 2011

Chaudhry Q, Scotter M, Blackburn J, Ross B, Boxall A, Castle L, Aitken R, Watkins R (2008) Applications and implications of nanotechnologies for the food sector. Food Additives & Contaminants: Part A 25 (3):241-258. doi:10.1080/02652030701744538

Chung SJ, Leonard JP, Nettleship I, Lee JK, Soong Y, Martello DV, Chyu MK (2009) Characterization of ZnO nanoparticle suspension in water: Effectiveness of ultrasonic dispersion. Powder Technol 194 (1–2):75-80. doi:10.1016/j.powtec.2009.03.025

Cioffi N, Torsi L, Ditaranto N, Tantillo G, Ghibelli L, Sabbatini L, Bleve-Zacheo T, D'Alessio M, Zambonin PG, Traversa E (2005) Copper nanoparticle/polymer composites with antifungal and bacteriostatic properties. Chem Mater 17 (21):5255-5262. doi:10.1021/cm0505244

CLSI (2002) Reference method for broth dilution antifungal susceptibility testing of yeast. Approved standard M27-A2. Clinical and Laboratory Standards Institute, Wayne, PA

CLSI (2003) Performance standards for antimicrobial disk susceptibility tests. Approved Standard M2-A8. Clinical and Laboratory Standards Institute, Wayne, PA

Devirgiliis C, Murgia C, Danscher G, Perozzi G (2004) Exchangeable zinc ions transiently accumulate in a vesicular compartment in the yeast *Saccharomyces cerevisiae*. Biochem Biophys Res Commun 323 (1):58-64. doi:10.1016/j.bbrc.2004.08.051

Emami-Karvani Z, Chehrazi P (2011) Antibacterial activity of ZnO nanoparticle on gram-positive and gram-negative bacteria. Afr J Microbiol Res 5 (12):1368-1373. doi:10.5897/AJMR10.159

Espitia P, Soares Nd, Coimbra J, de Andrade N, Cruz R, Medeiros E (2012) Zinc Oxide Nanoparticles: Synthesis, Antimicrobial Activity and Food Packaging Applications. Food Bioprocess Tech 5 (5):1447-1464. doi:10.1007/s11947-012-0797-6

FDA (2011) Part 182 - Substances generally recognized as safe. Food and drug administration. http://ecfr.gpoaccess.gov/cgi/t/text/text-idx?c=ecfr&sid=786bafc6f6343634fbf79fcdca7061e1&rgn=div5&view=text&node=21:3.0.1.1.13&idno=21#21:3.0.1.1.13.9. Accessed 28 March 2011

Gram L, Ravn L, Rasch M, Bruhn JB, Christensen AB, Givskov M (2002) Food spoilage—interactions between food spoilage bacteria. Int J Food Microbiol 78 (1–2):79-97. doi:10.1016/s0168-1605(02)00233-7

Gustavsson J, Cederberg C, Sonesson U (2011) Global food losses and food waste: extent, causes and prevention. The Swedish Institute for Food and Biotechnology (SIK), Rome, Italy.

He L, Liu Y, Mustapha A, Lin M (2011) Antifungal activity of zinc oxide nanoparticles against *Botrytis cinerea* and *Penicillium expansum*. Microbiol Res 166 (3):207-215. doi:10.1016/j.micres.2010.03.003

Huynh L, Jenkins P (2001) A rheological and electrokinetic investigation of the interactions between pigment particles dispersed in aqueous solutions of short-chain phosphates. Colloids Surf Physicochem Eng Aspects 190 (1):35-45. doi:10.1016/s0927-7757(01)00663-x

Jayaseelan C, Rahuman AA, Kirthi AV, Marimuthu S, Santhoshkumar T, Bagavan A, Gaurav K, Karthik L, Rao KVB (2012) Novel microbial route to synthesize ZnO nanoparticles using *Aeromonas hydrophila* and their activity against pathogenic bacteria and fungi. Spectrochim Acta, Pt A: Mol Biomol Spectrosc 90 (0):78-84. doi:10.1016/j.saa.2012.01.006

Jiang J, Oberdörster G, Biswas P (2009) Characterization of size, surface charge, and agglomeration state of nanoparticle dispersions for toxicological studies. J Nanopart Res 11 (1):77-89. doi:10.1007/s11051-008-9446-4

Jones N, Ray B, Ranjit KT, Manna AC (2008) Antibacterial activity of ZnO nanoparticle suspensions on a broad spectrum of microorganisms. FEMS Microbiol Lett 279 (1):71-76. doi:10.1111/j.1574-6968.2007.01012.x

Kasemets K, Ivask A, Dubourguier H-C, Kahru A (2009) Toxicity of nanoparticles of ZnO, CuO and TiO_2 to yeast *Saccharomyces cerevisiae*. Toxicol In Vitro 23 (6):1116-1122. doi:10.1016/j.tiv.2009.05.015

Khan R, Kaushik A, Solanki PR, Ansari AA, Pandey MK, Malhotra BD (2008) Zinc oxide nanoparticles-chitosan composite film for cholesterol biosensor. Anal Chim Acta 616 (2):207-213. doi:10.1016/j.aca.2008.04.010

Leong YK, Scales PJ, Healy TW, Boger DV, Buscall R (1993) Rheological evidence of adsorbate-mediated short-range steric forces in concentrated dispersions. J Chem Soc, Faraday Trans 89 (14):2473-2478

Mandzy N, Grulke E, Druffel T (2005) Breakage of TiO_2 agglomerates in electrostatically stabilized aqueous dispersions. Powder Technol 160 (2):121-126. doi:10.1016/j.powtec.2005.08.020

Michelmore A, Jenkins P, Ralston J (2003) The interaction of linear polyphosphates with zincite surfaces. Int J Miner Process 68 (1-4):1-16. doi:10.1016/s0301-7516(01)00085-0

Müller F, Peukert W, Polke R, Stenger F (2004) Dispersing nanoparticles in liquids. Int J Miner Process 74, Supplement (0):S31-S41. doi:10.1016/j.minpro.2004.07.023

Nair S, Sasidharan A, Divya Rani V, Menon D, Nair S, Manzoor K, Raina S (2009) Role of size scale of ZnO nanoparticles and microparticles on toxicity toward bacteria and osteoblast cancer cells. J Mater Sci Mater Med 20 (0):235-241. doi:10.1007/s10856-008-3548-5

Pal S, Tak YK, Song JM (2007) Does the antibacterial activity of silver nanoparticles depend on the shape of the nanoparticle? A study of the Gram-negative bacterium *Escherichia coli*. Appl Environ Microbiol 73 (6):1712-1720. doi:10.1128/aem.02218-06

Papo A, Piani L, Ricceri R (2002) Sodium tripolyphosphate and polyphosphate as dispersing agents for kaolin suspensions: rheological characterization. Colloids Surf Physicochem Eng Aspects 201 (1-3):219-230. doi:10.1016/s0927-7757(01)01024-x

Premanathan M, Karthikeyan K, Jeyasubramanian K, Manivannan G (2011) Selective toxicity of ZnO nanoparticles toward Gram-positive bacteria and cancer cells by apoptosis through lipid peroxidation. Nanomed Nanotechnol Biol Med 7 (2):184-192. doi:10.1016/j.nano.2010.10.001

Rai M, Yadav A, Gade A (2009) Silver nanoparticles as a new generation of antimicrobials. Biotechnol Adv 27 (1):76-83. doi:10.1016/j.biotechadv.2008.09.002

Reddy KM, Feris K, Bell J, Wingett DG, Hanley C, Punnoose A (2007) Selective toxicity of zinc oxide nanoparticles to prokaryotic and eukaryotic systems. Appl Phys Lett 90 (21):213902. doi:10.1063/1.2742324

Ren G, Hu D, Cheng EWC, Vargas-Reus MA, Reip P, Allaker RP (2009) Characterisation of copper oxide nanoparticles for antimicrobial applications. Int J Antimicrob Agents 33 (6):587-590

Rhodes R, Asghar S, Krakow R, Horie M, Wang Z, Turner ML, Saunders BR (2009) Hybrid polymer solar cells: From the role colloid science could play in bringing deployment closer to a study of factors affecting the stability of non-aqueous ZnO dispersions. Colloids Surf Physicochem Eng Aspects 343 (1–3):50-56. doi:10.1016/j.colsurfa.2009.01.028

Roselli M, Finamore A, Garaguso I, Britti MS, Mengheri E (2003) Zinc oxide protects cultured enterocytes from the damage induced by *Escherichia coli*. J Nutr 133 (12):4077-4082

Sawai J (2003) Quantitative evaluation of antibacterial activities of metallic oxide powders (ZnO, MgO and CaO) by conductimetric assay. J Microbiol Methods 54 (2):177-182. doi:10.1016/s0167-7012(03)00037-x

Sawai J, Kojima H, Ishizu N, Itoh M, Igarashi H, Sawaki T, Shimizu M (1997) Bactericidal action of magnesium oxide powder. J Inorg Biochem 67 (1-4):443-443. doi:10.1016/s0162-0134(97)80303-0

Sawai J, Shoji S, Igarashi H, Hashimoto A, Kokugan T, Shimizu M, Kojima H (1998) Hydrogen peroxide as an antibacterial factor in zinc oxide powder slurry. J Ferment Bioeng 86 (5):521-522. doi:10.1016/s0922-338x(98)80165-7

Scharff RL (2012) Economic Burden from Health Losses Due to Foodborne Illness in the United States. J Food Prot 75 (1):123-131. doi:10.4315/0362-028x.jfp-11-058

Schilde C, Mages-Sauter C, Kwade A, Schuchmann HP (2011) Efficiency of different dispersing devices for dispersing nanosized silica and alumina. Powder Technol 207 (1-3):353-361. doi:10.1016/j.powtec.2010.11.019

Sharma D, Sharma S, Kaith BS, Rajput J, Kaur M (2011) Synthesis of ZnO nanoparticles using surfactant free in-air and microwave method. Appl Surf Sci 257 (22):9661-9672. doi:10.1016/j.apsusc.2011.06.094

Shi L, Zhou J, Gunasekaran S (2008) Low temperature fabrication of ZnO-whey protein isolate nanocomposite. Mater Lett 62 (28):4383-4385. doi:10.1016/j.matlet.2008.07.038

Stanković A, Dimitrijević S, Uskoković D (2013) Influence of size scale and morphology on antibacterial properties of ZnO powders hydrothemally synthesized using different surface stabilizing agents. Colloids Surf B Biointerfaces 102 (0):21-28. doi:10.1016/j.colsurfb.2012.07.033

Stoimenov PK, Klinger RL, Marchin GL, Klabunde KJ (2002) Metal oxide nanoparticles as bactericidal agents. Langmuir 18 (17):6679-6686. doi:10.1021/la0202374

Teófilo RF, Ferreira MMC (2006) Quimiometria II: planilhas eletrônicas para cálculos de planejamentos experimentais, um tutorial. Quim Nova 29:338-350

Wei A (2006) Enzymatic glucose biosensor based on ZnO nanorod array grown by hydrothermal decomposition. Appl Phys Lett 89 (12):123902

Yamamoto O (2001) Influence of particle size on the antibacterial activity of zinc oxide. Int J Inorg Mater 3 (7):643-646. doi:10.1016/s1466-6049(01)00197-0

Ying K-L, Hsieh T-E, Hsieh Y-F (2009) Colloidal dispersion of nano-scale ZnO powders using amphibious and anionic polyelectrolytes. Ceram Int 35 (3):1165-1171. doi:10.1016/j.ceramint.2008.05.014

Zhang J, Fan Y, Smith E (2009) Experimental design for the optimization of lipid nanoparticles. J Pharm Sci 98 (5):1813-1819. doi:10.1002/jps.21549

ARTIGO CIENTÍFICO 4

PROPRIEDADES FÍSICO-MECÂNICAS E ANTIMICROBIANA DE FILMES NANOCOMPÓSITOS INCORPORADOS COM NANOPARTÍCULAS DE ZnO E PEDIOCINA

Resumo

Este trabalho objetivou desenvolver filmes nanocompósitos a base de metil celulose incorporados com pediocina e nanopartículas de óxido de zinco (nanoZnO), utilizando o delineamento estatístico composto central e a metodologia de superfície de resposta para análise de dados. Foram avaliadas as propriedades físico-mecânicas dos filmes (cristalografia por difração de raios X, resistência mecânica, inchamento, cor, características microscópicas e estabilidade térmica), bem como a sua atividade antimicrobiana contra *Staphylococcus aureus* e *Listeria monocytogenes*. A incorporação de nanoZnO e pediocina afetou a cristalinidade dos filmes. Os antimicrobianos afetaram significativamente a deformação na ruptura dos filmes. A incorporação de pediocina resultou em filmes amarelados, mas a presença de nanoZnO equilibrou este efeito, resultando em filmes com coloração esbranquiçada. O inchamento dos filmes diminuiu em relação ao controle. Os filmes com altas concentrações de NanoZnO apresentaram estabilidade térmica melhorada. Os filmes nanocompósitos apresentaram atividade contra os micro-organismos testados.

Palavras-chave: Atividade antimicrobiana, caracterização de embalagens, embalagens de alimentos, filmes nanocompósitos, nanopartículas de ZnO, pediocina.

Physical-mechanical and antimicrobial properties of nanocomposite films with pediocin and ZnO nanoparticles

Abstract

This work aimed to develop nanocomposite films of methyl cellulose (MC) incorporated with pediocin and zinc oxide nanoparticles (nanoZnO) using the central composite design and response surface methodology. This study evaluated film physical-mechanical properties, including crystallography by X-ray diffraction, mechanical resistance, swelling and color properties, microscopy characterization, thermal stability, as well as antimicrobial activity against *Staphylococcus aureus* and *Listeria monocytogenes*. NanoZnO and pediocin affected the crystallinity of MC. Load at break and tensile strength at break did not differ among films. NanoZnO and pediocin significantly affected the elongation at break. Pediocin produced yellowish films, but nanoZnO balanced this effect, resulting in a whitish coloration. NanoZnO exhibited good intercalation in MC and the addition of pediocin in high concentrations resulted in crater-like pits in the film surfaces. Swelling of films diminished significantly compared to control. Higher concentrations of NanoZnO resulted in enhanced thermal stability. Nanocomposite films presented antimicrobial activity against tested microorganisms.

Keywords: ZnO nanoparticles, pediocin, food packaging, nanocomposite films, foodborne pathogens, packaging characterization.

1. INTRODUCTION

World use of plastics has increased enormously, compounding the problem of waste contamination. In the United States alone, increased plastic production resulted in 31 million tons of plastic waste in 2010, representing 12.4 % of total Municipal Solid Waste (MSW)—commonly known as trash or garbage (EPA, 2011).

As plastic products continue to increase, they bring a number of environmental concerns. Such concerns have created increased interest in biopolymers research, due to their biodegradability.

Methyl cellulose (MC) has become an attractive alternative, due its ability to allow the development of environmental friendly products, its large availability in nature, low cost and easy processing. This biodegradable carbohydrate polymer is a modified type of cellulose and is the most abundant biopolymer in nature (Rimdusit et al., 2008).

However, biodegradable natural packaging materials usually have poor mechanical, barrier and thermal characteristics (Tunç & Duman, 2011).

Research has shown that new materials with improved properties can be developed using nanotechnology. These new materials are known as nanocomposites, which are hybrid materials where the filler incorporated in the polymeric matrix has at least one dimension in the nanometer scale (Espitia et al., 2012).

Polymer/clay nanocomposites have been one of the most widely studied nanocomposites and research has shown that the developed nanocomposites often exhibit enhanced thermal stability, physical-mechanical and barrier properties compared to neat polymer matrix (Arora & Padua, 2010).

However, studies dealing with nanocomposites of MC are scarce, and few have focused on the application of biopolymer nanocomposites as active packaging materials for food preservation (Lagarón & Fendler, 2009).

Antimicrobial packaging is a type of active packaging which interacts with the product or the headspace inside to reduce, inhibit or retard the growth of microorganisms that may be present on food surfaces (Soares et al., 2009).

In order to develop nanocomposite films for antimicrobial food packaging, zinc oxide (ZnO) nanoparticles and pediocin were incorporated into the MC matrix.

ZnO is an inorganic compound widely used in everyday applications, is currently listed as a generally recognized as safe (GRAS) material by the Food and Drug Administration (21CFR182.8991) and has previously shown antimicrobial activity against foodborne pathogens (Espitia et al., 2012; FDA, 2011).

Moreover, pediocin is a bacteriocin, also considered a bioactive peptide, which is ribosomally synthesized by *Pediococcus acidilactici* and has the

ability to kill closely related bacteria. Pediocin has many applications in food preservation due to its activity in controlling *Listeria monocytogenes*, a foodborne pathogen of special concern in the food industry (Rodríguez et al., 2002).

Therefore, this work aimed to develop nanocomposite films incorporated with pediocin and ZnO nanoparticles. Also, this work aimed to evaluate physical-mechanical properties, including microscopy analysis, tensile test, color properties and thermal stability, as well as antimicrobial activity against *S. aureus* and *L. monocytogenes* of developed nanocomposite films using the central composite design and statistical approaches of response surface methodology (RSM).

2. MATERIALS AND METHODS

2.1 Materials

Methyl cellulose (MC) and zinc oxide (ZnO) nanoparticles were purchased from Sigma–Aldrich Chemical Co., (USA). Pediocin was purchased in the form of a commercially available concentrate known as ALTA^{TM} 2341 (Kerry Bioscience, Ireland). Also, sodium pyrophosphate ($Na_4P_2O_7$) at 0.1 M was purchased from Sigma–Aldrich Chemical Co., (USA) and used as the dispersing agent of ZnO nanoparticles. Glycerol (Labsynth, Sao Paulo, Brazil) was used as a film plasticizer.

2.2 Film Production

For film production, ZnO nanoparticles were dispersed according to the following procedure: Different concentrations of ZnO nanoparticles (Table 1) were mixed with 150 mL of deionized water (Millipore Milli-Q system) and 0.1 M sodium pyrophosphate (0.13 g) was added. The ZnO nanoparticle dispersion process was done in a probe sonicator (DES500 Unique, Brazil) with a 1.1 cm diameter probe. ZnO nanoparticles were sonicated using 200 W of power for 23 min. After ZnO dispersion, glycerol (0.8 g) was added to the nanoparticle solution, which was heated at 80±2 ℃ to solubilize the polymer (methyl cellulose).

Pediocin was added to the nanoparticle solution at different concentrations according to the central composite design (Table 1) and with MC (7.5 g) in order to obtain the filmogenic solution.

The filmogenic solution was cast in cubic molds made from glass, with inner dimensions of 18x34 cm^2. Casted nanocomposite films were dried for 72 h at ambient conditions (18 ℃ and 65 % RH).

Table 1. Coded (in brackets) and decoded levels of ZnO nanoparticles and pediocin concentration for the CCD

Treatment codification* (TRT)	ZnO nanoparticles (% w/w)	Pediocin (% w/w)
8	11.0 (0)	50 (+1.41)
6	19.5 (+1.41)	33 (0)
3	5.0 (-1)	45 (+1)
11c	11.0 (0)	33 (0)
5	2.5 (-1.41)	33 (0)
10c	11.0 (0)	33 (0)
7	11.0 (0)	15 (-1.41)
1	5.0 (-1)	20 (-1)
13c	11.0 (0)	33 (0)
4	17.0 (1)	45 (+1)
9c	11.0 (0)	33 (0)
12c	11.0 (0)	33 (0)
2	17.0 (+1)	20 (-1)

*c is the central point. Coded levels are in parenthesis.

2.3 Experimental Design and Statistical Analysis

A central composite design (CCD) was used to study the combined effects of ZnO nanoparticles and pediocin on the engineering properties and antimicrobial activity of MC nanocomposite films. The experiment was carried out according to a CCD based on the Response Surface Methodology (RSM), with two variables: concentration of ZnO nanoparticles and pediocin in the filmogenic solution (each antimicrobial concentration was based on MC dry weight).

A statistical model representing the influence of ZnO nanoparticles and pediocin on the engineering properties and antimicrobial activity of nanocomposite film was developed and validated using the analysis of

variance (ANOVA). Treatment effects on response were assessed by RSM and the optimized condition was chosen to obtain an optimized nanocomposite film.

All calculations and graphics in this work were performed using electronic worksheets from Microsoft® Excel 2003 according to Teófilo and Ferreira (2006).

2.4 Optimization by the Desirability Function Approach

After the elaboration of response surface models, a simultaneous optimization of significant response variables was done using the desirability function approach according to Derringer and Suich (1980). Each estimated response variable, calculated by the fitted response surface associated with the CCD experimental design used in this work, was transformed using the desirability function into a desirable value (d_i), using the following equation:

$$d_i = \begin{cases} 0 & \hat{y}_i \le y_{i\min} \\ \left[\dfrac{\hat{y}_i - y_{i\min}}{y_{i\max} - y_{i\min}} \right] & y_{i\min} < \hat{y}_i < y_{i\max} \\ 1 & \hat{y}_i \ge y_{i\max} \end{cases} \qquad \text{(eq. 1)}$$

Where the values y_{imin} and y_{imax} are the minimum and maximum acceptable value of $\hat{y}_i$, respectively. The values of d_i vary in the interval $0 \le d_i \le 1$, increasing as the desirability of the corresponding response increases. The individual desirabilities were then combined using the geometric mean (Eq. 2) to give an overall desirability (D).

$$D = \left(d_1 \times d_2 \times \cdots \times d_k \right)^{1/k} \qquad \text{(eq. 2)}$$

The overall desirability was analyzed using a univariate search technique to optimize D over the independent variable domain, which resulted in the desirability of the combined response levels. In this work the desirability function varied between zero and one.

2.5 Film Characterization

2.5.1 X-ray diffraction (XRD) characterization

The diffraction pattern was obtained to confirm the crystalline structure of ZnO nanoparticles alone, as well as incorporated in the nanocomposite films. XRD patterns were taken with the X-ray Diffraction System X'Pert PRO model (PANalytical, Netherland), using an iron (Fe) filter and Co-Kα radiation (λ = 1.78890 Å). The diffraction pattern was obtained at diffraction angles between 10º and 80º (2θ).

2.5.2 Measurement of film thickness

Thickness of the samples was determined with a manual micrometer (0.01 mm, Mitutoyo Sul Americana, Suzano, São Paulo State, Brazil). The thickness of the nanocomposite films was measured at ten randomly selected points on each film to calculate the average value. Average values were used when necessary to calculate film properties.

2.5.3 Mechanical resistance

Mechanical properties of developed nanocomposite films (tensile strength at break, load at break and elongation at break) were determined according to the standard method ASTM D882–02 (ASTM, 2009) using an Instron Universal Testing Machine model 3367 (Instron Corporation, Norwood, MA, USA), equipped with a load cell of 1 kN. The nanocomposite film samples were cut in rectangular specimens (15x2.5 cm^2). Initial grip separation was 100 mm, and the cross-head speed was set at 50 mm/min. This test was repeated ten times for each treatment to confirm its repeatability.

2.5.4 Surface color measurement

Color values of films were measured with a colorimeter COLORQUEST XE HUNTERLAB (Reston, Virginia, USA). The instrument was used with a 9.5 mm diameter of measuring area. The measurements were done in the CIELAB scale, in which each measurement is expressed as L* (indicating the lightness), a* (positive in the red direction and negative in the green direction), and b* (positive in the yellow direction and negative in the blue

direction). Calculations were made for D-65 illuminant and 10° observation interval according to ASTM E308 (ASTM, 2008). Total color differences (ΔE) and opacity (OP) were calculated using the standard values of the white background (L* = 93.44; a* = -0.63; b* = 1.21). Also, the yellowness index (YI E313) and whiteness index (WI E313) were obtained using the Universal Software V4.10 according to ASTM E313-10 (ASTM, 2010). All color measurements were repeated three times for each type of nanocomposite film.

2.5.5 Microscopy characterization

Morphological analyses of nanocomposite films were observed directly by Scanning Electron Microscopy (SEM, Hitachi-TM 3000 Tabletop microscope, Japan).

The topography of nanocomposite films was studied using Atomic Force Microscopy (AFM, NT-MDT, Russia). AFM images were acquired in an intermittent contact mode in random areas of 50x50 μm^2. The samples were analyzed in air at room temperature (25 ℃).

2.5.6 Swelling tests

Swelling tests were done according to Jipa et al. (2012) with some modifications. Samples of nanocomposite films in triplicate (2x2 cm^2) were dried to constant weight, and immersed in distilled water at room temperature (25 ℃) for 2 h. The polymer mass dissolved in dist illed water was neglected considering the short time needed for the experiment. Also, the amount of both antimicrobial (ZnO nanoparticles and pediocin) incorporated in the active films and their released in aqueous media was considered negligible compared to the amount of absorbed water. Swelling degree was obtained by measuring the initial mass (m_i) and the mass of sample in swollen state (m_s) using Eq. (1):

$$SD = 100 * ((m_s - m_i)/ m_i) \quad (1)$$

The mass of swollen sample was measured after gently blotting film surface with tissue paper until the equilibrium was reached.

2.5.7 Thermogravimetric analysis

Analysis was performed on a thermogravimetric analyzer (TGA-1000, Navas instruments, Conway, S.C., USA). Samples of nanocomposite film (1 g approx.) were heated to 950 ℃, at a heating rate of 10 ℃/min under nitrogen atmosphere. Weight losses of samples were measured as a function of temperature.

2.5.8 Microorganisms and antimicrobial activity assay

Staphylococcus aureus (ATCC 6538) and *Listeria monocytogenes* (ATCC 15313) were used to test the antimicrobial activity of developed nanocomposite films. Bacteria stored at -80 ℃, were grown twice in Tryptic Soy Broth (TSB; Acumedia, Baltimore MD, USA) and incubated for 24 h at 35 ℃. Bacteria were streaked on non-selective culture media Tryptic Soy Agar (TSA; Acumedia, Baltimore MD, USA) and incubated for 24h at 35 ℃ to isolate bacterial colonies. Isolated colonies were selected from the TSA Petri dish and suspended in saline solution (0.85 % w/v). The bacterial suspension was adjusted to achieve the turbidity of McFarland standard solution 0.5, resulting in an inoculum containing approximately $1x10^8$ UFC/mL.

Bacterial inoculum of *S. aureus* was subcultured in Baird Parker Agar (Hi-Media Laboratories, Mumbai, India), while bacterial inoculum of *L. monocytogenes* was subcultured in Oxford agar (Difco Laboratories) for the antimicrobial activity assay.

Following this, discs (1 cm diameter) of each treatment of nanocomposite films were placed on the surface of the previously inoculated agar culture media. Petri dishes with microorganism and discs of nanocomposite films were incubated at 12±1 ℃ for 24 h to allow the diffusion of antimicrobial compounds (pediocin and ZnO nanoparticles) from the films without microbial growth. Petri dishes were incubated at 35±1 ℃ for 24 h.

The antimicrobial activity of nanocomposite films was determined by measuring the inhibition zone around each disc of films (cm). All samples were tested in triplicate.

3. RESULTS AND DISCUSSION

3.1 X-ray Diffraction (XRD) Characterization

The XRD technique uses the scattered intensity of an X-ray beam on the sample, revealing information about the crystallographic structure, chemical composition, and physical properties of the material studied. This technique is widely used in materials characterization since is nondestructive and does not require elaborated sample preparation (Espitia et al., 2012).

Pure ZnO nanoparticles, film of neat MC and nancomposite films were analyzed using XRD technique (Figure 1). In this work we report the results obtained for nancomposite films regarding treatments TRT6 and TRT8, since these treatments present the maximum levels of ZnO nanoparticles and pediocin.

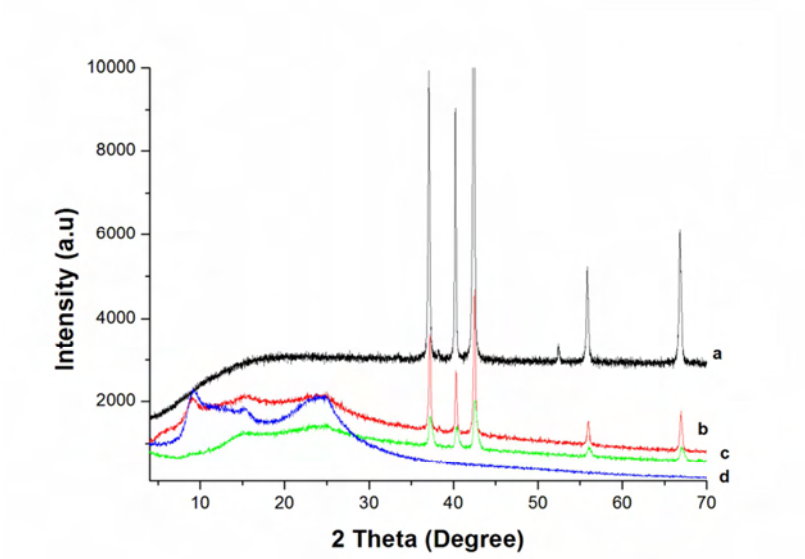

Figure 1. XRD patterns of: **a)** pure ZnO nanoparticles; **b)** 19 % ZnO and 33 % PED (TRT 6); **c)** 11 % ZnO and 50 % PED (TRT 8); and **d)** MC control film.

Moreover, the interplanar spacing (d) of ZnO nanoparticles was calculated to compare with the standard d values of ZnO according to JCPDS Nº. 036–1451. The calculated d values matched with the standard (Table 2), confirming the hexagonal wurtzite structure of ZnO nanoparticles.

Table 2. Computed *d* values of ZnO nanoparticles sample and standard *d* value from JCPDS card Nº. 036–1451

Θ Angle	Calculated *d* value (Å)	Standard *d* value (Å)
18.53	2.814	2.816
20.10	2.602	2.602
21.19	2.475	2.476
27.91	1.911	1.911
33.39	1.625	1.626
37.26	1.477	1.477
38.97	1.422	1.407

These results showed main characteristic peaks of ZnO nanoparticles (observed at 2θ = 37.2°, 2 θ = 40.3°, 2 θ = 42.5°, 2 θ = 55.9°), confirming that the hexagonal wurtzite structure of ZnO nanoparticles was not affected after their incorporation in MC matrix. Moreover, the intensity of main characteristic peaks of ZnO was higher as the concentration of ZnO nanoparticles in MC matrix increased.

For the film of neat MC, main diffraction peaks were observed at 2θ = 9.1°, 2θ = 15.6°, and a broad peak around 2 θ = 25°, which represent its partial crystallinity structure. According to Espinoza-Herrera et al. (2011), MC has a high proportion of amorphous structure and a natural partial crystallinity.

Moreover, as observed in the XRD patterns of nanocomposite films, the addition of ZnO nanoparticles and pediocin affected the crystallinity of MC matrix. In this way, the addition of ZnO nanoparticles resulted in narrow peaks of MC, indicating more crystallinity structure of films; on the other hand, higher concentrations of pediocin resulted in broader peaks, mainly observed in XRD pattern of TRT8, indicating that the addition of pediocin resulted in lower crystallinity.

3.2 Thickness and Mechanical Resistance of Nanocomposite Films

Results of thickness showed that this property had no significant difference among developed nanocomposite films based on the CCD, indicating that the process of elaboration resulted in homogenous films. Moreover, a T-test was applied to compare thickness mean value of nanocomposite films (0.140±0.02 mm) and control film (0.098±0.01 mm), showing a significant difference ($p<0.05$) among them.

This difference resulted from the incorporation of both antimicrobials, ZnO nanoparticles and pediocin, in the polymeric matrix. Previous works have indicated the modification of thickness caused by incorporation of ZnO nanoparticles and pediocin to a polymeric matrix (Li et al., 2010; Santiago-Silva et al., 2009; Seo et al., 2011).

Mechanical properties of films are important characteristics for food packaging materials. They measure stretchability prior to breakage and film strength. In this way, the mechanical performance of developed nanocomposite films was studied by determining the tensile strength at break (MPa), load at break (N) and elongation at break (%).

Load at break and tensile strength at break did not present significant differences among developed nanocomposite films. Also, the mean values of load at break (148.22±20.69 N) and tensile strength at break (44.14±6.89 MPa) of nanocomposite films were not significant different ($p>0.05$) from mean values of control film (126.67±25.65 N and 46.43±4.47 MPa). These results indicated that the mechanical resistance of MC films was not affected after incorporation of ZnO nanoparticles and pediocin.

According to Bastarrachea et al. (2011), a significant effect in the tensile properties is not expected when the molar mass of the antimicrobial molecule is smaller than the molar mass of the polymeric material. In this case, the molar mass of ZnO is 81.408 g/mol and the molar mass of pediocin is 4,629 g/mol, while the molar mass of MC is much higher, varying from 14,000 to 88,000 g/mol depending on its degree of substitution.

Bastarrachea et al. (2011) indicated that the incorporation of the antimicrobial should not alter the conformation of the packaging material's polymer structure, thereby not influencing its tensile properties.

On the other hand, maximum value of elongation at break was observed at 54.57 %, while the minimum was 30.29 % (Table 3).

Table 3. Coded, decoded levels and responses for the CCD of MC films incorporated with ZnO nanoparticles and pediocin

	Runs	x_1	x_2	*Elong.*	*L**	*b**	*OP*	ΔE	*WI*	*YI*
Factorial points	2	-1	-1	31.93	91.29	8.15	41.24	6.98	40.67	14.17
	9	1	-1	33.42	91.82	8.57	61.25	7.07	40.09	15.08
	11	-1	1	54.57	89.56	13.08	43.39	11.56	12.66	23.25
	3	1	1	38.98	89.42	13.06	65.39	11.59	12.47	23.71
Center points	1	0	0	35.79	90.46	11.01	56.67	9.56	24.96	19.69
	6	0	0	30.29	90.30	11.28	55.07	9.86	23.24	20.03
	8	0	0	35.08	90.61	11.36	55.74	9.80	23.71	20.04
	12	0	0	32.97	90.06	10.77	54.73	9.56	25.07	19.27
	10	0	0	39.48	91.04	11.00	54.20	9.34	26.55	19.34
Axial points $\alpha=2^{1/2} \approx 1.414$	7	-1.414	0	51.95	89.59	12.19	31.53	10.94	16.93	21.36
	5	1.414	0	39.38	90.74	10.45	65.86	8.99	28.42	18.78
	12	0	-1.414	33.12	91.21	7.91	55.51	6.81	41.62	13.84
	4	0	1.414	45.51	88.81	14.91	58.32	13.23	4.15	26.32

	Experimental Domain				
Variables	-1.414	-1	0	1	1.414
x_1: ***ZnO***	2.5	5	11	17	19.5
x_2: ***Pediocin***	15	20	33	45	50

The abbreviation *Elong.* stands for elongation at break (%).

The elongation at break of nanocomposite films was influenced by the linear effect of ZnO nanoparticles and pediocin, as well as by the quadratic effect of ZnO nanoparticles (p<0.05) according to the analysis of regression coefficients of the response function (Table 4).

Table 4. Coefficient estimates from CCD and statistical analysis for the elongation at break (%) of nanocomposite films incorporated with ZnO nanoparticle and pediocin

	Size of ZnO			
	Coefficient[a]	Std. err.	*t* (4)	*p*
Mean	***34.72***	1.52683	22.7418	2.21E-05
ZnO	***-3.985***	1.20706	3.30177	0.029884
PED	***5.716***	1.20706	4.73507	0.00907
ZnO^2	***4.781***	1.29444	3.69354	0.020954
PED^2	1.605	1.29444	1.23954	0.2829
ZnO×PED	-4.269	1.70705	2.50059	0.066724

ZnO: nanoparticles; PED: pediocin. [a] Values in bold and italics are significant at α=0.05 with 4 degrees of freedom for the response variable.

The regression model for elongation at break was validated with ANOVA, which presented statistical significance among developed nanocomposite films, with a non-significant lack of fit (Table 5).

Table 5. ANOVA results for the elongation at break (%) of nanocomposite films incorporated with ZnO nanoparticle and pediocin

Variation	Elongation at break				
	SS[af]	df[b]	MS[c]	*F*[d]	*p*[e]
Regression	***627.1***	5	125.423	11.27	0.003044
Residues	77.92	7	11.1313		
Lack of fit	31.3	3	10.4317	0.895	0.517008
Pure Error	46.62	4	11.656		
Total SS	705	12			

[a] Sum of squares; [b] Degree of freedom; [c] Mean squares; [d] *F* distribution; [e] *p* value; [f] Bold and italic values are significant at α = 0.05.

The linear regression coefficient of ZnO nanoparticles was negative, indicating that a lower concentration of this antimicrobial allows more elongation of nanocomposite films. The linear regression coefficient of pediocin, which is positive, indicates that higher concentrations of this bioactive peptide result in higher values of elongation at break of nanocomposite films. Moreover, the significant quadratic coefficient of ZnO nanoparticles indicates that the elongation at break of nanocomposite films decreases quadratically when the concentration of ZnO increases (Figure 2).

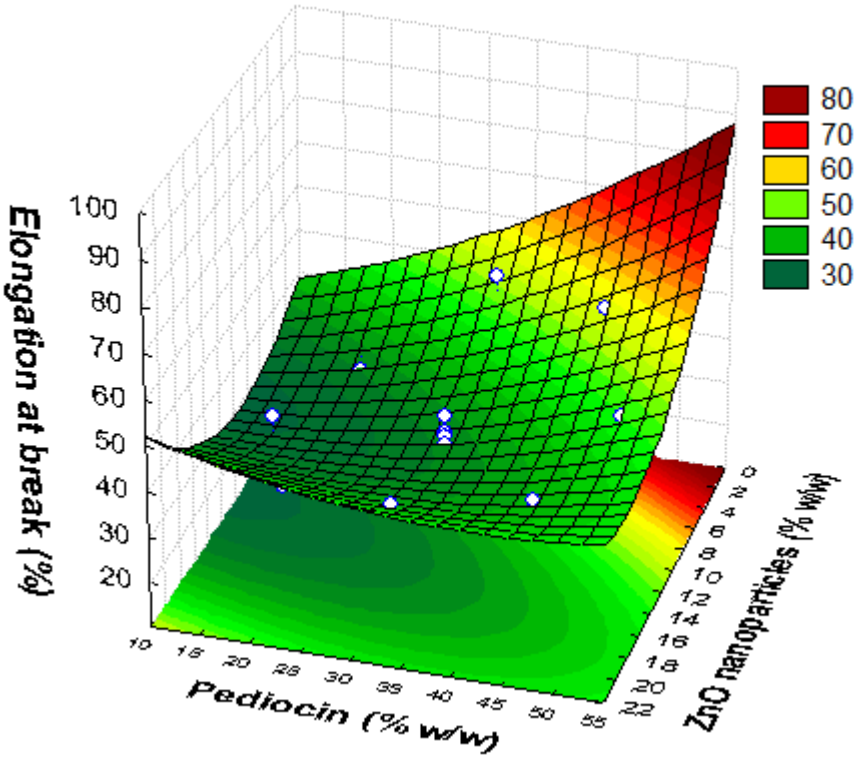

Figure 2. Response surface of elongation at break (%) as a function of pediocin (% w/w) and ZnO nanoparticles (% w/w).

Results of elongation at break regarding ZnO concentration are in agreement with Li et al. (2009), who indicated the reverse effect of ZnO nanoparticles in the flexibility of the films.

Moreover, the addition of pediocin resulted in increased values of elongation at break, indicating that this bioactive peptide acted as a plasticizer in the cellulosic matrix. This result is related to XRD patterns, which showed that higher concentration of pediocin resulted in diminished crystallinity of nanocomposite films.

On the other hand, the elongation at rupture of packaging materials is inversely related to tensile strength, and a decrease in the values of load at break and tensile strength at break of developed nanocomposite films was expected.

However, mechanical resistance of nanocomposite films, measured as load at break and tensile strength at break, presented no difference when compared to control film. This is probably because ZnO incorporation prevented the decrease of mechanical resistance after pediocin

incorporation, since previous works have indicated that the incorporation of ZnO nanoparticles can enhance the strength but not the flexibility of nanocomposite films (Ma et al., 2009).

3.3 Surface Color Measurement

The color of food packaging is an important factor in terms of general appearance and consumer acceptance (Bourtoom & Chinnan, 2008; Srinivasa et al., 2003).

The addition of active compounds that structurally bind with films-forming solutions, could change the native color of the film (Rhim et al., 2000). In this way, the color of control film was transparent, while nanocomposite films incorporated with different concentrations of ZnO and pediocin presented a yellowish and whitish color (Figure 3).

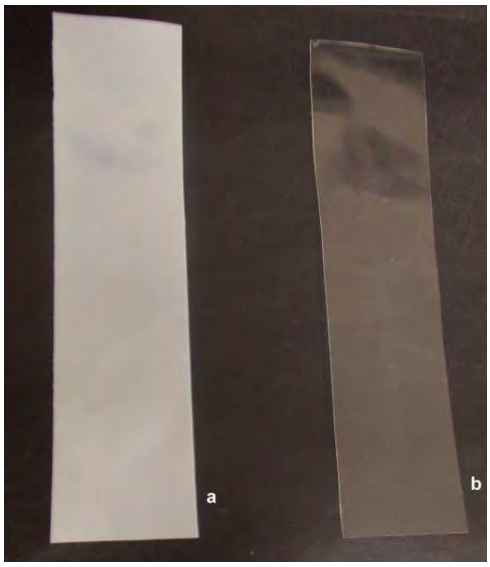

Figure 3. Nanocomposite film incorporated with 11 % (w/w) of ZnO nanoparticles and 33 % of pediocin (a), and control film (b).

Moreover, statistical analysis showed that the regression model for the colorimetric parameters L*, b*, total color difference (ΔE), opacity (OP), yellowness index (YI E313) and whiteness index (WI E313) presented significance differences among nanocomposite films, with a non-significant lack of fit (Table 6).

Table 6. Estimated regression coefficients for colorimetric parameters of nanocomposite films incorporated with ZnO nanoparticles and pediocin

Term		Colorimetric parameter					
		L*	b*	OP	ΔE	WI E313	YI E313
Mean		***90.49***	***11.08***	***55.28***	***9.627***	***24.71***	***19.67***
ZnO		0.251	***-0.259***	***11.32***	***-0.331***	***1.936***	-0.283
PED		***-0.942***	***2.416***	***1.282***	***2.27***	***-13.58***	***4.418***
ZnO^2		-0.055	-0.044	***-3.291***	-0.005	-0.093	-0.058
PED^2		-0.134	0.001	0.819	0.023	0.009	-0.053
ZnO×PED		-0.17	-0.11	0.5	-0.014	0.096	-0.111
Regression	F^a	9.366	31.2	162.7	27.21	29.65	38.12
	P^b	0.005246	0.000121	$4.4 \cdot 10^{-07}$	0.00019	0.000143	$6.23 \cdot 10^{-05}$
Lack of fit	F^a	1.59	11.22	2.203	15.28	12.76	13.01
	P^b	0.324352	0.020388	0.230201	0.011755	0.016248	0.015697

ZnO: nanoparticles; PED: pediocin. Values in bold and italics are significant at α=0.05 with 4 degrees of freedom for the response variable; [a] *F* distribution; [b] *p*-value.

The colorimetric parameter L* was influenced by the linear effect of pediocin (*p<0.05*), while the addition of ZnO nanoparticles in tested conditions had no effect on this parameter. The linear regression coefficient of pediocin was negative, indicating that when higher concentrations of this bioactive peptide are incorporated, the luminosity of nanocomposite films is significantly diminished (Figure 4.a).

Also, the colorimetric parameter b* was influenced by the linear effect of ZnO nanoparticles and pediocin (*p<0.05*) according to the analysis of regression coefficients of the response function. Positive values of this parameter indicate a trend in the yellow direction and negative values indicate a trend in the blue direction.

In this case, the linear regression coefficient of both antimicrobials affected the colorimetric parameter b*, with the coefficient of ZnO nanoparticles being negative, indicating that higher concentrations of ZnO nanoparticles result in lower values of b*. The coefficient of pediocin was positive, indicating that higher concentration of pediocin allows higher values of b* (Figure 4.b).

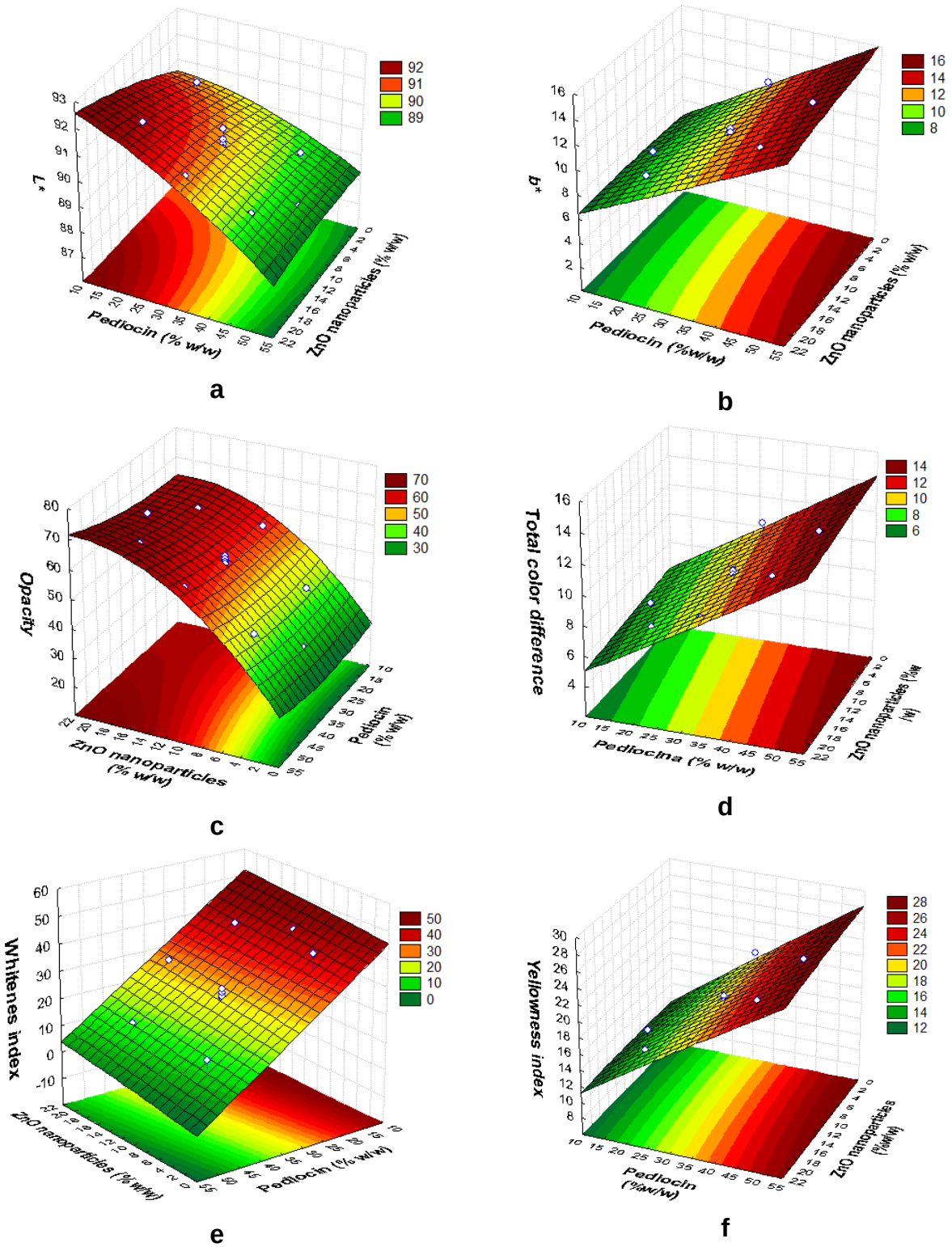

Figure 4. Response surface of the colorimetric parameters: **a)** L*; **b)** b*; **c)** opacity; **d)** total color difference; **e)** whiteness index; and **f)** yellowness index as a function of pediocin (% w/w) and ZnO nanoparticles (% w/w).

On the other hand, the colorimetric parameter a* made no significant difference to the developed nanocomposite films. This is probably due to the color that this coordinate represents, which are green, when negative values are obtained, or red, when positive values are obtained.

Moreover, the opacity (OP) of developed nanocoposite films was affected by the linear effect of ZnO nanoparticles and pediocin, indicating that increased concentrations of both antimicrobials results in increased values of OP. However, the quadratic and negative effect of ZnO indicates that the OP increase until certain ZnO concentration, and after reaching this critical concentration this parameter decreased quadratically (Figure 4.c).

Total color difference (ΔE) was affected by the linear and negative effect of ZnO and the positive linear effect of pediocin, indicating that high concentrations of ZnO results in low values of ΔE while high concentrations of pediocin results in high values of this colorimetric parameter (Figure 4.d).

As expected, whiteness index (WI E313) of nanocomposite films was affected by linear effect of both antimicrobials; nevertheless pediocin presented a negative coefficient indicating that high concentrations of pediocin results in lower values of this index (Figure 4.e).

Moreover, yellowness index (YI E313) was affected by the addition of pediocin, since this antimicrobial in the form of concentrated powder presents naturally a yellow color and the presence of ZnO did not have influence on this parameter (Figure 4.f).

Similar to our results, Chandramouleeswaran et al. (2007) developed ZnO-polypropylene (PP) nanocomposites and indicated that the whitening effect on PP is due to the presence of ZnO nanoparticles.

Moreover, similar to pediocin other bacteriocins have shown similar effects on color parameters after incorporation in polymeric matrixes. In this way, alginate and PVOH films showed a significant decrease of L* values (lightness) and an increase of b* values (yellowness) due to enterocin incorporation, a bacteriocin produced by *Enterococcus faecium* CTC492 isolated from meat products (Marcos et al., 2010). Also, the incorporation of nisin, a bacteriocin produced by certain strains of *Lactococcus lactis*, in tapioca starch films and its mixtures with hydroxypropyl methylcellulose

resulted in a decrease of L* values and increase of b* and YI values compared to control films (Basch et al., 2012). The authors attributed the yellowish trend of the films to the own color of nisin.

Thus, based on our results and related works, the presence of pediocin in the formulation of developed nanocomposite films produced slightly yellowish films; however, this effect was balanced by the incorporation of ZnO nanoparticle, resulting in a whitish coloration.

3.4 Microscopy Characterization

Morphological analyses by Scanning Electron Microscopy (SEM) of MC film (control film) showed a homogeneous surface, with the presence of scarce undissolved polymeric resin. Moreover, nanocomposite films showed the presence of ZnO nanoparticles. The addition of pediocin in high concentrations resulted in the formation of crater-like pits (Figure 5).

The formation of crater-like pits as an effect of pediocin was verified by the elaboration and SEM analysis of a MC film incorporated only with the maximum concentration of pediocin (50 % w/w) tested in this work. Also, MC film incorporated only with 20 % (w/w) of ZnO nanoparticles was observed in the SEM for comparison (Figures 5.e and 5.f).

A high number of crater-like pits were observed in the surface of the film with 50 % pediocin, presenting a sponge-like and loosely filled structure. The greater formation of crater-like pits revealed a weak interaction of the polymeric matrix, which failed to retain microscopic surface integrity. Moreover, images of nanocomposite films showed ZnO nanoparticles trapped in crater-like pits created by pediocin (Figure 5.d). This probably caused the lack of improvement of mechanical resistance of nanocomposite films after ZnO incorporation, as observed for load at break and tensile strength.

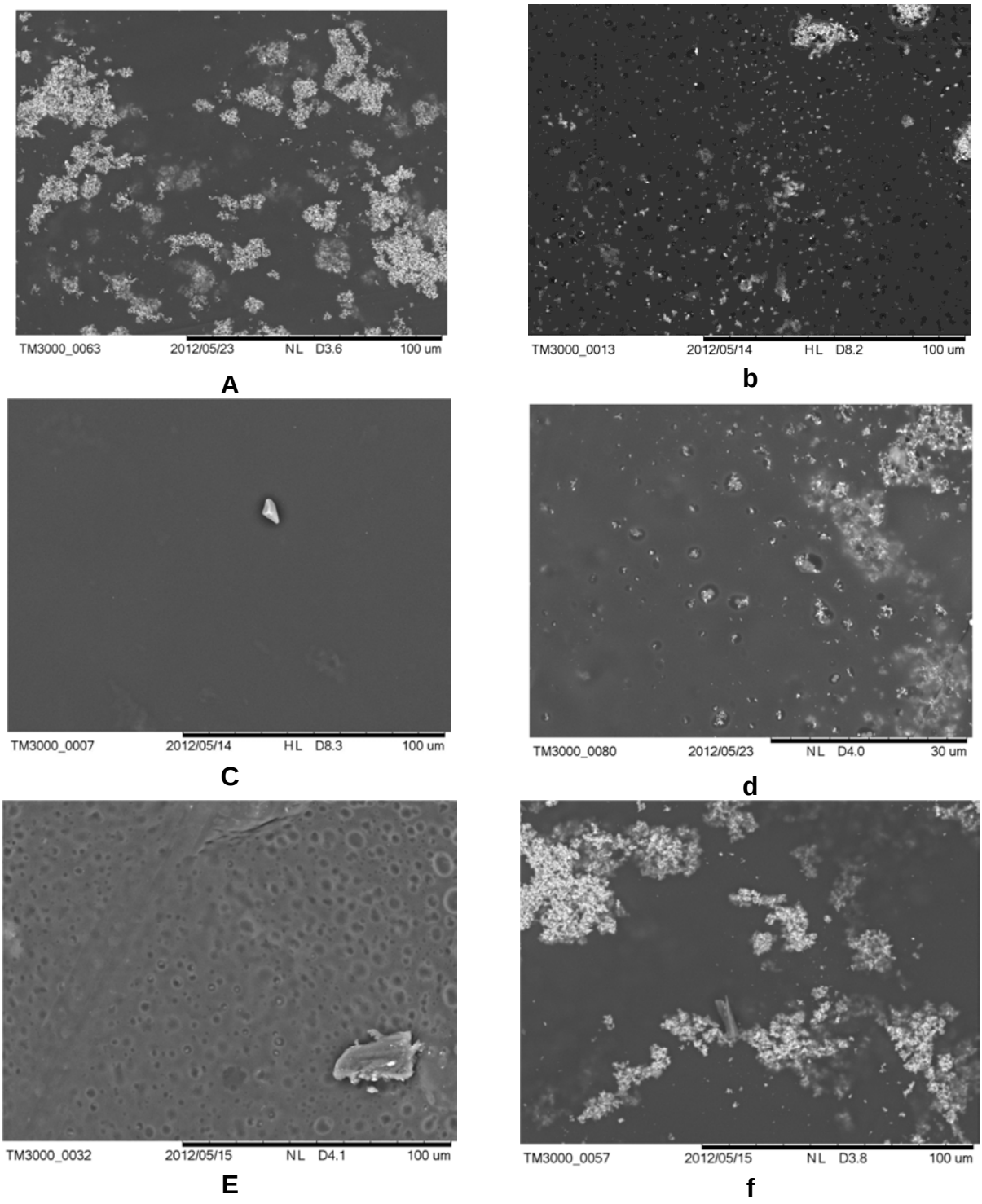

Figure 5. SEM photomicrograph of nanocomposite films incorporated with: **a)** 19.5 % ZnO and 33 % PED (TRT6); **b)** 11 % ZnO and 50 % PED (TRT8); **c)** control film; **d)** 2.5 % ZnO and 33 % of pediocin (TRT5); **e)** 50 % of pediocin; and **f)** 20 % of ZnO. Images at 1000X magnification; image (d) at 2500X magnification.

In addition, atomic force microscopy (AFM) presented 3D topographic images of nanocomposite film surfaces (Figure 6).

These images confirmed the results observed by SEM, showing the formation of crater-like pits in nanocomposite films. These crater-like pits are clearly observed in image of treatment 8 (Figure 6.b), where the concentration of pediocin was considerably higher than the concentration of ZnO. On the other hand, the control film had a very homogeneous surface with few points of undissolved polymeric resin, as observed in the SEM microphotograph. The crater-like pits, as observed in the nanocomposite films, were not observed in the control film, indicating that these cavities form as a result of the addition of pediocin.

In order to prove our theory about the formation of the crater-like pits, we used AFM to analyze the surface of MC film incorporated only with the highest concentration of pediocin (50 % w/w) or ZnO nanoparticles (20 % w/w) used in this study (Figures 6.d and 6.e). In agreement with the SEM images, AFM showed the formation of crater-like pits created by pediocin.

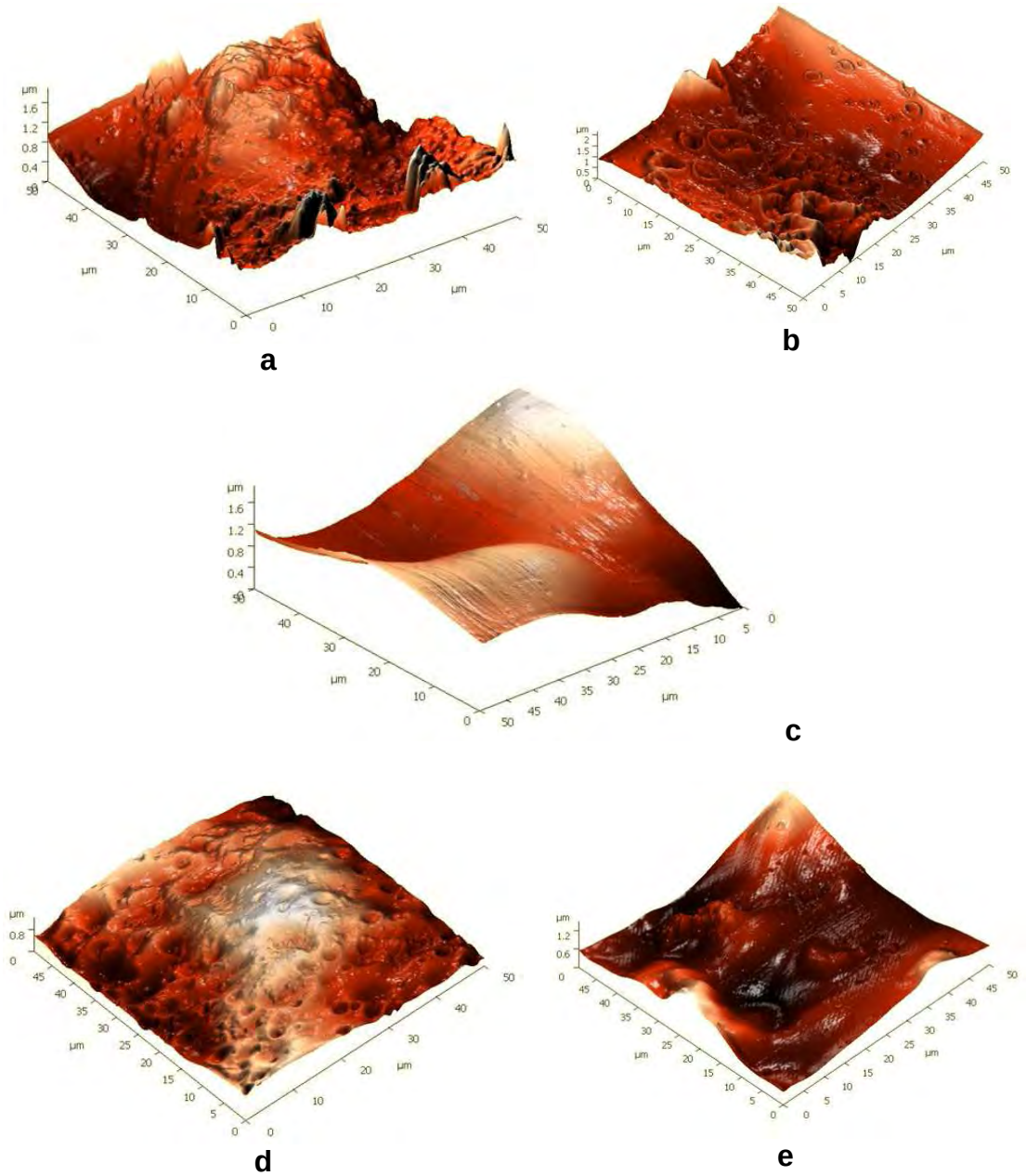

Figure 6. AFM photomicrograph of nanocomposite films incorporated with: **a)** 19.5 % ZnO and 33 % PED (TRT6); **b)** 11 % ZnO and 50 % PED (TRT8); **c)** control film; **d)** 50 % of pediocin; and **e)** 20 % of ZnO. Images analyzed at area of 50x50 μm^2.

Espinoza-Herrera et al. (2011) indicated that the formation of crater-like pits, also known as pores, in the cellulosic polymeric matrix is probably due to a smaller transference of mass, related to solvent evaporation, and consequently a slower drying speed. Particularly in this work, it is probable that polysaccharides that constitute the matrix film are bonded to pediocin and form a more compact structure that reduce the transference rate of solvent (in this case water) from the film forming solution, leading to the formation of crater-like pits and consequently to a rougher surface.

These results are related to the results obtained by XRD, which showed that increased pediocin concentration resulted in diminished crystallinity of nanocomposite films.

3.5 Swelling Tests

The sensitivity of developed nanocomposite films to water was investigated by means of their swelling degree. Swelling degree is an important parameter in order to know the stability and quality changes of packaging materials during packaging and storage of food product (Abdollahi et al., 2012; Srinivasa et al., 2007).

Results of the swelling test showed that this property had no significant difference among developed nanocomposite films according to the CCD. However, when the T-test was applied, a significant difference ($p<0.05$) was observed among the mean value of swelling degree of nanocomposite films (16.4±2.1 g of H_2O/g of film) and control film (21.3±3.2 g of H_2O/g of film), indicating that the control film absorbed large amount of water compared to developed nanocomposite films. To prove adequate barrier properties, films must exhibit low swelling ability (Guiga et al., 2010; Jipa et al., 2012); therefore this is a promising result.

We attribute the reduction of swelling degree of nanoacomposite films to the presence of ZnO nanoparticles in MC matrix since, although the incorporation of pediocin in the MC matrix resulted in the formation of crater-like pits, ZnO nanoparticles exhibited good intercalation in the MC matrix, as observed in the AFM images, which avoided the absorption of water.

Studies are scarce regarding the effect of ZnO nanoparticles on the swelling degree of nanocomposite films. However, Liu and Kim (2012) reported that ZnO nanoparticles have previously been shown to diminish the swelling degree of nanocomposites. In this way, they have indicated that the incorporation of ZnO and silver nanoparticles in genipin-crosslinked chitosan nanocomposites leads to decreased swelling compared to control film.

3.6 Thermogravimetric Analysis

Determining the thermal resistance allows studying structural changes caused by temperature variations on packaging (Espitia et al., 2012). The thermal stability of developed nanocomposite films was investigated by means of thermogravimetric analysis (Figure 7).

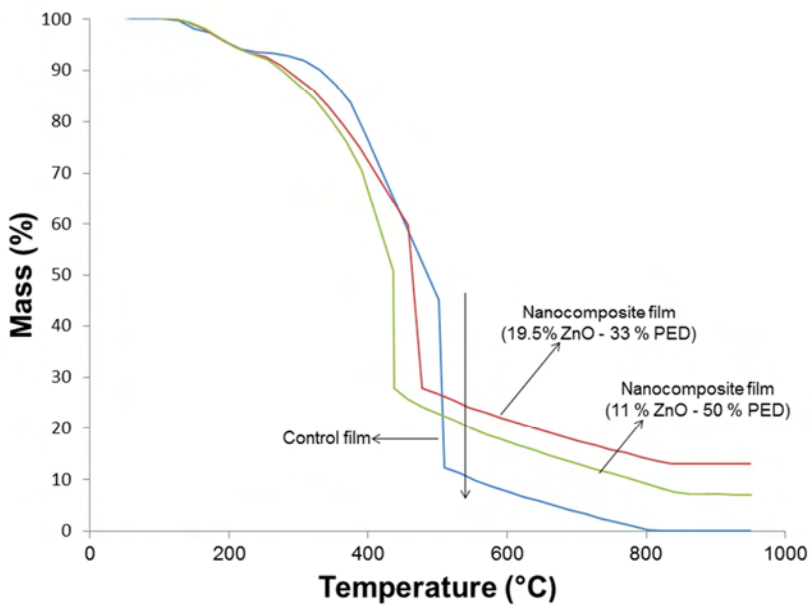

Figure 7. TGA curve of nanocomposite films with highest concentration of ZnO nanoparticles (TRT6: 19.5 % ZnO; 33 % PED), highest concentration of pediocin (TRT8: 11 % ZnO; 50 % PED) and control film.

The temperature value at the maximum decomposition rate, obtained from the derivative thermogravimetric (DTG) curves, of nanocomposite film with the highest concentration of ZnO (TRT 6; 19.5 % ZnO) was higher compared to control film or to nanocomposite film with 11 % of ZnO and 50 % of pediocin (Table 7). Thus, the nanocomposite film with a high concentration of

ZnO nanoparticles showed enhanced thermal stability in comparison with control film and nancomposite film with high concentration of pediocin.

Table 7. Temperature at maximum decomposition rate of nanocomposite films

Treatment codification (TRT)	ZnO nanoparticles (% w/w)	Pediocin (% w/w)	Temperature at maximum decomposition rate (℃)	Total weight loss (% w/w)
6	19.5	33	458	86.98
8	11.0	50	438	92.92
Control film	-	-	450	99.71

Similar to our results, Yu et al. (2009) reported that the decomposed temperature of carboxymethylcellulose (CMC) sodium nanocomposites with ZnO nanoparticles was 295.4 ℃, while the control was 293.7 ℃, indicating that ZnO–CMC nanocomposite film exhibited better thermal stability than control CMC film. They ascribed this result to the interaction between ZnO and CMC.

Moreover, our results are in agreement with XRD analysis, which indicated that the presence of ZnO nanoparticles affected MC crystallinity, resulting in narrows peaks. Vicentini et al. (2010) reported similar results, indicating that the thermal resistance improvement of biopolymer films by ZnO is due to a decrease in the interatomic distances, and therefore more energy is being required to decompose these films.

Moreover, the nanocomposite film incorporated with the high pediocin concentration showed the lowest thermal resistance, presenting the lowest thermal decomposition at which the maximum decomposition rate is achieved.

This result is probably due to the organic nature of pediocin. Pediocin is a heat-stable peptide, and its antimicrobial activity is retained at 100 ºC, but reduced at 121 ºC (Bhunia et al., 1988; Rodríguez et al., 2002), presenting thermal decomposition above this temperature range.

Moreover, a total weight loss was observed in control film, as expected, while nanocomposite films with ZnO nanoparticles lost less weight (Table 6). Diminished weight loss was observed with increasing concentrations of ZnO

nanoparticles incorporated in the film. This is attributed to the amount of ZnO nanoparticles deposited on each nanocomposite film.

3.7 Antimicrobial Activity Assay

Developed nanocomposite films presented antimicrobial activity against tested microorganisms, *L. monocytogenes* and *S. aureus* (Figure 8).

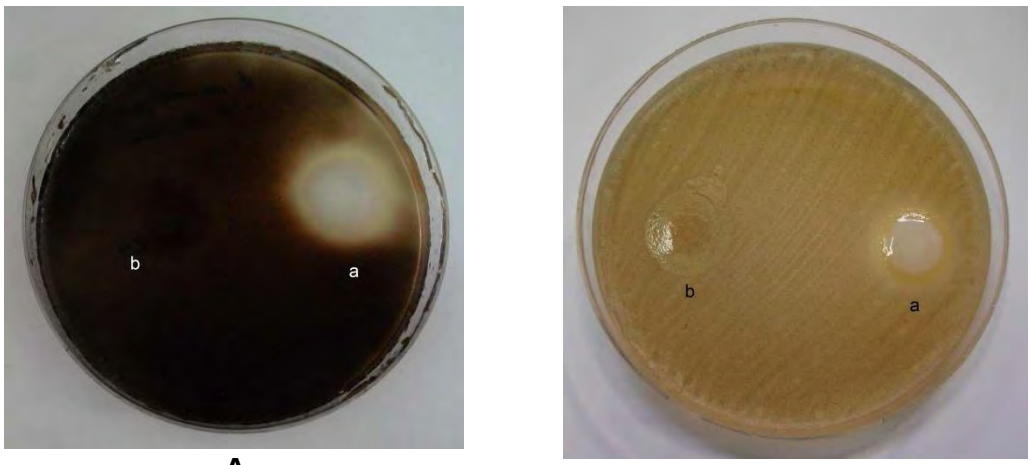

A **B**

Figure 8. Antimicrobial activity of nanocomposite films (a) incorporated with ZnO nanoparticles (17 % w/w) and pediocin (20 %) and control film (b) against *L. monocytogenes* **(A)** and *S. aureus* **(B)**.

However, nanocomposite films had no significant difference among treatments. The average values of the measured inhibition zone around each disc of films (cm) were calculated for each microorganism. The average inhibition zone for *L. monocytogenes* was 2±0.1 cm, while for *S. aureus* was 1.6±0.2 cm.

Antimicrobial activity *in vitro* of ZnO nanoparticles against Gram-positive bacteria, such as *S. aureus*, has been previously reported (Adams et al., 2006; Premanathan et al., 2011; Reddy et al., 2007).

Moreover, studies have indicated the antimicrobial activity of ZnO nanoparticles when incorporated in polymeric matrixes. Li et al. (2009) observed that the growth of *S. aureus* was affected significantly by ZnO-coated films compared to control film. Also, Nafchi et al. (2012) indicated that

ZnO nanoparticles (rod shape) incorporated in sago starch films exhibited excellent antimicrobial activity against *S. aureus*.

Although studies regarding antimicrobial activity of ZnO nanoparticles against *L. monocytongenes* are limited, Jin et al. (2009) have indicated that ZnO nanoparticles suspended in polyvinylprolidone (PVP) gel resulted in a 5.3 log reduction of *L. monocytogenes*, showing significant antimicrobial activities in growth media.

Moreover, pediocin is a bioactive peptide with high specific activity against *L. monocytogenes*, and the potential of this bioactive peptide in food packaging application has been reported (Coma, 2008; Santiago-Silva et al., 2009). In addition, *in vitro* studies indicate that pediocin is adsorbed to Gram-positive bacteria, including *S. aureus*, which results in cell death (Bhunia et al., 1988; Bhunia et al., 1991).

Thus, developed nanocomposite films incorporated with ZnO nanoparticles and pediocin have potential use for controlling *S. aureus* and *L. monocytogenes* in food preservation.

3.8 Optimization by the Desirability Function Approach

Elongation at break and colorimetric parameters L*, b*, OP, YI and WI of developed films were selected for simultaneous optimization by the desirability approach. The optimization was performed in order to achieve films with good mechanical and colorimetric properties. Other responses were not considered in this analysis since they presented no statistical significance according to the RSM.

The optimization showed that films with desired characteristics can be obtained incorporating 20 % (w/w) ZnO nanoparticles and 15 % (w/w) pediocin (Figure 9).

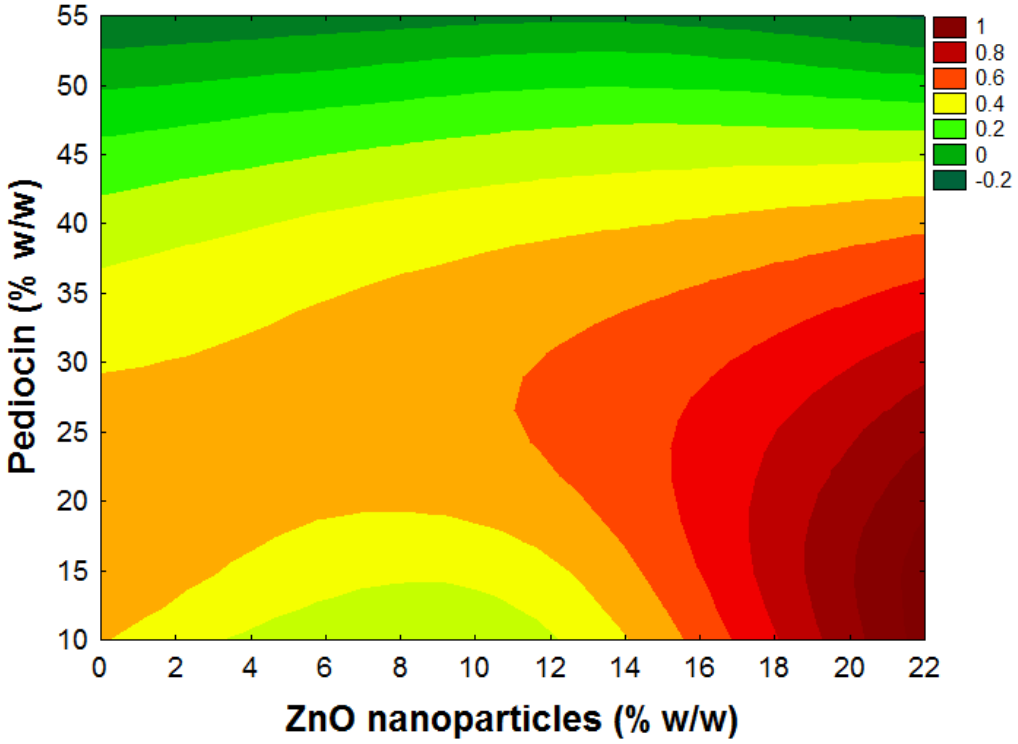

Figure 9. Overall desirability of MC films incorporated with ZnO nanoparticles and pediocin. Desirability function varied from zero (non-desired condition) to one (desired condition).

4. CONCLUSION

The use of natural antimicrobial agents, such as pediocin, associated to nanotechnology allowed the development of new antimicrobial packaging for food preservation. In this experiment, methyl cellulose was used as a polymeric matrix due to its biodegradability, large availability in nature, low cost and easy processing.

Results from XRD showed that the addition of ZnO nanoparticles and pediocin affected the crystallinity of methyl cellulose matrix. Mechanical resistance of nanocomposite films, measured as load at break and tensile strength at break, did not present significant differences among films. However, elongation at break presented statistical significance, indicating that ZnO incorporation resulted in more rigid films, while the addition of pediocin resulted in increased values of elongation at break. The presence of pediocin in nanocomposite films produced slightly yellowish films. However, this effect was balanced by the incorporation of ZnO nanoparticles, resulting in a whitish coloration.

SEM and AFM images showed that ZnO nanoparticles exhibited good intercalation in MC matrix and the addition of pediocin in high concentrations resulted in the formation of crater-like pits in nanocomposite film surface. The swelling degree of nanocomposite films was significantly diminished compared to control due to ZnO nanoparticles. Also, incorporation of ZnO in higher concentration allowed enhanced thermal stability when compared to control and nancomposite film with high concentration of pediocin.

Developed nanocomposite films presented antimicrobial activity against *L. monocytogenes* and *S. aureus*.

Based on the results of the desirability function analysis, optimal concentrations of tested antimicrobials are 20 % (w/w) ZnO nanoparticles and 15 % (w/w) pediocin. The results of this research indicated the potential use of developed nanocomposite films for the control of these food borne pathogens. Finally, more studies are needed to test the antimicrobial activity of developed nanocomposite films on food matrixes.

ACKNOWLEDGMENTS

The authors thank Mr. Nicholas J. Walker for providing language help and writing assistance, Professor Maurício P.F. Fontes for the XRD analysis and Professor Angélica C.O Carneiro for TGA analysis. The authors gratefully acknowledge the financial support for this research provided by a doctoral scholarship from Coordenação de Aperfeiçoamento de Pessoal de Nível Superior (CAPES) and a grant from Conselho Nacional de Desenvolvimento Científico e Tecnológico (CNPq).

5. REFERENCES

Abdollahi, M., Rezaei, M., & Farzi, G. (2012). A novel active bionanocomposite film incorporating rosemary essential oil and nanoclay into chitosan. *Journal of Food Engineering, 111*(2), 343-350.

Adams, L. K., Lyon, D. Y., & Alvarez, P. J. J. (2006). Comparative eco-toxicity of nanoscale TiO_2, SiO_2, and ZnO water suspensions. *Water Research, 40*(19), 3527-3532.

Arora, A., & Padua, G. W. (2010). Review: Nanocomposites in food packaging. *Journal of Food Science, 75*(1), R43-R49.

ASTM. (2008). ASTM E308 – 08 Standard practice for computing the colors of objects by using the CIE system. West Conshohocken, PA: ASTM International.

ASTM. (2009). ASTM D 882 – 09 Standard test method for tensile properties of thin plastic sheeting. West Conshohocken, PA: ASTM International.

ASTM. (2010). ASTM E313 – 10 Standard practice for calculating yellowness and whiteness indices from instrumentally measured color coordinates. West Conshohocken, PA: ASTM International.

Basch, C., Jagus, R., & Flores, S. (2012). Physical and antimicrobial properties of tapioca starch-HPMC edible films incorporated with nisin and/or potassium sorbate. *Food and Bioprocess Technology,* 10.1007/s11947-012-0860-3, 1-10.

Bastarrachea, L., Dhawan, S., & Sablani, S. (2011). Engineering properties of polymeric-based antimicrobial films for food packaging: A review. *Food Engineering Reviews, 3*(2), 79-93.

Bhunia, A. K., Johnson, M. C., & Ray, B. (1988). Purification, characterization and antimicrobial spectrum of a bacteriocin produced by *Pediococcus acidilactici*. *Journal of Applied Microbiology, 65*(4), 261-268.

Bhunia, A. K., Johnson, M. C., Ray, B., & Kalchayanand, N. (1991). Mode of action of pediocin AcH from *Pediococcus acidilactici* H on sensitive bacterial strains. *Journal of Applied Microbiology, 70*(1), 25-33.

Bourtoom, T., & Chinnan, M. S. (2008). Preparation and properties of rice starch–chitosan blend biodegradable film. *LWT - Food Science and Technology, 41*(9), 1633-1641.

Chandramouleeswaran, S., Mhaske, S. T., Kathe, A. A., Varadarajan, P. V., Prasad, V., & Vigneshwaran, N. (2007). Functional behaviour of polypropylene/ZnO–soluble starch nanocomposites. *Nanotechnology, 18*(385702), 8pp.

Coma, V. (2008). Bioactive packaging technologies for extended shelf life of meat-based products. *Meat Science, 78*(1–2), 90-103.

EPA. (2011). Municipal solid waste. Retrieved September 23, 2012, from http://www.epa.gov/osw/nonhaz/municipal/index.htm

Espinoza-Herrera, N., Pedroza-Islas, R., San Martín-Martinez, E., Cruz-Orea, A., & Tomás, S. (2011). Thermal, mechanical and microstructures properties of cellulose derivatives films: A comparative study. *Food Biophysics, 6*(1), 106-114.

Espitia, P., Soares, N. d. F., Coimbra, J. S. d. R., Andrade, N. J., Cruz, R. S., & Medeiros, E. A. A. (2012). Zinc oxide nanoparticles: Synthesis, antimicrobial activity and food packaging applications. *Food and Bioprocess Technology, 5*(5), 1447-1464.

FDA. (2011). Part 182 - Substances generally recognized as safe Retrieved 28 March, 2011, from http://ecfr.gpoaccess.gov/cgi/t/text/text-idx?c=ecfr&sid=786bafc6f6343634fbf79fcdca7061e1&rgn=div5&view=text&node=21:3.0.1.1.13&idno=21#21:3.0.1.1.13.9

Guiga, W., Swesi, Y., Galland, S., Peyrol, E., Degraeve, P., & Sebti, I. (2010). Innovative multilayer antimicrobial films made with Nisaplin® or nisin and cellulosic ethers: Physico-chemical characterization, bioactivity and nisin desorption kinetics. *Innovative Food Science and Emerging Technologies, 11*(2), 352-360.

Jin, T., Sun, D., Su, J. Y., Zhang, H., & Sue, H. J. (2009). Antimicrobial efficacy of zinc oxide quantum dots against *Listeria monocytogenes*, *Salmonella Enteritidis*, and *Escherichia coli* O157:H7. *Journal of Food Science, 74*(1), M46-M52.

Jipa, I. M., Stoica-Guzun, A., & Stroescu, M. (2012). Controlled release of sorbic acid from bacterial cellulose based mono and multilayer antimicrobial films. *LWT - Food Science and Technology, 47*(2), 400-406.

Lagarón, J. M., & Fendler, A. (2009). High water barrier nanobiocomposites of methyl cellulose and chitosan for film and coating applications. *Journal of Plastic Film and Sheeting, 25*(1), 47-59.

Li, X., Xing, Y., Jiang, Y., Ding, Y., & Li, W. (2009). Antimicrobial activities of ZnO powder-coated PVC film to inactivate food pathogens. *International Journal of Food Science & Technology, 44*(11), 2161-2168.

Li, X., Xing, Y., Li, W., Jiang, Y., & Ding, Y. (2010). Antibacterial and physical properties of poly(vinyl chloride)-based film coated with ZnO nanoparticles. *Food Science and Technology International, 16*(3), 225-232.

Liu, Y., & Kim, H.-I. (2012). Characterization and antibacterial properties of genipin-crosslinked chitosan/poly(ethylene glycol)/ZnO/Ag nanocomposites. *Carbohydrate Polymers, 89*(1), 111-116.

Ma, X., Chang, P. R., Yang, J., & Yu, J. (2009). Preparation and properties of glycerol plasticized-pea starch/zinc oxide-starch bionanocomposites. *Carbohydrate Polymers, 75*(3), 472-478.

Marcos, B., Aymerich, T., Monfort, J. M., & Garriga, M. (2010). Physical performance of biodegradable films intended for antimicrobial food packaging. *Journal of Food Science, 75*(8), E502-E507.

Nafchi, A. M., Alias, A. K., Mahmud, S., & Robal, M. (2012). Antimicrobial, rheological, and physicochemical properties of sago starch films filled with nanorod-rich zinc oxide. *Journal of Food Engineering, 113*(4), 511-519.

Premanathan, M., Karthikeyan, K., Jeyasubramanian, K., & Manivannan, G. (2011). Selective toxicity of ZnO nanoparticles toward Gram-positive bacteria and cancer cells by apoptosis through lipid peroxidation. *Nanomedicine: Nanotechnology, Biology and Medicine, 7*(2), 184-192.

Reddy, K. M., Feris, K., Bell, J., Wingett, D. G., Hanley, C., & Punnoose, A. (2007). Selective toxicity of zinc oxide nanoparticles to prokaryotic and eukaryotic systems. *Applied Physics Letters, 90*(21), 213902.

Rhim, J. W., Gennadios, A., Handa, A., Weller, C. L., & Hanna, M. A. (2000). Solubility, tensile, and color properties of modified soy protein isolate films. *Journal of Agricultural and Food Chemistry, 48*(10), 4937-4941.

Rimdusit, S., Jingjid, S., Damrongsakkul, S., Tiptipakorn, S., & Takeichi, T. (2008). Biodegradability and property characterizations of methyl cellulose: Effect of nanocompositing and chemical crosslinking. *Carbohydrate Polymers, 72*(3), 444-455.

Rodríguez, J. M., Martínez, M. I., & Kok, J. (2002). Pediocin PA-1, a wide-spectrum bacteriocin from lactic acid bacteria. *Critical Reviews in Food Science and Nutrition, 42*(2), 91-121.

Santiago-Silva, P., Soares, N. F. F., Nóbrega, J. E., Júnior, M. A. W., Barbosa, K. B. F., Volp, A. C. P., . . . Würlitzer, N. J. (2009). Antimicrobial efficiency of film incorporated with pediocin (ALTA® 2351) on preservation of sliced ham. *Food Control, 20*(1), 85-89.

Seo, J., Jeon, G., Jang, E. S., Bahadar Khan, S., & Han, H. (2011). Preparation and properties of poly(propylene carbonate) and nanosized ZnO composite films for packaging applications. *Journal of Applied Polymer Science, 122*(2), 1101-1108.

Soares, N. F. F., Pires, A. C. S., Camilloto, G. P., Santiago-Silva, P., Espitia, P. J. P., & Silva, W. A. (2009). Recent patents on active packaging for food application. *Recent Patents on Food, Nutrition & Agriculture, 1*(1), 171-178.

Srinivasa, P. C., Ramesh, M. N., Kumar, K. R., & Tharanathan, R. N. (2003). Properties and sorption studies of chitosan–polyvinyl alcohol blend films. *Carbohydrate Polymers, 53*(4), 431-438.

Srinivasa, P. C., Ramesh, M. N., & Tharanathan, R. N. (2007). Effect of plasticizers and fatty acids on mechanical and permeability characteristics of chitosan films. *Food Hydrocolloids, 21*(7), 1113-1122.

Teófilo, R. F., & Ferreira, M. M. C. (2006). Quimiometria II: planilhas eletrônicas para cálculos de planejamentos experimentais, um tutorial. *Química Nova, 29*, 338-350.

Tunç, S., & Duman, O. (2011). Preparation of active antimicrobial methyl cellulose/carvacrol/montmorillonite nanocomposite films and investigation of carvacrol release. *LWT - Food Science and Technology, 44*(2), 465-472.

Vicentini, D. S., Smania Jr, A., & Laranjeira, M. C. M. (2010). Chitosan/poly (vinyl alcohol) films containing ZnO nanoparticles and plasticizers. *Materials Science and Engineering: C, 30*(4), 503-508.

Yu, J., Yang, J., Liu, B., & Ma, X. (2009). Preparation and characterization of glycerol plasticized-pea starch/ZnO–carboxymethylcellulose sodium nanocomposites. *Bioresource Technology, 100*(11), 2832-2841.

SEGUNDA PARTE

Information is not knowledge. The only source of knowledge is experience.
Albert Einstein

ARTIGO CIENTÍFICO 5

ATIVIDADE ANTIMICROBIANA E PROPRIEDADES FÍSICO-MECÂNICAS DE FILMES COMESTÍVEIS A BASE DE AÇAÍ

Resumo

Este trabalho objetivou desenvolver filmes comestíveis a base de açaí incorporados com polifenóis obtidos de casca de maçã (ASP), óleo essencial de tomilho (TEO) e uma mistura de ambos, para a conservação de alimentos. A atividade antimicrobiana dos filmes comestíveis de açaí foi avaliada contra *Listeria monocytogenes*. Foi avaliado o efeito de ambos os agentes antimicrobianos sobre as propriedades físico-mecânicas dos filmes desenvolvidos. Os filmes incorporados com TEO, ASP e sua mistura, apresentaram atividade antimicrobiana contra *L. monocytogenes*. A adição de ASP resultou em maior resistência mecânica dos filmes, enquanto a incorporação de TEO diminuiu sua resistência. A incorporação de ASP ou TEO não teve efeito significativo na permeabilidade ao vapor de água dos filmes. Os filmes de açaí apresentaram tendência à luminosidade e vermelho, e a incorporação de ASP resultou no incremento desses parâmetros. Os filmes com ASP apresentaram estabilidade térmica melhorada. Entretanto, TEO causou uma rápida decomposição térmica dos filmes. Este trabalho demonstrou o potencial de aplicação de filmes a base de açaí na conservação de alimentos, devido à atividade antimicrobiana de ambos os compostos usados, bem como às suas boas propriedades físico-mecânicas.

Palavras-chave: Açaí, atividade antimicrobiana, filme comestível, óleo essencial de tomilho, pectina, polifenóis, propriedades mecânicas, resistência térmica.

Antimicrobial Activity and Physical-Mechanical Properties of Edible Films Based on Açaí Berries

Abstract

Açaí edible films incorporated with apple skin polyphenol (ASP), thyme essential oil (TEO) or their mixture were developed as antimicrobial active packaging for food preservation. Antimicrobial activity of açaí edible films against *Listeria monocytogenes* was evaluated. The effects of both antimicrobial compounds on physical-mechanical properties of açaí edible film, including mechanical properties, water vapor permeability, color, thermal stability and microstructure, were also assessed. Açaí edible films incorporated with TEO, ASP or their mixture showed antimicrobial activity against *L. monocytogenes*. Incorporation of both compounds in the films resulted in synergistic antimicrobial interaction. Addition of ASP resulted in improved mechanical properties, whereas incorporation of TEO diminished film mechanical resistance. Incorporation of ASP or TEO had no significant effect on water vapor permeability of films. Açaí edible films containing ASP were lighter and had more red color than the control film. Incorporation of ASP resulted in improved film thermal stability, whereas addition of TEO caused rapid thermal decomposition. Presence of clusters was observed on the surface of açaí edible films. Addition of ASP resulted in a smother surface, whereas addition of TEO led to the formation of crater-like pits on the film surface. The results of this study indicated that açaí edible films formulated with ASP and TEO have the potential to be used for food preservation due to their combined antibacterial activity as well as their good physical-mechanical properties.

Keywords: Edible film, pectin, açaí, antimicrobial activity, mechanical properties, thermal stability, polyphenols, thyme essential oil.

1. INTRODUCTION

Edible film research has undergone rapid expansion in the past twenty years, in part due to increased consumer interest in health, nutrition, food safety, and environmental issues. World production of plastic resins has increased

around 25-fold, with less than 5 % of all plastics being recycled, leading to a rapid accumulation of plastics in the environment (Sutherland et al., 2010).

Food wraps account for millions of tons of waste in landfills every year, putting a serious burden on the environment. As a result, biopolymers have emerged as an alternative to plastics, due to their biodegradability. Biopolymers have been studied for their film-forming properties to produce edible films in food packaging applications (Azeredo et al., 2009).

Edible films can be prepared from proteins, such as gelatin, whey protein, casein, and zein, and polysaccharides, such as starch, cellulose derivatives, alginates, and pectin. In this study, pectin and açaí berries have been used to produce antimicrobial edible films.

Pectin is a polysaccharide that is able to form cohesive and transparent films (Alves et al., 2011). This polysaccharide is a structural component of cell walls, which consists primarily of partially methyl esterified poly α-d-1,4-linked galacturonic acid (homogalacturonan, “smooth” ordered regions). Pectin also has kinks of (1→2)-linked α-l-rhamnose residues as “hairy” regions due to side chains of arabinogalactan I, constituting the disordered regions (Pérez et al., 2009). Moreover, pectin is an ingredient used in the food industry and is considered as generally recognized as safe (GRAS) by the U.S. Food and Drug Administration (FDA) (FDA 2012).

Pectin had been previously used in combination with fruit to produce edible films. In those studies, apple (Du et al., 2008a; Mild et al., 2011), tomato (Du et al., 2008b), carrot and hibiscus (Ravishankar et al., 2012) had been used as the primary ingredients for the preparation of edible films. However, to the best of our knowledge, there are no studies using açaí berries as the polymeric matrix for the development of edible films in food packaging.

Recently, açaí (*Euterpe oleracea*), a tropical fruit from Brazil, has received great attention due to the presence of bioactive compounds. Açaí is a palm berry, which is round and dark purple when mature, with an average diameter of 2 cm. Açaí berries are described as having a nutty flavor with lingering metallic undertones and a creamy, yet oily texture (Schreckinger et al., 2010). Studies of açaí berries regarding their phytochemical composition have revealed a variety of phenolic acids, anthocyanins, proanthocyanidins

and other flavonoids, which have high antioxidant capacity and potential anti-inflammatory effects (Kang et al., 2012). According to Azeredo et al., (2009), edible films produced with fruit can have sufficient mechanical and barrier properties along with the color and flavor provided by the pigments and volatile compounds of the fruit. Thus, açaí has potential to be used in conjunction with pectin as the polymeric matrix for the production of edible films in antimicrobial food packaging.

Antimicrobial packaging is a type of active packaging that interacts with the product to reduce, inhibit or retard the growth of microorganisms that may be present on food surfaces (Soares et al., 2009). To obtain packaging with antimicrobial properties, several antimicrobial compounds have been incorporated in polymeric matrixes. This includes apple skin polyphenols, which are flavoring components and listed ("apple essence, natural") as GRAS by the FDA. Apples contain a variety of phytochemicals, including quercetin, catechin, phloridzin and chlorogenic acid, all of which are strong antioxidants (Boyer & Liu 2004). Also, these phenolic compounds have shown antimicrobial activity against foodborne pathogens, such as *Escherichia coli* and *Staphylococcus aureus* (Alberto et al., 2006).

Moreover, essential oils (such as thyme essential oil) are natural substances and are also considered as GRAS by the FDA (López et al., 2007). Their biological effects, including antibacterial activity, antifungal activity, pharmaceutical and therapeutic potentials, have been previously reported (Bakkali et al., 2008; Edris 2007; Espitia et al., 2012).

In this study, edible films using açaí berries as the polymeric matrix were developed. The açaí edible films were incorporated with apple skin polyphenol and thyme essential oil. The antimicrobial activity of these edible films was tested against *L. monocytogenes*. The physical-mechanical properties of açaí edible films, including mechanical resistance, water vapor permeability, color properties, thermal stability and microstructure, were also evaluated.

2. MATERIALS AND METHODS

2.1 Edible Film Preparation

Açaí puree (Amafruits, Orland Park, IL) and pectin were the primary ingredient in all açaí-based film forming solutions. Glycerol, also known as vegetable glycerin (Starwest Botanical, Rancho Cordova, CA), was added as a plasticizing agent. Ascorbic acid (Bronson®, Lindon, UT) and citric acid (Archer Daniels Midland Co., Decatur, IL) were used as browning inhibitors. Pectin solution (3 % w/w) was prepared with high methoxyl (1400) pectin (Tic Gum, White Marsh, MD) and added to açaí puree.

Preparation of pectin and açaí solutions was done according to Ravishankar et al., (2012). The açaí film forming solution was prepared using the Kitchen Aid mixer by adding açaí puree (26 % w/w), citric acid (0.25 % w/w), ascorbic acid (0.25 % w/w) and vegetable glycerin (3 % w/w) to the pectin solution (70.5 % w/w) and mixing at low speed for 15 min. A control sample, which consisted of an edible film based only on pectin, was prepared for comparison purposes.

The film forming solution was homogenized in the Kinematica Polytron (Beckman Instruments Inc., Westbury, N.Y., U.S.A.) for 3 min at 20000-24000 rpm. The solution was then degassed under vacuum for 30 min before casting of the films.

The edible films were prepared by placing a polyethylene terephthalate film (PET) on a glass plate (30.5 × 30.5 cm), followed by pouring the film forming solution (60±1 g) on the PET film. The film was then cast using a draw down bar (45 mil = 1.143 mm). The edible films were dried for approximately 12±1 h at room temperature (23 to 25 ℃).

2.2 Antimicrobial Compounds

Apple skin polyphenol powder was an apple skin extract produced by Apple Poly LLC (Morrill, Nebr., U.S.A.) as Apple Poly brand. Thyme essential oil was obtained from Lhasa Karnak Herb Co. (Berkeley, Calif., U.S.A.). Both antimicrobial compounds were incorporated individually in the edible films at concentrations of 3 and 6 % (w/w), respectively. Moreover, to test the possible combined effect of the antimicrobial activity between these two

compounds, 6 % (w/w) of each antimicrobial compound was incorporated into the açaí edible film.

2.3 Edible Film Characterization

2.3.1 Antimicrobial activity

L. monocytogenes was obtained from University of California, Berkeley (our strain designation RM2199; original designation strain F2379) and was isolated from cheese associated with an outbreak. Frozen cultures of *L. monocytogenes* were streaked on Trypticase Soy Agar (TSA) and then incubated at 37 ℃ for 24 h. One isolated colony was re-streaked on TSA and then incubated at 37 ℃ for 24 h. This was followed by inoculating one isolated colony into a tube with 5 mL Trypticase Soy Broth (TSB) and incubating at 37 ℃ for 24 h with agitation. The microbial broth was then serially diluted (10×) in 0.1 % peptone water.

For overlay diffusion tests, 0.1 mL of 10^5 CFU/mL of bacterial culture was plated onto each of the TSA plates. The inoculum was spread evenly throughout each plate and then let to dry for 5 min. Following this, one edible film disc (12 mm diameter) was placed on the center of each previously inoculated TSA plate with the film's shiny side down. The plates were incubated at 37 ℃ for 24 h. The inhibition radius around the film disc (colony-free perimeter) was measured with a digital caliper (Neiko Tools, Ontario, Calif., U.S.A.) in triplicate after 24 h of incubation. The inhibition area was then calculated.

2.3.2 Film thickness

Film thickness was measured with a digital micrometer (Mitutoyo Manufacturing, Tokyo, Japan) at 5 random positions on the film samples for water vapor permeability (WVP) and tensile tests.

2.3.3 Mechanical properties

Mechanical properties of films were studied by characterizing the tensile properties: maximum load, tensile strength at break, elongation at break, and Young's modulus (elastic modulus). Tensile properties were measured

according to standard method D882-09 (ASTM 2009) using an Instron Model 55R4502 Universal Testing Machine (Instron, Canton, Mass., U.S.A.) with a 100 N load cell. The test speed was 10 mm/min and the distance between the grips was 10 cm. Ten specimens of edible films from each treatment were used for measuring tensile properties.

2.3.4 Water vapor permeability

The water vapor permeability of edible films was determined using the gravimetric modified cup method according to McHugh et al., (1993) based on the standard method ASTM (1980). Eight specimens of açaí edible films from each treatment were used for measuring water vapor permeability.

Cabinets used for measuring water vapor permeability were pre-equilibrated to 0 % relative humidity (RH) using calcium sulfate desiccant (drierite). Test cups made of poly(methyl methacrylate) (Plexiglas) were filled with 6 mL of deionized water to expose the film to a high water activity inside the test cups. The edible film was placed at the top of the cup. The sample film was sealed to the cup base with a ring containing a 19.6 cm^2 opening using four screws symmetrically located around the cup circumference. Eight weights were taken for each cup at 2 h intervals.

2.3.5 Colorimetric analysis

Color of edible films was measured using a Minolta Chroma Meter (Model CR-400, Minolta, Inc., Tokyo, Japan). The color was measured using the CIE L*, a* and b* coordinates and illuminant D65 and 10° observer angle. The instrument was calibrated using a Minolta standard white reflector plate. A total of 10 films were evaluated for each treatment and five readings were made for each replicate.

2.3.6 Thermogravimetric analysis

A thermogravimetric analyzer from TA Instruments TGA 2950 (New Castle, DE) was used to characterize the thermal stability of edible films. Sample from each treatment (10±1 mg) was heated to 800 ℃ at a rate of 10 ℃/min. The sample chamber was purged with nitrogen gas at a flow rate of 40

cm^3/min. Weight losses of samples were measured as a function of temperature. The derivative of TGA curves was obtained using TA analysis software.

2.3.7 Field emission scanning electron microscopy (FESEM)

Morphological analyses of edible films were done using a Hitachi S-4700 Field Emission Scanning Electron Microscope (FESEM, Hitachi, Tokyo, Japan). Samples were prepared by dropping a 1 cm^2 piece of film into liquid nitrogen and allowing the piece to equilibrate in the liquid nitrogen. The film piece was then fractured into several smaller pieces. Selected smaller pieces were mounted edge-up on a small aluminum cube, which was then mounted on a specimen stub using double adhesive coated carbon tabs (Ted Pella, Inc, Redding, Calif., U.S.A.). The samples were coated with gold-palladium in a Denton Desk II sputter coating unit (Denton Vacuum, LLC, Moorestown, N.J., U.S.A.). Finally, edible film samples were viewed in the FESEM. Images were captured at 2650x1920 pixel resolution.

2.3.8 Statistical analysis

Data from antimicrobial activity and physical-mechanical properties of edible films were evaluated by analysis of variance (ANOVA) and Tukey's multiple comparison tests at 95 % confidence level using the Statistical Analysis System (SAS) version 9.1 (SAS Inc., Cary, N.C., U.S.A.).

3. RESULTS AND DISCUSSION

3.1 Antimicrobial Activity

Açaí edible films incorporated with apple skin polyphenol, thyme essential oil or their mixture showed antimicrobial activity against *L. monocytogenes* (Figure 1).

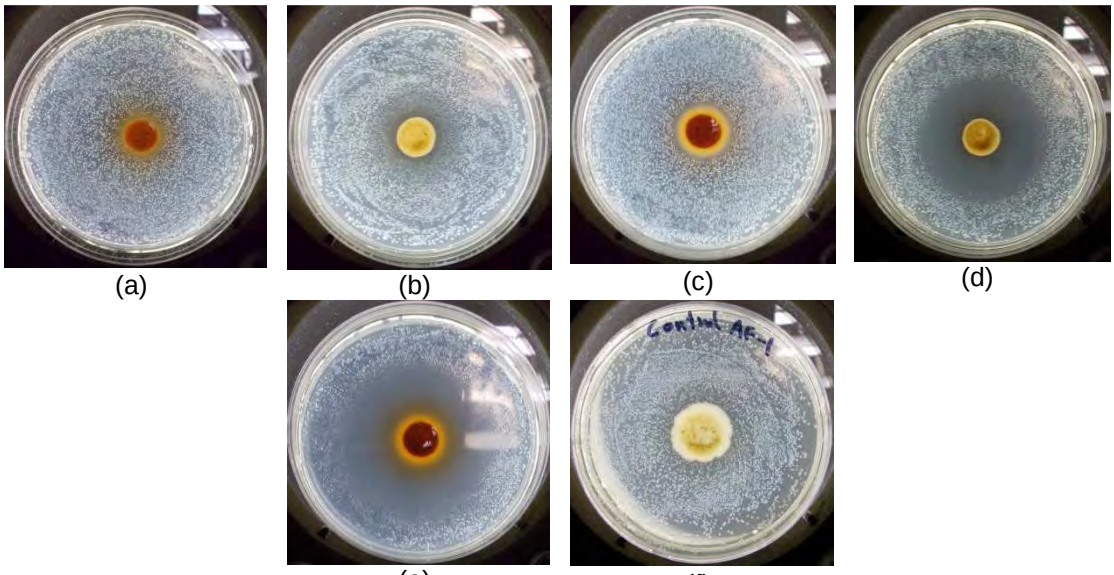

Figure 1. Antimicrobial activity against *L. monocytogenes* of edible films incorporated with 3 % (w/w) apple skin polyphenol (a), 3 % (w/w) thyme essential oil (b), 6 % (w/w) apple skin polyphenol (c), 6 % (w/w) thyme essential oil (d), combination of both antimicrobial at 6% (w/w) (e) and control film (f).

Statistical analysis indicated that antimicrobial activity was significantly different ($p<0.05$) among açaí edible films incorporated with the antimicrobial compounds (Table 1).

Table 1. Antimicrobial activity of açaí edible films incorporated with apple skin polyphenol and thyme essential oil

Treatment	Inhibition zone (mm^2)*
3 % ASP	42.45 ± 18.04^{c}
3 % TEO	37.83 ± 21.06^{c}
6 % ASP	108.52 ± 21.62^{c}
6 % TEO	844.36 ± 119.98^{b}
6 % ASP+ 6 %TEO	1297.75 ± 248.88^{a}

ASP: apple skin polyphenol; TEO: thyme essential oil. *Data reported are mean values ± standard deviation, mean values followed by the different letters are significantly different at $p<0.05$.

The high antimicrobial activity of plant and herb extracts has been recognized for centuries, resulting in their use as natural medicine. Recently, the antimicrobial activity of thyme essential oil has been widely studied, with

thymol and carvacrol being the two major flavor components in the oil responsible for its antimicrobial activity (Burt 2004; Tajkarimi et al., 2010).

Additionally, polyphenols are natural compounds with recognized antimicrobial, antioxidative and anti-inflammatory properties. These molecules are abundant in apples and are especially concentrated in the peel (Pastene et al., 2009). Apple skin polyphenols constitute ≥80 % polyphenols, 5-8 % phloridzin, 15-18 % chorogenic acid and ≥4 % proanthocyanidins B2 (data provided by supplier). Main polyphenols include procyanidin, catechin, epicatechin, chlorogenic acid and phlorizin; however, their fractions vary with variety, ripening degree, storage, processing and the degree to which the polyphenols are standardized (Boyer & Liu 2004; Du et al., 2011).

The açaí edible film incorporated with both antimicrobial compounds had the highest inhibition zone, indicating the potential benefit of combining apple skin polyphenol with thyme essential oil in edible films to control *L. monocytogenes*.

3.2 Mechanical Properties

Antimicrobial substances incorporated into a polymeric matrix have an important function in packaging since they constitute another barrier to microbial growth and contribute to food preservation. Therefore, mechanical properties of packaging materials incorporated with antimicrobials is essential for practical applications (Espitia et al., 2011).

The mechanical performance of açaí edible films was characterized by determining their maximum load, tensile strength, elongation and elastic modulus. The results showed that these properties were significantly different between treatments, except for elongation (Table 2).

Table 2. Mechanical properties of edible films based on açaí berries and pectin incorporated with apple skin polyphenol and thyme essential oil*

Treatment	Evaluated properties			
	Maximum load (N)	Tensile strength (MPa)	Elongation (%)	Elastic modulus (MPa)
ASP	5.501±0.315^{a}	2.742±0.498^{a}	67.341±15.802^{NS}	9.385±6.390^{ab}
TEO	1.207±0.004^{b}	0.593±0.108^{c}	89.176±9.227^{NS}	3.168±0.585^{c}
Control	1.423±0.323^{b}	1.430±0.347^{b}	99.125±42.537^{NS}	6.716±1.360^{bc}

ASP: 6 % (w/w) Apple skin polyphenol; TEO: 6 % (w/w) Thyme essential oil. *Data reported are mean values ± standard deviation, mean values in the same column followed by different letters are significantly different at $p<0.05$. ^{NS} No significant differences between films.

The addition of apple skin polyphenol resulted in the highest maximum load value. The tensile strength and elastic modulus also improved with the addition of apple skin polyphenol. These results are probably due to the presence of fiber in the apple skin polyphenol powder. Several researchers have reported that the dietary fiber content is higher in apple peel when compared to other edible parts of the fruit (Gorinstein et al., 2002; Leontowicz et al., 2003). Dietary fiber consists mainly of cellulose, hemicelluloses, lignins, pectins and gums. (Sudha et al., 2007). Henríquez et al., (2010) found that total dietary fiber (TDF) in apple peel represented about 47.8 % of the dry weight of Granny Smith apple peel. Moreover, they indicated that differences in TDF could be attributed to different evaluated cultivars and different fruit growing conditions.

Studies have shown that incorporation of fibers in biodegradable polymers can improve their mechanical properties. Luo & Netravali (1999) reported that pineapple fibers improved the tensile strength of poly(hydroxybutyrate-co-valerate) (PHBV), a biodegradable polymer produced from a wide range of microorganisms. Also, they indicated that compared to virgin PHBV resin, composites incorporated with 30 % pineapple fibers showed an increase in Young's modulus. Moreover, the incorporation of cotton fiber or coconut husk fiber (whisker) into edible fruit films improved their overall tensile properties (Azeredo et al., 2012).

In contrast, the incorporation of thyme essential oil resulted in intermediate values of maximum load, and in the lowest values of elastic modulus and

tensile strength. Similar results were observed by Espitia et al., (2011), who incorporated oregano, cinnamon and lemongrass essential oil in cellulose acetate films. They found that the maximum load at break of the films decreased with addition of each essential oil. The diminished mechanical properties were attributed to the plasticization effect of these essential oils in the polymeric matrix (Espitia et al., 2011).

3.3 Water Vapor Permeability

The water vapor permeability (WVP) results showed significant differences among treatments (Table 3).

Table 3. Water vapor permeability of edible films based on açaí berries and pectin incorporated with apple skin polyphenol and thyme essential oil*

Treatment	Film thickness (mm)	Relative humidity inside the cups (% RH)	Water vapor permeability ($g \cdot mm/kPa \cdot h \cdot m^2$)
ASP	0.199 ± 0.034^{a}	84.5 ± 0.9^{a}	3.64 ± 0.56^{a}
TEO	0.137 ± 0.016^{b}	81.7 ± 2.2^{b}	3.09 ± 0.45^{ab}
Control	0.101 ± 0.008^{c}	79.4 ± 2.6^{b}	2.62 ± 0.40^{b}

ASP:6 % (w/w) Apple skin polyphenol; TEO: 6 % (w/w) Thyme essential oil. *Data reported are mean values ± standard deviation, mean values in the same column followed by different letters are significantly different at $p < 0.05$.

Edible films incorporated with apple skin polyphenol had the highest thickness, followed by edible films incorporated with thyme essential oil. These results indicated that the addition of antimicrobials altered the thickness and microstructure of the films. This was later confirmed by microscopic analysis.

Furthermore, the higher WVP of the edible films with apple skin polyphenol can be explained by the higher relative humidity at the film underside. This was probably due to differences in film thickness. Consequently, we conclude that addition of apple skin polyphenol and thyme essential oil should not affect WVP of the films if the thickness of all treatments is maintained at the same value.

3.4 Colorimetric Analysis

The colorimetric parameters, L*, a* and b*, showed significant differences among açaí edible films (Table 4).

Table 4. Effect of apple skin polyphenol and thyme essential oil on color parameters of açaí edible films[1]

Treatment	Colorimetric parameters		
	L*	a*	b*
ASP	27.71±0.13[a]	8.14±0.35[a]	2.27±0.16[b]
TEO	25.41±0.32[c]	3.74±0.11[c]	2.35±0.14[b]
Control	25.87±0.17[b]	4.45±0.08[b]	2.61±0.12[a]

ASP:6 % (w/w) Apple skin polyphenol; TEO: 6 % (w/w) Thyme essential oil. [1]Data reported are mean values ± standard deviation, mean values in the same column followed by different letters are significantly different at $p<0.05$.

The color parameter L* is a measurement of the lightness or darkness of the film. Its value ranges from 0 to 100 as indication of dark to light. All treatments were significantly different from each other. The incorporation of apple skin polyphenol resulted in lighter films, whereas the addition of thyme essential oil resulted in darker films.

Positive values of the colorimetric parameter a* indicate the redness of the material, whereas negative values indicate greenness. The addition of apple skin polyphenol resulted in the highest value of a*. This result was expected since the natural color of apple skin polyphenol is red. The control film had an intermediate value, whereas the presence of thyme essential oil showed a decrease in this color parameter.

The natural color of açaí berries is green when immature. However, açaí has a dark purple color when ripe (Pompeu et al., 2009). Two predominant anthocyanins, cyanidin-3-rutino-side and cyanidin-3-glucoside, are responsible for most of açaí's characteristic dark purple color, and are often a major source of color in açaí-containing juices and beverages (Pacheco-Palencia & Talcott 2010). Anthocyanins have been categorized as the most important group of water-soluble pigments in plants and are responsible for most blue, red, and related colors in flowers and fruits (Clifford 2000). Thus,

the natural red color of açaí edible films resulted from anthocyanins present naturally in açaí pulp. The red color of apple skin polyphenols also contributed to the increase in this parameter.

In addition, positive values of b* indicate yellowness, whereas negative values indicate blueness. The incorporation of both antimicrobial compounds resulted in reduced values of b* when compared to control.

3.5 Thermogravimetric Analysis

The thermal stability of açaí edible films and of individual components used in the preparation of the edible films was investigated by thermogravimetric analysis. The thermograms shown in Figure 2 indicate that each component had an initial weight loss at temperatures ranging from 50-100 ℃, which corresponds to water loss. After this, a maximum decomposition step was observed at a temperature around 226 ℃ for pectin powder, 347 ℃ for açaí, 274 ℃ for pure apple skin polyphenol and 125 ℃ fo r pure thyme essential oil from the derivative thermogravimetric (DTG) curves (data not shown).

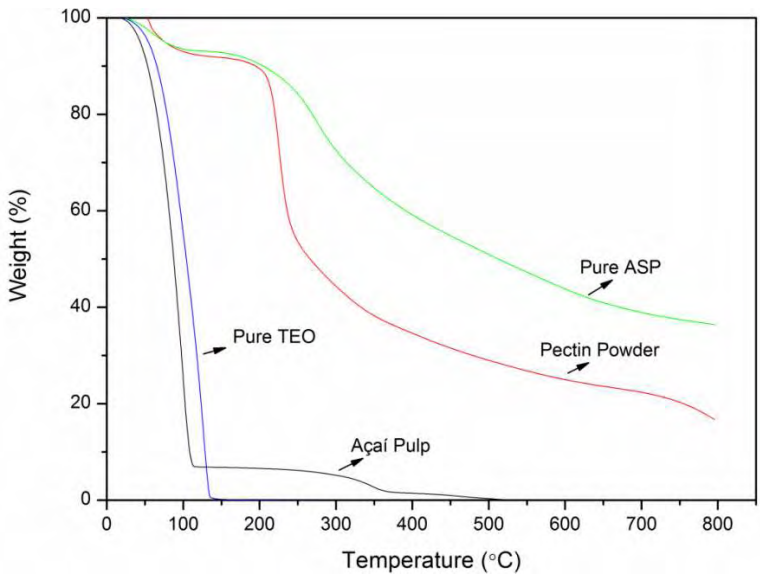

Figure 2. Thermograms of main components used for the production of edible films based on açaí berries and pectin: açaí pulp, pectin powder, apple skin polyphenol (ASP) and thyme essential oil (TEO).

These results are in agreement with previous work. Gohil (2011) reported that maximum weight loss of pectin occurred at 220°C. Pectin decomposition in the range from 200 to 400 ℃ was related to degr adation from pyrolytic decomposition (Mangiacapra et al., 2006). The high decomposition temperature observed for açaí is related to açaí fiber. According to Martins et al., (2008), cellulose and lignin have decomposition peaks around 340 ℃.

Açaí and apple skin polyphenol were the most thermally stable components. Although açaí had the highest thermal decomposition temperature, apple skin polyphenol and pectin powder suffered lower total weight losses. Pure thyme essential oil had the lowest thermal decomposition temperature due to its volatile nature.

Moreover, açaí edible films prepared for each treatment followed a similar trend observed in the thermograms of the individual components (Figure 3). The açaí edible film incorporated with 6 % (w/w) apple skin polyphenol had the highest remaining weight (22.9 %), indicating the highest thermal stability. This is probably due to the presence of fibers from apple peel.

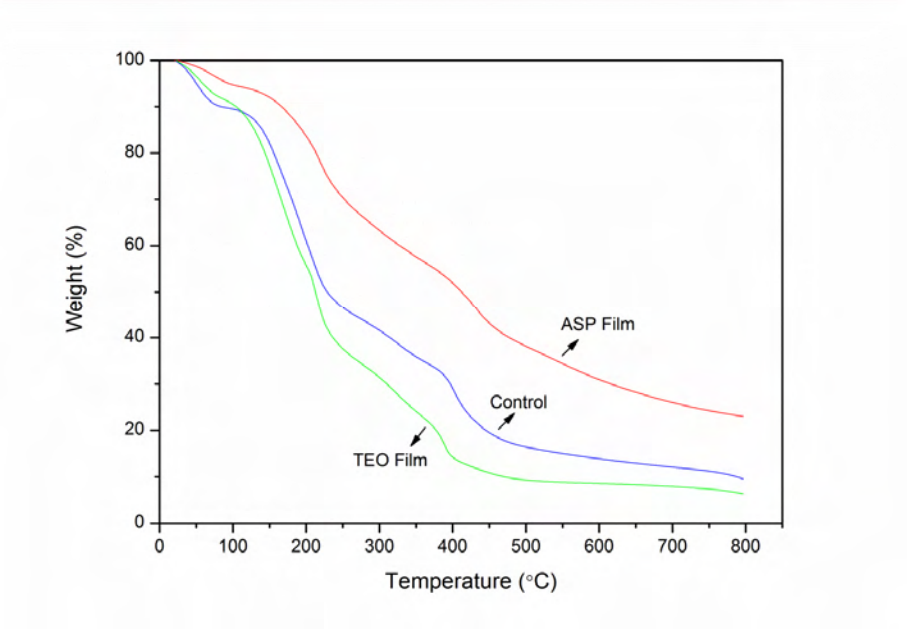

Figure 3. Thermograms of different treatments of edible films based on açaí berries and pectin: pectin film; edible film incorporated with 6 % (w/w) apple skin polyphenol (ASP); and 6 % (w/w) thyme essential oil (TEO).

Previous studies have shown the relationship between increased thermal stability and fiber content in films. Lu et al., (2008) observed that the incorporation of microfibrillated cellulose resulted in slightly increased thermal stability of polyvinyl alcohol composite films. Moreover, Visakh et al., (2012) reported that the thermal stability of natural rubber (latex) nanocomposites improved with increasing content of fiber from waste bamboo cellulose pulp.

The control film showed intermediate thermal stability between the ASP and TEO films. The slightly higher thermal stability of the control film compared to the thyme essential oil film resulted from the presence of açaí fibers and the absence of the highly volatile oil in the polymeric matrix. According to the açaí pulp supplier, açaí pulp has 12 % fiber. Moreover, Martins et al., (2008) reported that açaí is almost round (1-2 cm diameter) with a smooth external epidermis (peel) and contains one light brown seed, which is about 80 % of the fruit size. It is covered with a layer of rough fibers and a small edible layer of pulp (Figure 4).

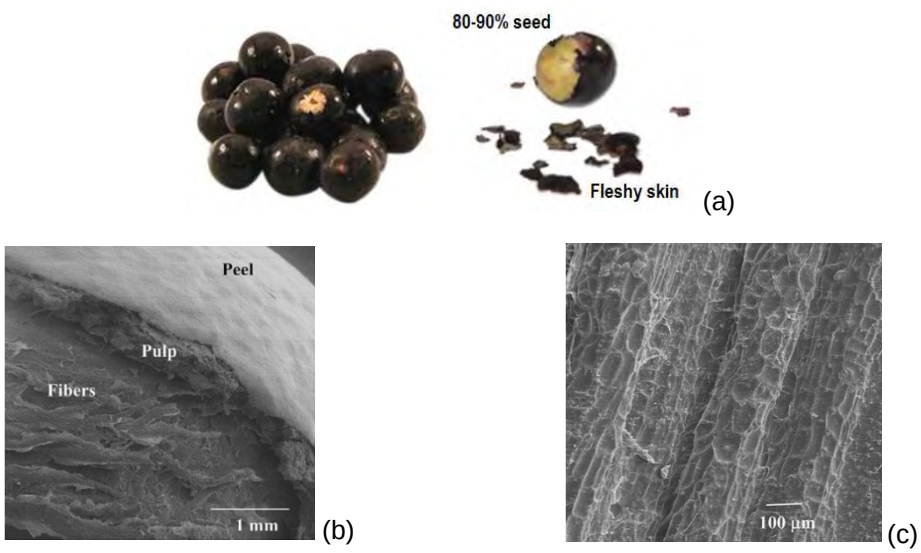

Figure 4. Images of açaí berries (a) and scanning electron micrographs (SEM) of the cross section of açaí berry (b*) and açaí fibers (c*). *Images from Martins et al. (2008).

In addition, açaí edible film incorporated with thyme essential oil had the lowest thermal stability. This film had the highest weight loss (93.71 % mass lost) at the end of the analysis. Tongnuanchan et al., (2012) had shown that fish skin gelatin film incorporated with citrus essential oils (bergamot, kaffir

lime, lemon and lime essential oils) had lower thermal degradation temperature and higher weight loss than the control film.

3.6 Field Emission Scanning Electron Microscopy (FESEM)

The control film showed a heterogeneous surface and protruding structures with the presence of clusters, probably as a result of the fleshy açaí skin and fiber (Figure 5.a). The protrusions were more evident in the cross section of the film (Figure 5.b). The images showed that the protrusions were large, thickened portions of the film. The formation of the thickened areas was due to açaí rather than pectin. This was verified by the neat pectin film, which was more homogenous and lacked the thickened areas (Figure 5.c and d) found in the açaí films.

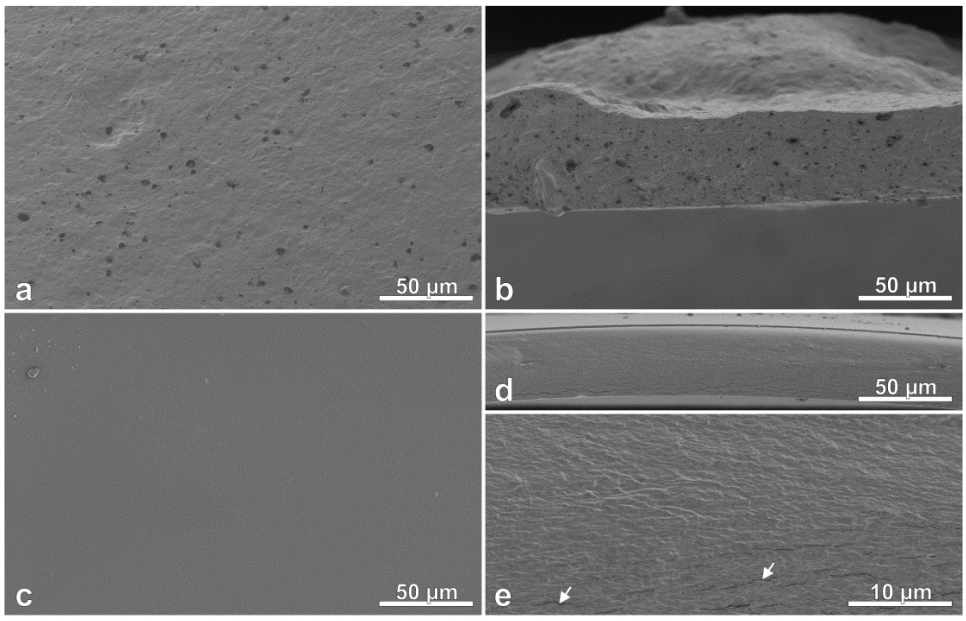

Figure 5. FESEM photomicrograph of edible film based on açaí berries and pectin (a-b) and neat pectin film (c-e).

These results agree with those of Giancone et al., (2011), who found that pectin films contained tightly packed clusters. Their micrographs were taken using a conventional SEM, whereas the micrographs in this study were taken using a field emission SEM. The conditions in the present study allowed for the visualization of finer surface details than those from a conventional SEM. Nevertheless, the micrographs from the two types of SEM's were quite

similar. Figure 5.e showed the tightly packed structures as well as the hairline separations of pectin film. These were probably artifacts resulting from compression stress (arrows) due to the pressure exerted on the film during fracture with liquid nitrogen.

Moreover, the photomicrograph of the açaí edible film containing 6 % (w/w) apple skin polyphenol had a smoother surface than the control film (Figure 6.a). However, there are pits in the inner structure of the edible film (Figure 6.b).

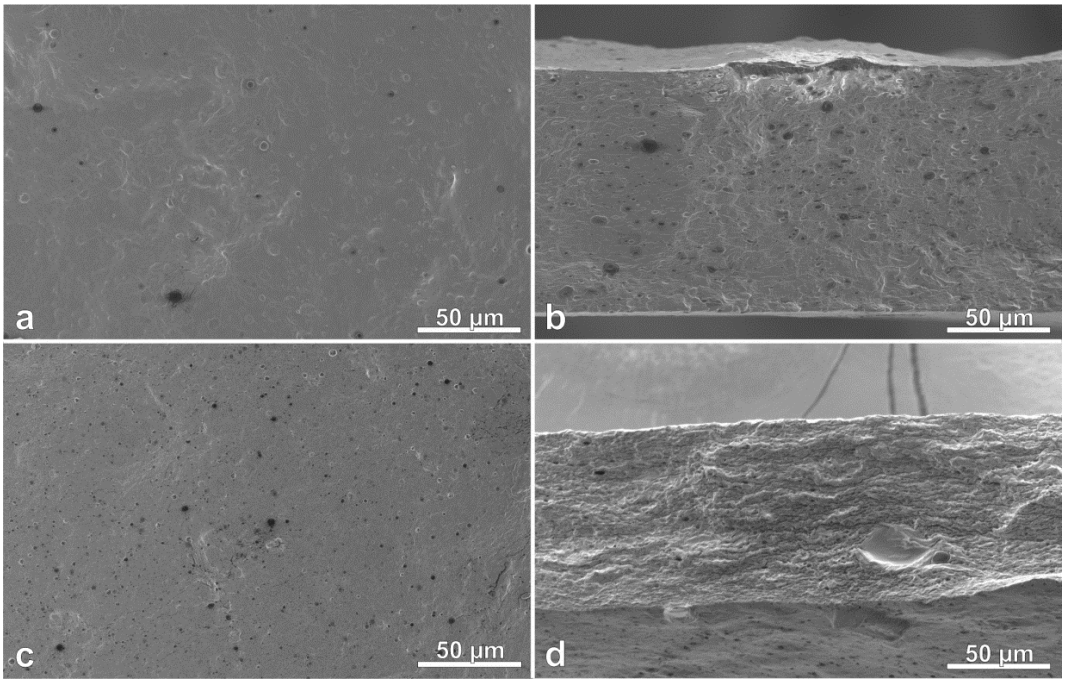

Figure 6. FESEM photomicrograph of edible film based on açaí berries and pectin incorporated with 6 % (w/w) of apple skin polyphenol (a-b) and 6 % (w/w) of thyme essential oil (c-d).

The surface of the açaí edible film containing 6 % (w/w) thyme essential oil showed crater-like pits on its surface (Figure 6.c) and linear structures in the cross section (Figure 6.d). There were also fewer inner pits compared with the other films. Crater-like pits on surfaces of pectin-based films have been previously reported by Murillo-Martínez et al., (2011), who developed edible films from emulsion of mineral oil and water, stabilized with low-methoxyl pectin-whey protein isolate complex. They indicated that the oriented

microstructure of the films consisted mainly of fibrous-like structures attributed to aggregates of the biopolymers and the presence of voids originally occupied by the relatively large-sized droplets of the emulsion.

4. CONCLUSIONS

A new antimicrobial food packaging material for food preservation applications was developed by the incorporation of thyme essential oil and apple skin polyphenols into an edible polymeric matrix based on açaí berries and pectin. Açaí edible films incorporated with thyme essential oil, apple skin polyphenol or the mixture of both compounds showed antimicrobial activity against *L. monocytogenes*. Moreover, the açaí edible film with both antimicrobial compounds showed combined antimicrobial effect. Mechanical properties of açaí edible films improved after addition of apple skin polyphenol, whereas incorporation of thyme essential oil resulted in weaker mechanical properties. Water vapor permeability was not affected by incorporation of apple skin polyphenol or thyme essential oil in açaí edible films. Açaí edible films had a natural red color due to natural anthocyanins present in açaí pulp. Moreover, the reddish color from apple skin polyphenols contributed to increase in lightness and redness of the films. TGA analyses showed that açaí and apple skin polyphenol were the most thermally stable components. Therefore, incorporation of apple skin polyphenol resulted in improved thermal stability of films, whereas incorporation of thyme essential oil caused rapid thermal decomposition. FESEM images showed the presence of clusters in the control film, resulting in a heterogeneous film surface. This effect was diminished by incorporation of apple skin polyphenol, which resulted in a smother surface. Incorporation of thyme essential oil resulted in the formation of crater-like pits on the film surface. This study showed the potential application of antimicrobial açaí edible films in food preservation applications due to synergistic effects of the antibacterial compounds. Also, the films had good physical-mechanical properties. Finally, further studies are needed to examine the synergistic behavior of the antimicrobial compounds in açaí edible films.

ACKNOWLEDGMENTS

The authors thank Mr. Carl Olsen (PFR Unit, USDA/ARS) for providing technical support. The authors gratefully acknowledge the financial support for this research provided by a doctoral scholarship from Coordenação de Aperfeiçoamento de Pessoal de Nível Superior (CAPES).

5. REFERENCES

Alberto MR, Canavosio MAR & Nadra MCMd (2006) Antimicrobial effect of polyphenols from apple skins on human bacterial pathogens. Electronic Journal of Biotechnology, 9 (3), 205-209.

Alves VD, Castelló R, Ferreira AR, Costa N, Fonseca IM & Coelhoso IM (2011) Barrier properties of carrageenan/pectin biodegradable composite films. Procedia Food Science, 1 (0), 240-245.

ASTM (1980) ASTM E96-80. Standard test methods for water vapor transmission of materials. ASTM International, Philadelphia, PA.

ASTM (2009) ASTM D 882 – 09. Standard test method for tensile properties of thin plastic sheeting. ASTM International, West Conshohocken, PA.

Azeredo HMC, Mattoso LHC, Wood D, Williams TG, Avena-Bustillos RJ & McHugh TH (2009) Nanocomposite edible films from mango puree reinforced with cellulose nanofibers. Journal of Food Science, 74 (5), N31-N35.

Azeredo HMC, Miranda KWE, Rosa MF, Nascimento DM & de Moura MR (2012) Edible films from alginate-acerola puree reinforced with cellulose whiskers. LWT - Food Science and Technology, 46 (1), 294-297.

Bakkali F, Averbeck S, Averbeck D & Idaomar M (2008) Biological effects of essential oils – A review. Food and Chemical Toxicology, 46 (2), 446-475.

Boyer J & Liu RH (2004) Apple phytochemicals and their health benefits. Nutrition Journal, 3 (5), 1-15.

Burt S (2004) Essential oils: their antibacterial properties and potential applications in foods—A review. International Journal of Food Microbiology, 94 (3), 223-253.

Clifford MN (2000) Anthocyanins – nature, occurrence and dietary burden. Journal of the Science of Food and Agriculture, 80 (7), 1063-1072.

Du W-X, Olsen CW, Avena-Bustillos RJ, McHugh TH, Levin CE & Friedman M (2008a) Storage stability and antibacterial activity against *Escherichia coli* O157:H7 of carvacrol in edible apple films made by two different casting methods. Journal of Agricultural and Food Chemistry, 56 (9), 3082-3088.

Du WX, Olsen CW, Avena-Bustillos RJ, Friedman M & McHugh TH (2011) Physical and antibacterial properties of edible films formulated with apple skin polyphenols. Journal of Food Science, 76 (2), M149-M155.

Du WX, Olsen CW, Avena-Bustillos RJ, McHugh TH, Levin CE & Friedman M (2008b) Antibacterial activity against *E. coli* O157:H7, physical properties, and storage stability of novel carvacrol-containing edible tomato films. Journal of Food Science, 73 (7), M378-M383.

Edris AE (2007) Pharmaceutical and therapeutic potentials of essential oils and their individual volatile constituents: a review. Phytotherapy Research, 21 (4), 308-323.

Espitia PJP, Soares NDFF, Botti LCM & Silva WA (2011) Effect of essential oils in the properties of cellulosic active packaging. Macromolecular Symposia, 299-300 (1), 199-205.

Espitia PJP, Soares NFF, Botti LCM, Melo NR, Pereira OL & Silva WA (2012) Assessment of the efficiency of essential oils in the preservation of postharvest papaya in an antimicrobial packaging system. Brazilian Journal of Food Technology, 15, 333-342.

FDA (2012) Part 184 - Direct Food Substances Affirmed As Generally Recognized As Safe. Food and Drug Administration. Available at: http://www.accessdata.fda.gov/scripts/cdrh/cfdocs/cfCFR/CFRSearch.cfm?fr=184.1588. Accessed 20 Dember 2012.

Giancone T, Torrieri E, Di Pierro P, Cavella S, Giosafatto CL & Masi P (2011) Effect of surface density on the engineering properties of high

methoxyl pectin-based edible films. Food & Bioprocess Technology, 4 (7), 1228-1236.

Gohil RM (2011) Synergistic blends of natural polymers, pectin and sodium alginate. Journal of Applied Polymer Science, 120 (4), 2324-2336.

Gorinstein S, Martin-Belloso O, Lojek A, Číž M, Soliva-Fortuny R, Park Y-S, Caspi A, Libman I & Trakhtenberg S (2002) Comparative content of some phytochemicals in Spanish apples, peaches and pears. Journal of the Science of Food and Agriculture, 82 (10), 1166-1170.

Henríquez C, Speisky H, Chiffelle I, Valenzuela T, Araya M, Simpson R & Almonacid S (2010) Development of an ingredient containing apple peel, as a source of polyphenols and dietary fiber. Journal of Food Science, 75 (6), H172-H181.

Kang J, Thakali KM, Xie C, Kondo M, Tong Y, Ou B, Jensen G, Medina MB, Schauss AG & Wu X (2012) Bioactivities of açaí (*Euterpe precatoria* Mart.) fruit pulp, superior antioxidant and anti-inflammatory properties to *Euterpe oleracea* Mart. Food Chemistry, 133 (3), 671-677.

Leontowicz M, Gorinstein S, Leontowicz H, Krzeminski R, Lojek A, Katrich E, Číž M, Martin-Belloso O, Soliva-Fortuny R, Haruenkit R & Trakhtenberg S (2003) Apple and pear peel and pulp and their influence on plasma lipids and antioxidant potentials in rats fed cholesterol-containing diets. Journal of Agricultural and Food Chemistry, 51 (19), 5780-5785.

López P, Sánchez C, Batlle R & Nerín C (2007) Development of flexible antimicrobial films using essential oils as active agents. Journal of Agricultural and Food Chemistry, 55 (21), 8814-8824.

Lu J, Wang T & Drzal LT (2008) Preparation and properties of microfibrillated cellulose polyvinyl alcohol composite materials. Composites Part A: Applied Science and Manufacturing, 39 (5), 738-746.

Luo S & Netravali AN (1999) Interfacial and mechanical properties of environment-friendly “green” composites made from pineapple fibers and poly(hydroxybutyrate-co-valerate) resin. Journal of Materials Science, 34 (15), 3709-3719.

Mangiacapra P, Gorrasi G, Sorrentino A & Vittoria V (2006) Biodegradable nanocomposites obtained by ball milling of pectin and montmorillonites. Carbohydrate Polymers, 64 (4), 516-523.

Martins MA, Pessoa JDC, Gonçalves PS, Souza FI & Mattoso LHC (2008) Thermal and mechanical properties of the açaí fiber/natural rubber composites. Journal of Materials Science, 43 (19), 6531-6538.

McHugh TH, Avena-Bustillos R & Krochta JM (1993) Hydrophilic edible films: Modified procedure for water vapor permeability and explanation of thickness effects. Journal of Food Science, 58 (4), 899-903.

Mild RM, Joens LA, Friedman M, Olsen CW, McHugh TH, Law B & Ravishankar S (2011) Antimicrobial edible apple films inactivate antibiotic resistant and susceptible *Campylobacter jejuni* strains on chicken breast. Journal of Food Science, 76 (3), M163-M168.

Murillo-Martínez MM, Pedroza-Islas R, Lobato-Calleros C, Martínez-Ferez A & Vernon-Carter EJ (2011) Designing W1/O/W2 double emulsions stabilized by protein–polysaccharide complexes for producing edible films: Rheological, mechanical and water vapour properties. Food Hydrocolloids, 25 (4), 577-585.

Pacheco-Palencia LA & Talcott ST (2010) Chemical stability of açai fruit (*Euterpe oleracea* Mart.) anthocyanins as influenced by naturally occurring and externally added polyphenolic cofactors in model systems. Food Chemistry, 118 (1), 17-25.

Pastene E, Speisky H, Troncoso M, Alarcón J & Figueroa G (2009) *In vitro* inhibitory effect of apple peel extract on the growth of *Helicobacter pylori* and respiratory burst induced on human neutrophils. Journal of Agricultural and Food Chemistry, 57 (17), 7743-7749.

Pérez CD, Flores SK, Marangoni AG, Gerschenson LN & Rojas AM (2009) Development of a high methoxyl pectin edible film for retention of L-(+)-Ascorbic acid. Journal of Agricultural and Food Chemistry, 57 (15), 6844-6855.

Pompeu DR, Silva EM & Rogez H (2009) Optimisation of the solvent extraction of phenolic antioxidants from fruits of *Euterpe oleracea* using Response Surface Methodology. Bioresource Technology, 100 (23), 6076-6082.

Ravishankar S, Jaroni D, Zhu L, Olsen C, McHugh T & Friedman M (2012) Inactivation of *Listeria monocytogenes* on ham and bologna using pectin-based apple, carrot, and hibiscus edible films containing carvacrol and cinnamaldehyde. Journal of Food Science, 77 (7), M377-M382.

Schreckinger ME, Lotton J, Lila MA & Mejia EGd (2010) Berries from South America: A comprehensive review on chemistry, health potential, and commercialization. Journal of Medicinal Food, 13 (2), 233-246.

Soares NFF, Pires ACS, Camilloto GP, Santiago-Silva P, Espitia PJP & Silva WA (2009) Recent patents on active packaging for food application. Recent Patents on Food, Nutrition & Agriculture, 1 (1), 171-178.

Sudha ML, Baskaran V & Leelavathi K (2007) Apple pomace as a source of dietary fiber and polyphenols and its effect on the rheological characteristics and cake making. Food Chemistry, 104 (2), 686-692.

Sutherland WJ, Clout M, Côté IM, Daszak P, Depledge MH, Fellman L, Fleishman E, Garthwaite R, Gibbons DW, De Lurio J, Impey AJ, Lickorish F, Lindenmayer D, Madgwick J, Margerison C, Maynard T, Peck LS, Pretty J, Prior S, Redford KH, Scharlemann JPW, Spalding M & Watkinson AR (2010) A horizon scan of global conservation issues for 2010. Trends in Ecology & Evolution, 25 (1), 1-7.

Tajkarimi MM, Ibrahim SA & Cliver DO (2010) Antimicrobial herb and spice compounds in food. Food Control, 21 (9), 1199-1218.

Tongnuanchan P, Benjakul S & Prodpran T (2012) Properties and antioxidant activity of fish skin gelatin film incorporated with citrus essential oils. Food Chemistry, 134 (3), 1571-1579.

Visakh PM, Thomas S, Oksman K & Mathew AP (2012) Crosslinked natural rubber nanocomposites reinforced with cellulose whiskers isolated from bamboo waste: Processing and mechanical/thermal properties. Composites Part A: Applied Science and Manufacturing, 43 (4), 735-741.

ARTIGO CIENTÍFICO 6

OTIMIZAÇÃO DA FORMULAÇÃO DE POLIFENOIS DE CASCA DE MAÇÃ E ÓLEO ESSENCIAL DE TOMILHO EM FILMES COMESTÍVEIS ANTIMICROBIANOS DE AÇAÍ

Resumo

Este trabalho teve como objetivo desenvolver filmes comestíveis a base de açaí incorporados com polifenóis de casca de maçã (ASP) e óleo essencial de tomilho (TEO), utilizando o planejamento composto central e a metodologia de superfície de resposta. As principais propriedades físico-mecânicas dos filmes de açaí avaliadas foram: resistência mecânica, permeabilidade ao vapor de água (PVA), cor, estabilidade térmica e análise da microestrutura dos filmes, além da atividade antimicrobiana conta *Listeria monocytogenes*. Os filmes de açaí inibiram o crescimento de *L. monocytogenes*. A resistência mecânica dos filmes foi melhorada pela incorporação de ASP, enquanto TEO diminuiu essa propriedade. A PVA não foi influenciada pela incorporação dos antimicrobianos. A cor dos filmes de açaí foi influenciada pela incorporação de ambos os antimicrobianos e pela sua interação. A incorporação de ASP resultou na estabilidade térmica melhorada dos filmes. Os filmes com maior concentração de ASP apresentaram superfície mais suave. Já os filmes com concentração elevada de TEO apresentaram a formação de crateras na superfície.

Palavras-chave: Açaí, caracterização de embalagens, embalagem ativa de alimentos, filme comestível, *Listeria monocytogenes*, óleo essencial de tomilho, polifenóis de maçã.

Optimization of Apple Skin Polyphenols and Thyme Essential Oil Formulation on Açaí Antimicrobial Edible Films

Abstract

This work aimed to develop açaí edible films incorporated with apple skin polyphenols (ASP) and thyme essential oil (TEO) using the central composite design, response surface methodology and the desirability function for multi-response optimization. The antimicrobial activity of açaí edible films was evaluated against *Listeria monocytogenes*. The main physical-mechanical properties of açaí edible films, including mechanical resistance, water vapor permeability (WVP), color, thermal stability and microstructure, were also evaluated. Açaí edible films inhibited the growth of *L. monocytogenes*. Film mechanical resistance was improved by adding ASP, while TEO reduced resistance. Antimicrobial incorporation did not influence film WVP. Film color was influenced by the incorporation of both antimicrobials. The addition of ASP resulted in improved film thermal stability. ASP incorporation resulted in smoother surface of edible films while high TEO concentration resulted in crater-like pits.

Keywords: Açaí, characterization, food active packaging, edible film, *Listeria monocytogenes*, thyme essential oil, apple skin polyphenols.

1. INTRODUCTION

Waste contamination generated from domestic and industrial plastic use continues to grow, exacerbating environmental concerns, increasing interest in biopolymers, due to their biodegradability.

The film-forming properties of biopolymers have been studied in order to produce edible films intended for food packaging (Azeredo, Mattoso, Wood, Williams, Avena-Bustillos, & McHugh, 2009). Fruit purees have recently been studied as edible film-forming materials and according to Azeredo, Mattoso, Wood, Williams, Avena-Bustillos, and McHugh (2009) edible films produced from fruit purees can combine the mechanical and barrier properties from the film-forming components with the color and flavor provided by the fruit

pigments. Edible film production is an interesting and promising way of using the co-products of fruit processing.

Previous research in this area includes the development of edible films using pectin and tomatoes (Du, Olsen, Avena-Bustillos, McHugh, Levin, & Friedman, 2008a), apple (Du, Olsen, Avena-Bustillos, McHugh, Levin, & Friedman, 2008b), carrot and hibiscus as a polymeric base (Ravishankar, Jaroni, Zhu, Olsen, McHugh, & Friedman, 2012). Açaí fruit puree has the potential to be used with pectin to form a polymer matrix to develop edible films.

Açaí fibers have been used as reinforcement fillers in the production of recycled thermoplastics, such as high impact polystyrene cups and polyproplynene bottles (Castro, Dias, & Faria, 2010). However, there are few studies regarding the use of açaí pulp as a polymeric matrix for developing edible film intended as food packaging.

Açaí (*Euterpe oleracea* Mart.) is a tropical palm tree that occurs naturally in the Amazon region, especially in the city of Belém in Pará State, Brazil. Açaí berries are spherical grape-sized fruits, which are green when young and gradually become dark purple when ripe (Martins, Pessoa, Gonçalves, Souza, & Mattoso, 2008). Recently, açaí has attracted much attention due to its nutritional value, such as a high anthocyanins content as well as antioxidant and anti-inflammatory activities (Kang, et al., 2012; Kang, et al., 2011).

Edible films have been used to prevent moisture, lipid, solute, or aroma compound migration between foods and their environments as well as between different compartments in the same food (Bilbao-Sáinz, Avena-Bustillos, Wood, Williams, & McHugh, 2010). Moreover, edible films, when incorporated with antimicrobial compounds, have the potential to be used as antimicrobial active packaging to control foodborne pathogens and spoilage microorganisms, thus enhancing food safety and extending the shelf-life of packaged food.

In order to create packaging with antimicrobial properties, several antimicrobial compounds have been incorporated into polymeric matrixes. Among antimicrobials, polyphenol obtained from apple skin has emerged as

new natural alternative. Polyphenols are secondary metabolites of plants and are important determinants in the sensory and nutritional quality of fruits and vegetables (Ignat, Volf, & Popa, 2011). Polyphenols are classified according to their structure as phenolic acids derivatives, flavonoids, and tannins. Apple pulp contains catechin, procyanidin, caffeic acid and chlorogenic acid, while apple skin contains the forementioned substances as well as flavonoids not present in pulp, such as quercetin glycosides and cyanidin glycosides (Alberto, Canavosio, & Nadra, 2006).

Previous research has described the antimicrobial activity of phenolic compounds extracted from apple skin (Fratianni, Coppola, & Nazzaro, 2011). According to Ignat, Volf, and Popa (2011) these compounds have potential use as food preservatives and play important roles in protecting against pathological disturbances, including atherosclerosis, brain dysfunction and cancer.

Moreover, plant essential oils have been used for thousands of years, especially in food preservation, pharmaceuticals, alternative medicine and natural therapies. Essential oils are natural substances, generally recognized as safe (GRAS) by the U.S. Food and Drug Administration (López, Sánchez, Batlle, & Nerín, 2007). The ability of plant essential oils to protect foods against bacteria and fungi has been previously reported (Burt & Reinders, 2003; Espitia, Soares, Botti, Melo, Pereira, & Silva, 2012).

Although direct application of essential oils in food has shown potential for food preservation, it has some limitations due to the high concentrations needed to achieve antimicrobial activity in food matrixes, in some cases generating undesirable sensory quality. As a result, the incorporation of essential oils into edible films, which can be used in conjunction with other antimicrobials in the packaging system, has emerged as an alternative to food preservation.

The aim of this work was to develop antimicrobial edible films from açaí fruit formulated with both apple skin polyphenols and thyme essential oil. The influence of both compounds on the antimicrobial activity, physical-mechanical properties and microstructure of developed açaí edible films was

studied by means of the central composite design and statistical approaches of response surface methodology (RSM).

2. MATERIALS AND METHODS

2.1 Açaí Edible Film Elaboration

Açaí puree (Amafruits, Orland Park, IL) was the primary ingredient in all açaí-based film-forming solutions. Glycerol, also known as vegetable glycerin, (Starwest Botanical, Rancho Cordova, CA) was added as a plasticizing agent. Ascorbic acid (Bronson®, Lindon, UT) and citric acid (Archer Daniels Midland Co., Decatur, IL) were used as browning inhibitors. Pectin solution (3 % w/w) was prepared with high methoxyl (1400) pectin (Tic Gum, White Marsh, MD) and added to açaí puree to increase film strength and facilitate film release from cast surfaces. Preparation of açaí film-forming solution was done according to Ravishankar, Jaroni, Zhu, Olsen, McHugh, and Friedman (2012). Ingredient concentrations used in this formulation are shown (Table 1).

Table 1. Composition of açaí film forming solution

Ingredient	Concentration (%w/w)	Amount* (g)
Açaí puree	26	52
Pectin solution	70.5	141
Glycerol	3	6
Citric acid	0.25	0.5
Ascorbic acid	0.25	0.5

The açaí film-forming solution was prepared using a Kitchen Aid mixer by adding açaí puree, citric acid, ascorbic acid and vegetable glycerin to the pectin solution and mixing at low speed for 15 min. Açaí film-forming solution was homogenized on the Kinematica Polytron (Beckman Instruments Inc., Westbury, N.Y., U.S.A.) for 3 min at 20000-24000 rpm. Açaí film-forming solutions were degassed under vacuum for 30 min before used for film casting.

Açaí films were prepared by placing a polyethylene terephthalate film (PET) on a glass plate (30.5 × 30.5 cm), followed by placing the açaí film-forming solution (60±1 g) on the PET film. The film was cast using a draw down bar

(45 mil = 1.143 mm). Açaí edible films were dried for approximately 12±1 h at room temperature (23 to 25 ℃).

2.2 Antimicrobials

Apple skin polyphenol powder was an apple skin extract produced by Apple Poly LLC (Morrill, Nebr., U.S.A.) as Apple Poly brand. Thyme essential oil was obtained from Lhasa Karnak Herb Co. (Berkeley, Calif., U.S.A.).

2.3 Experimental Design and Statistical Analysis

Finding the optimum experimental conditions is more efficient when multivariate statistical techniques are employed since all variables (factors) are simultaneously considered, accompanied with significant experimental savings (Box & Draper, 1989; Teófilo & Ferreira, 2006).

To perform this task, experimental designs such as response surface methodology (RSM) are the procedures employed in the majority of optimization studies (Brereton, 2003). Experimental designs are helpful in determining the effects of individual variables (factors) and their interactions (Teófilo & Ferreira, 2006).

A central composite design (CCD) with two independent variables was the protocol chosen for carrying out the RSM. The design consisted of a total of 11 experiments: 4 in the factorial points, 4 in the axial points and 3 central points. The independent variables investigated were the concentration of apple skin polyphenols and thyme essential oil (Table 2).

Table 2. Variables and levels of antimicrobials incorporated in açaí edible films

Variables	Levels (% w/w)				
	-1.41	-1	0	1	+1.41
Apple skin polyphenols	0.13	1	3.1	5.2	6.07
Thyme essential oil	0.13	1	3.1	5.2	6.07

These ranges were selected based on prior knowledge about the system under study to asses in detail the interaction and synergistic effect of

incorporated antimicrobials on the physical-mechanical properties, microstructure and antibacterial activity of açaí edible films.

All experiments were performed randomly to minimize the effects of uncontrolled factors that may introduce bias. For the statistical analysis, the model coefficients were calculated by multiple linear regression and validated by analysis of variance (ANOVA). A control treatment was performed using açaí edible film without the incorporation of any antimicrobial. All calculations and graphs in this work were done using electronic spreadsheets from Microsoft® Excel 2003 according to Teófilo and Ferreira (2006).

2.4 Optimization by the Desirability Function Approach

After the elaboration of response surface models, a simultaneous optimization of significant response variables was done using the desirability function approach according to Derringer and Suich (1980). Each estimated response variable used in this work, calculated by the fitted response surface associated with the CCD experimental design, was transformed using the desirability function into a desirable value (d_i), using the following equation:

$$d_i = \begin{cases} 0 & \hat{y}_i \le y_{i\min} \\ \left[\dfrac{\hat{y}_i - y_{i\min}}{y_{i\max} - y_{i\min}} \right] & y_{i\min} < \hat{y}_i < y_{i\max} \\ 1 & \hat{y}_i \ge y_{i\max} \end{cases} \qquad \text{(eq. 1)}$$

Where the values y_{imin} and y_{imax} are the minimum and maximum acceptable value of $\hat{y}_i$ (each response variable), respectively. The values of d_i vary in the interval $0 \le d_i \le 1$, increasing as the desirability of the corresponding response increases. Each individual desirability was combined using the geometric mean (eq. 2) to give an overall desirability (D).

$$D = \left(d_1 \times d_2 \times \cdots \times d_k \right)^{1/k} \qquad \text{(eq. 2)}$$

The overall desirability was analyzed using a univariate search technique to optimize D over the independent variable domain, which resulted in the desirability of the combined response levels. In this work the desirability

function varied linearly between zero (undesirable response) to one (desirable response).

2.5 Açaí Edible Film Characterization

2.5.1 Antimicrobial activity against pathogenic bacteria

Listeria monocytogenes was obtained from the University of California Berkeley (our strain designation RM2199; original designation strain F2379) isolated from cheese associated with an outbreak. Frozen cultures of *L. monocytogenes* were streaked on Trypticase Soy Agar (TSA) and incubated at 37 ℃ for 24 h. One isolated colony was re-strea ked on TSA and incubated at 37 ℃ for 24 h. This was followed by inoculating one isolated colony into a tube with 5 mL Trypticase Soy Broth (TSB) and incubating at 37 ℃ for 24 h with agitation. The microbial broth was serially diluted (10×) in 0.1 % peptone water.

For overlay diffusion tests, 0.1 mL of 10^5 CFU/mL of bacterial culture were plated onto each of the TSA plates. The inoculum was spread evenly throughout each plate, then left to dry for 5 min. One açaí edible film disc (12 mm diameter) was placed on the center of each previously inoculated agar plate with the film's shiny side down. The plates were incubated at 37 ℃ for 24 h. The inhibition radius around the film disc (colony-free perimeter) was measured with a digital caliper (Neiko Tools, On-tario, Calif., U.S.A.) in triplicate after 24 h of incubation. The inhibition area was then calculated.

2.5.2 Film thickness

Film thicknesses was measured with a digital micrometer (Mitutoyo Manufacturing, Tokyo, Japan), at 5 random positions on the film samples for further analyses of water vapor permeability (WVP) and tensile tests.

2.5.3 Mechanical resistance

Mechanical resistance of açaí edible films was studied by determining the elastic modulus. Tensile properties was measured according to standard method D882-09 (ASTM 2009), using an Instron Model 55R4502 Universal Testing Machine (Instron, Canton, Mass., U.S.A.) with a 100 N load cell. The

test speed was 10 mm/min and the distance among the grips was 100 mm. Ten specimens of açaí edible film from each treatment were used for measuring tensile properties.

2.5.4 Water vapor permeability

The water vapor permeability (WVP) of açaí edible films was determined using the gravimetric modified cup method according to McHugh, Avena-Bustillos, and Krochta (1993) based on the standard method E96-80 (ASTM, 1980). Eight specimens of açaí edible films from each treatment were used to measure WVP.

Cabinets used for measuring WVP were pre-equilibrated to 0 % RH using calcium sulfate desiccant (drierite). Eight cups made of poly(methyl methacrylate) (Plexiglas) were filled with deionized water to expose the film to high water activity inside the cups. Samples of açaí edible films from each treatment were placed at the top of the cups. Sample films were sealed to the cup base with a ring containing a 19.6 cm^2 opening using four screws symmetrically located around the circumference of the cup. Eight measurements of weights were taken for each cup at 2 h intervals.

2.5.5 Colorimetric analysis

Color of açaí edible films was measured using a Minolta Chroma Meter (Model CR-400, Minolta, Inc., Tokyo, Japan). The color was measured using the CIE L*, a*, and b* coordinates. Illuminant D65 and 10° observer angle were used. The instrument was calibrated using a Minolta standard white reflector plate. Measurements were done according to Du, Olsen, Avena-Bustillos, McHugh, Levin, and Friedman (2008a). A total of 10 films were evaluated for each treatment and five readings were made in each replicate.

2.5.6 Thermogravimetric analysis

Thermal stability of developed açaí edible films was performed on a thermogravimetric analyzer (TGA 2950, TA Instruments, New Castle). Samples of each film (10±1 mg) were heated to 800 °C at a rate of 10 ℃/min. The sample chamber was purged with nitrogen gas at a flow rate of

40 cm^3/min. Weight losses of samples were measured as a function of temperature. The derivative of TGA curves was obtained using TA analysis software.

2.5.7 Field emission scanning electron microscopy

Morphological analyses of açaí edible films were done according to Azeredo, Mattoso, Wood, Williams, Avena-Bustillos, and McHugh (2009) using a Hitachi S-4700 Field Emission Scanning Electron Microscope (FESEM, Hitachi, Tokyo, Japan). Samples of açaí edible films were prepared by dropping a 1 cm^2 piece cut from the center of the film into liquid nitrogen and allowing the piece to equilibrate under the liquid nitrogen. The film piece was then fractured into several smaller pieces. Selected smaller pieces were mounted, edge-up on a small aluminum cube that was mounted on a specimen stub using double adhesive coated carbon tabs (Ted Pella, Inc, Redding, Calif., U.S.A.). The film samples were coated with gold-palladium in a Denton Desk II sputter coating unit (Denton Vacuum, LLC, Moorestown, N.J., U.S.A.). Finally, açaí edible film samples were viewed in the FESEM. Images were captured at 2650x1920 pixel resolution.

3. RESULTS AND DISCUSSION

3.1 Antimicrobial Activity

Açaí edible films presented antimicrobial activity against *L. monocytogenes* (Figure 1).

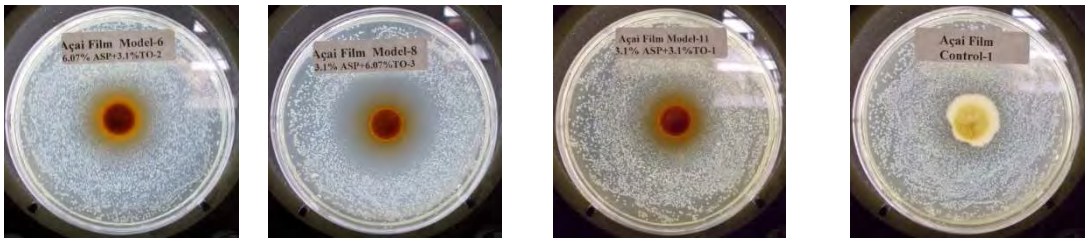

(a) (b) (c) (d)

Figure 1. Antimicrobial activity against *Listeria monocytogenes* of açaí edible films incorporated with 6.07 % (w/w) ASP and 3.1 % (w/w) TEO (a); 3.1 % (w/w) ASP and 6.07 % TEO (b); 3.1 % (w/w) of both antimicrobials (c) and control film (d). *ASP: Apple skin polyphenols; TEO: Thyme essential oil.

The antimicrobial activity of açaí edible films against *L. monocytogenes* was influenced by the linear effect of apple skin polyphenols concentration and the linear and quadratic effect of thyme essential oil concentration (*p<0.05*) according to the analysis of regression coefficients of the response function (Table 3).

Table 3. Coefficient estimates from CCD and statistical analysis for the antimicrobial activity of açaí edible films incorporated with apple skin polyphenols and thyme essential oil

Independent variable	Antimicrobial activity			
	Coefficient[a]	Std. err.	*t* (5)	*p*
Mean	***126.110***	21.044	5.993	0.001856
ASP	***40.015***	12.887	3.105	0.026696
TEO	***231.034***	12.887	17.928	0.000010
ASP²	16.307	15.338	1.063	0.336336
TEO^2	***122.238***	15.338	7.970	0.000502
ASP×TEO	32.365	18.224	1.776	0.135911

ASP: Apple skin polyphenols; TEO: Thyme essential oil. [a] Values in bold and italics are significant at α=0.05 with 5 degrees of freedom for the response variable.

The model was validated with ANOVA and results showed that the regression model for the antimicrobial activity presented statistical significance for tested açaí edible films, with a non-significant lack of fit (Table 4).

Table 4. ANOVA results for the antimicrobial activity of açaí edible films incorporated with apple skin polyphenols and thyme essential oil

Variation	Antimicrobial activity				
	SS[af]	df[b]	MS[c]	*F*[d]	*p*[e]
Regression	***530775.2***	5	106155.047	79.91	0.000091
Residues	6642.6	5	1328.512		
Lack of fit	6419.1	3	2139.698	19.15	0.050036
Pure Error	223.5	2	111.733		
Total SS	537417.8	10			

[a] Sum of squares; [b] Degree of freedom; [c] Mean squares; [d] *F* distribution; [e] *p* value; [f] Bold and italic values are significant at α = 0.05.

The effect of TEO against *L. monocytogenes* was stronger than the effect caused by ASP incorporation in açaí films. In addition, all coefficients were positive, indicating that increasing concentration of both antimicrobials allows high antimicrobial activity. Moreover, the significant quadratic coefficient for thyme essential oil indicates that the antimicrobial activity of developed edible films increases quadratically when the concentration of this antimicrobial increases (Figure 2).

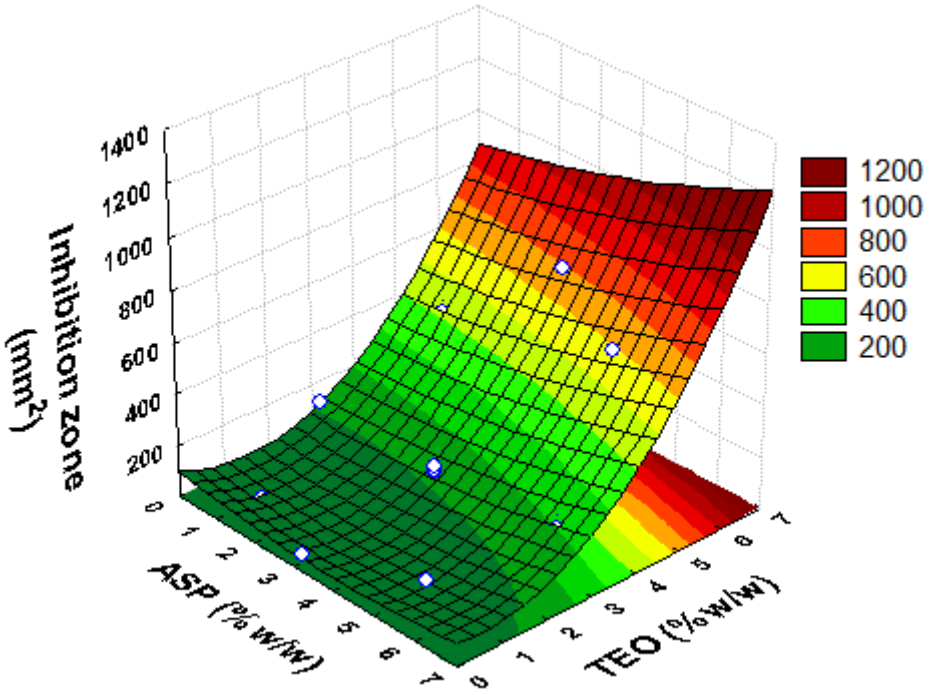

Figure 2. Response surface of antimicrobial activity against *Listeria monocytogenes* as a function of apple skin polyphenols (ASP; % w/w) and thyme essential oil (TEO; % w/w).

Previous works reported the antimicrobial activity of these natural compounds individually against food borne pathogens. Fratianni, Coppola, and Nazzaro (2011) reported the antimicrobial activity of ethanolic extracts of phenolic compounds from apple skin *in vitro* against *Bacillus cereus* and *Escherichia coli*, and Rounds, Havens, Feinstein, Friedman, and Ravishankar (2012) indicated antimicrobial activity of apple skin polyphenols against *E. coli* when incorporated directly in hamburger patties. Moreover, Du, Olsen, Avena-Bustillos, Friedman, and McHugh (2011) indicated that

apple skin polyphenols were highly effective against *L. monocytogenes* when incorporated in edible films made from apple.

Similarly, the antimicrobial activity of thyme essential oil has been previously reported. Govaris, Botsoglou, Sergelidis, and Chatzopoulou (2011) added thyme essential oil to feta cheese and observed the strong antimicrobial activity against *L. monocytogenes*. Moreover, Hosseini, Razavi, and Mousavi (2009) incorporated thyme essential oil in chitosan-based films and indicated its higher antimicrobial activity against *L. monocytogenes* compared to chitosan-based films containing clove and cinnamon essential oils.

The influence of apple skin polyphenols and thyme essential oil demonstrated the antimicrobial activity of both compounds after incorporation and mixture on açaí edible films. Thus, açaí edible films incorporated with a mixture of both natural compounds have potential application to control *L. monocytogenes*.

3.2 Mechanical Resistance

Packaging material resistance is important because this parameter describes the mechanical and structural properties of packaging materials (Espitia, Soares, Botti, & Silva, 2011). The mechanical performance of açaí edible films was studied by determining the elastic modulus (MPa).

The elastic modulus, a measure of the stiffness of the film, was influenced by the linear effect of apple skin polyphenols and thyme essential oil, as well as by the quadratic effect of thyme essential oil and the interaction of both antimicrobials ($p<0.08$) according to the analysis of regression coefficients of the response function (Table 5).

Table 5. Coefficient estimates from CCD and statistical analysis for the elastic modulus of açaí edible films incorporated with apple skin polyphenols and thyme essential oil

	Elastic modulus			
Independent variable	Coefficient[a]	Std. err.	*t* (5)	*p*
Mean	***4.958***	0.674	7.355	0.000729
ASP	***0.909***	0.413	2.203	0.078824
TEO	***-2.827***	0.413	-6.851	0.001012
ASP^2	-0.037	0.491	-0.076	0.942184
TEO^2	***2.17***	0.491	4.418	0.006908
ASP×TEO	***-2.652***	0.5837	-4.543	0.006154

ASP: Apple skin polyphenols; TEO: Thyme essential oil. [a] Values in bold and italics are significant at α=0.08 with 5 degrees of freedom for the response variable.

The model was validated with ANOVA and the results showed that the regression model for elastic modulus presented statistical significance among açaí edible films, with a non-significant lack of fit (Table 6).

Table 6. ANOVA results for the elastic modulus of açaí edible films incorporated with apple skin polyphenols and thyme essential oil

Variation	Elastic modulus				
	SS[af]	df[b]	MS[c]	*F*[d]	*p*[e]
Regression	***128.11***	5	25.622	18.801	0.00295
Residues	6.81	5	1.363		
Lack of fit	5.64	3	1.879	3.188	0.24784
Pure Error	1.18	2	0.589		
Total SS	134.92	10			

[a] Sum of squares; [b] Degree of freedom; [c] Mean squares; [d] *F* distribution; [e] *p* value; [f] Bold and italic values are significant at α = 0.05.

The linear regression coefficient of apple skin polyphenol is positive, indicating that increasing concentrations of this antimicrobial result in a stiffer film. On the other hand, the linear regression coefficient of thyme essential oil, which is negative, indicated that high concentrations of this antimicrobial result in low elastic modulus values of açaí edible films. Moreover, the significant quadratic coefficient of thyme essential oil indicates that the elastic modulus of açaí edible films increases quadratically when the concentration of this antimicrobial decreases (Figure 3).

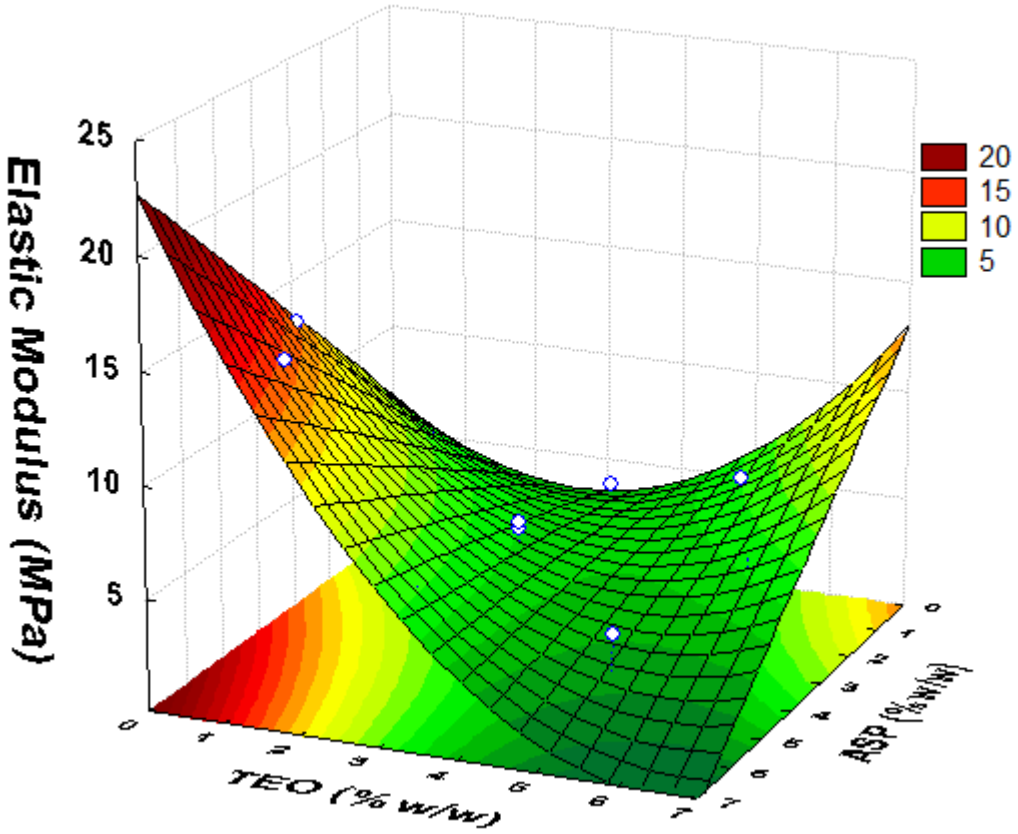

Figure 3. Response surface of elastic modulus as a function of apple skin polyphenols (ASP, % w/w) and thyme essential oil (TEO, % w/w).

In addition, the response surface shows that maximum value of elastic modulus can be achieved when concentration of apple skin polyphenols is the highest and thyme essential oil is equal to zero. These results indicate the antagonistic effect of thyme essential oil regarding the stiffness of açaí edible film.

High mechanical resistance of edible films corresponding to the increase in the concentration of apple skin polyphenols has been reported by Du, Olsen, Avena-Bustillos, Friedman, and McHugh (2011), who observed an increase of the elastic modulus in apple edible films incorporated with apple skin polyphenols in concentrations ranging from 4.5 % to 6 % (w/w).

The effect of apple skin polyphenols on the stiffness of açaí edible films can be attributed to the interaction of fiber, from apple skin polyphenols, with the fruit matrix. Henríquez, et al. (2010) reported that the dietary fiber and mineral content are higher in apple peel when compared to other edible parts of this fruit. They indicated that the Granny Smith apple peel has 47.8±1.8 %

of total dietary fiber (TDF), while the apple peel ingredient has 39.7±0.5% TDF.

Previous studies showed that incorporating fibers in polymeric matrixes resulted in improved mechanical resistance. Okubo, Fujii, and Thostenson (2009) reported that a hybrid biocomposite composed of a biodegradable poly(lactic acid) (PLA) matrix reinforced with microfibrillated cellulose (MFC) and bamboo fiber bundles presented increasing in both stiffness and strength with the addition of MFC. Moreover, Araujo, Mano, Teixeira, Spinacé, and De Paoli (2010) observed the improvement on mechanical properties of high density polyethylene (HDPE) due to the use of curauá fiber from *Ananas erectifolius* plant (plant closely related to the pineapple). The incorporation of this fiber efficiently promoted the reinforcement effect in the HDPE matrix.

On the other hand, the incorporation of thyme essential oil resulted in diminishing mechanical resistance of açaí edible films. Similar to our results, apple edible films presented a significant reduction in tensile strength and elastic modulus after incorporation with cinnamon, allspice or clove bud essential oil (Du, Olsen, Avena-Bustillos, McHugh, Levin, & Friedman, 2009). Rojas-Graü, Avena-Bustillos, Friedman, Henika, Martín-Belloso, and McHugh (2006) also reported diminishing mechanical resistance on apple edible films when incorporated with lemongrass essential oil.

In addition, our results are in agreement with those of Hosseini, Razavi, and Mousavi (2009), who reported that chitosan-based films containing thyme essential oil presented reduced mechanical resistance compared to the control film. They attributed the loss of mechanical resistance to the breakup of film network caused by the addition of essential oils. Similarly, Pranoto, Rakshit, and Salokhe (2005) incorporated garlic essential oil in edible films and indicated that the incorporation of additives other than crosslinking agents generally results in lower mechanical resistance.

3.3 Water Vapor Permeability

The concentration of apple skin polyphenols and thyme essential oil at studied levels did not show any influence ($p>0.05$) on the thickness and water vapor permeability (WVP) of açaí edible films, with mean values of

0.175 mm for thickness and 3.562 g·mm/kPa·h·m^2 for WVP. Our results were in agreement with those of Du, Olsen, Avena-Bustillos, McHugh, Levin, and Friedman (2009), who reported that the WVP of apple edible films was not affected by the incorporation of essential oils (cinnamon, allspice, and clove bud). They indicated that this result was due to the nature of essential oil constituents, which are mostly composed of terpene-like compounds and not lipids.

Moreover, the presence of fibers from apple skin polyphenols had no effect on WVP of açaí edible films. This result was expected since natural cellulosic fibers are highly polar due to the presence of hydroxyl groups (Majeed, et al., 2013) and the content of numerous hydroxyl groups made natural fibers strongly hydrophilic (Bledzki & Faruk, 2004).

3.4 Colorimetric Analysis

The color of food packaging is an important factor in terms of general appearance and consumer acceptance (Bourtoom & Chinnan, 2008; Srinivasa, Ramesh, Kumar, & Tharanathan, 2003). Açaí edible films presented color tones ranging from red to orange-yellow (Figure 4).

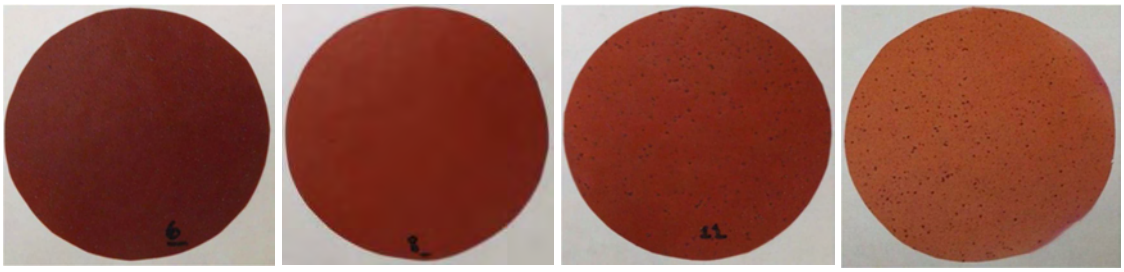

(a) (b) (c) (d)

Figure 4. Visual and color appearance of açaí edible films incorporated with 6.07 % (w/w) ASP and 3.1 % (w/w) TEO (a); 3.1 % (w/w) ASP and 6.07 % TEO (b); 3.1 % (w/w) of both antimicrobials (c) and control film (d).
*ASP: Apple skin polyphenols; TEO: Thyme essential oil.

Moreover, statistical analysis showed that the regression model for the colorimetric parameters L*, a* and b* presented statistical significance for açaí edible films, with a non-significant lack of fit (Table 7).

Table 7. Estimated regression coefficients for colorimetric parameters of açaí edible films incorporated with apple skin polyphenols and thyme essential oil

Term		Colorimetric parameter		
		L*	a*	b*
Mean		***26.963***	***7.169***	***2.666***
ASP		***0.875***	***1.623***	0.031
TEO		-0.066	***0.306***	0.058
ASP^2		***-0.250***	***-0.439***	-0.027
TEO^2		0.109	0.131	0.147
ASP×TEO		***0.348***	***0.425***	***0.429***
Regression	F^a	**27.365**	**89.949**	**8.496**
	P^b	0.001220	0.000068	0.017389
Lack of fit	F^a	2.525	2.484	0.391
	P^b	0.296294	0.299970	0.775466

ASP: Apple skin polyphenols; TEO: Thyme essential oil. [a] Values in bold and italics are significant at α=0.07 for L* and at α=0.05 for a* and b*, with 5 degrees of freedom for the response variable.

The color parameter L* provides a measure of the lightness and darkness of the analyzed material. Its values range from 0 to 100 as indication of dark to light. The analysis of the estimated regression coefficients showed that the colorimetric parameter L* was influenced by the linear effect of apple skin polyphenols ($p<0.05$), while the addition of thyme essential oil had no effect on this parameter. However, the interaction of both antimicrobials had a significant effect in the L* parameter. Moreover, L* values of açaí edible films were affected by the quadratic effect of apple skin polyphenols (Figure 5.a).

The colorimetric parameter a* indicates a measure of redness when presents positive values and a measure of greenness when negative values are observed. The analysis of the estimated regression coefficients showed that the linear effect of both antimicrobials influenced the colorimetric parameter a*. Positive values of these coefficients indicated that an increase in the concentration of both antimicrobials results in high values of a*, with a strong redness tendency. In addition, the quadratic effect of apple skin polyphenols negatively influenced the parameter a*. The estimated regression coefficients showed a positive interaction of both antimicrobials regarding this parameter. In contrast, at higher concentrations, indicating that high concentrations of this antimicrobial result in a slightly decrease of a* values (Figure 5.b).

On the other hand, the regression model for the b* parameter presented statistical significance for açaí edible films, with a non-significant lack of fit.

The analysis of estimated regression coefficients indicated that the interaction of both antimicrobials presented significant influence over this parameter, indicating that increasing concentration of both antimicrobials contribute positively to the yellowness of açaí edible films. The color of an object absorbs part of the light source and reflects the remaining light. Thus, according to our results, açaí edible films absorb light in the blue wavelength region while reflect light in the red and yellow wavelength regions.

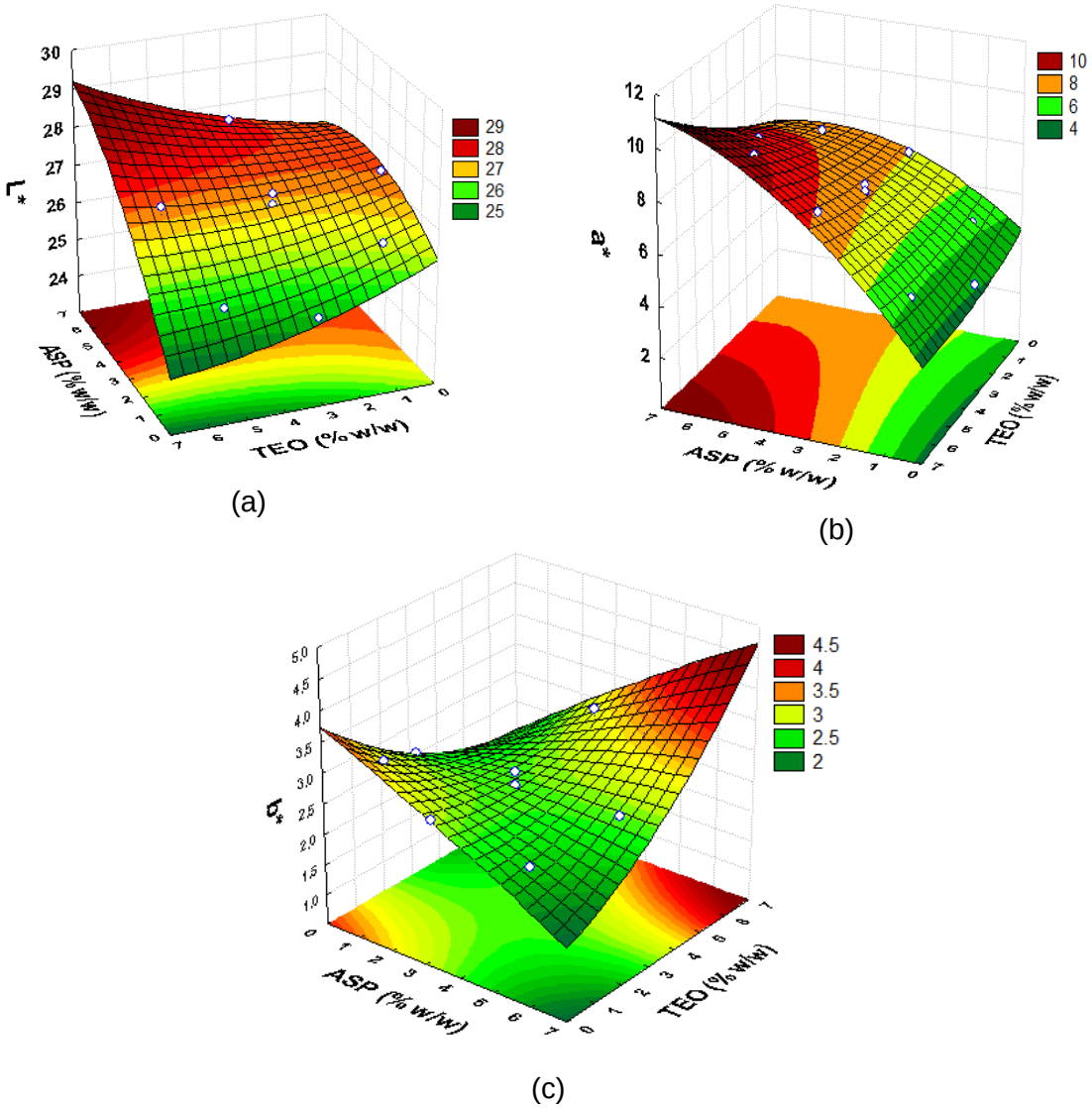

(a) (b) (c)

Figure 5. Response surface of the colorimetric parameters: (a) L*; (b) a*; (c) b* of açaí edible films as a function of apple skin polyphenols (% w/w) and thyme essential oil (% w/w).

3.5 Thermogravimetric Analysis

Determining the thermal resistance of packaging allows the study of structural changes caused by temperature variations (Espitia, Soares, Coimbra, Andrade, Cruz, & Medeiros, 2012). The thermal stability of açaí edible films was investigated by means of thermogravimetric analysis. The thermograms showed that açaí edible films have a multi-degradation-step process in inert atmosphere (Figure 6).

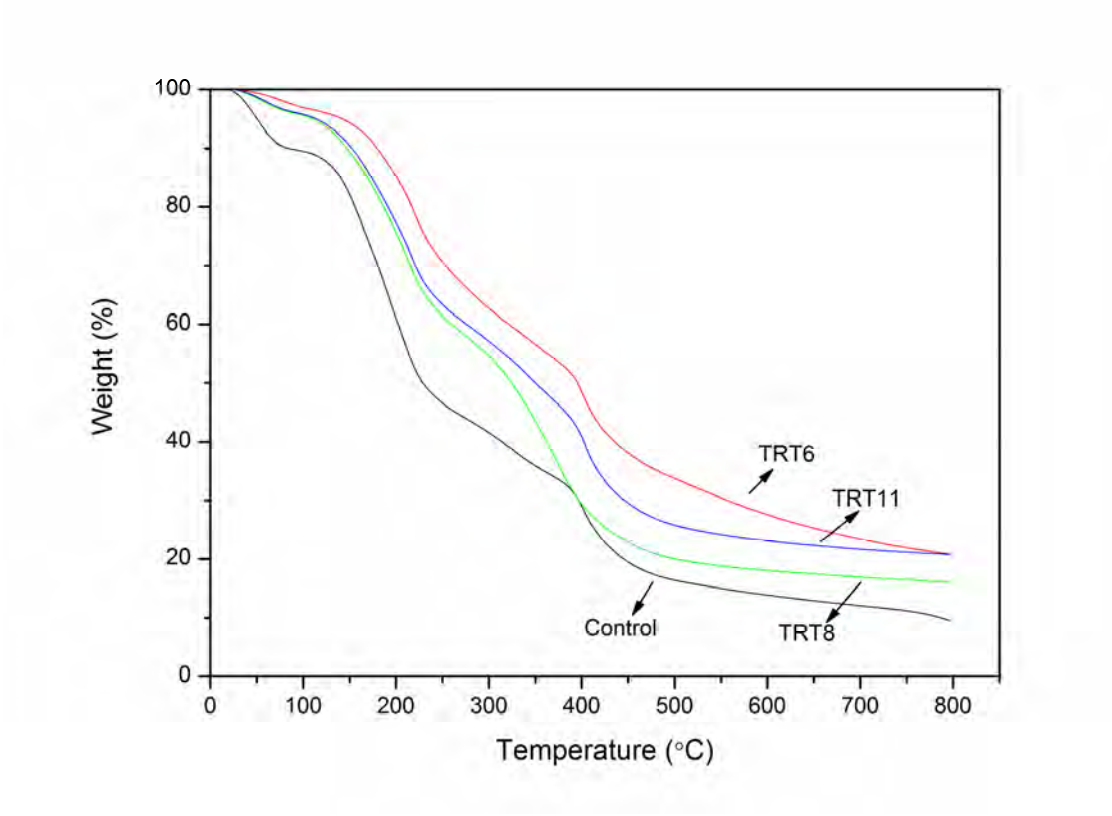

Figure 6. Thermograms of main tested treatments from CCD of açaí edible films: Control film; açaí edible film incorporated with 6.07 % ASP and 3.10 % TEO (TRT6); 6.07 % TEO and 3.10 % ASP (TRT8); and intermediary concentrations of CCD (TRT11).*ASP: Apple skin polyphenols; TEO: Thyme essential oil.

An initial loss of weight was observed at temperatures between 50-100 ℃, which corresponded to water loss. After this, a decomposition step observed at around 150 ℃ was attributed to pectin decomposi tion, which presented the maximum decomposition rate at 226 ℃. The next decomposition step, which occurred at an onset temperature around 300 °C, was attributed to glycerol decomposition. The last decomposition step, observed at 400 ℃,

was attributed to thermal decomposition of fibers from açaí and apple skin, composed mainly of cellulose and lignin.

Moreover, the thermograms also showed that the incorporation of apple skin polyphenols resulted in less weight loss, indicating that the thermal stability of açaí edible films was enhanced with the addition of this antimicrobial. According to the supplier of açaí pulp, 12 % of the açaí pulp corresponds to fiber. In addition, the fiber content probably increases with the addition of apple skin polyphenols. Leontowicz, et al. (2003) indicated that the total, soluble, and insoluble dietary fiber in apple peels is significantly higher than in pulp.

The incorporation of natural fibers used as filler or reinforcement to the matrix polymers changed their thermal stability (Majeed, et al., 2013). Fiber from wheat straw have been used as filler in a biocomposite polymer based on an aromatic copolyester (polybutylene adipate-co-terephthalate), which is a biodegradable polymer completely synthesized by petrochemical processes. The authors reported that the addition of fiber fillers increased the thermal degradation temperature of the polymeric matrix, as a function of the reinforcing content (Avérous & Le Digabel, 2006). Moreover, the incorporation of pulp fiber and wood flour in polyvinyl chloride (PVC) has resulted in composites with increased thermal property (Kiani, Ashori, & Mozaffari, 2011).

3.6 Field Emission Scanning Electron Microscopy

Açaí edible film (control film) had a heterogeneous surface with structures that protruded from the air-side surface of the film, probably as a result of differential surface tension during drying (Figure 7.a, b). The protrusions were more evident in the cross section of the film (Figure 7.b) where it became evident that the protrusions were large, thickened portions of the film. The formation of the thickened areas was an effect of açaí, rather than pectin. This was verified by the observation of pectin-only film, which was more homogenous and lacked of the thickened areas (Figure 7.c, d) found in the açaí-only films.

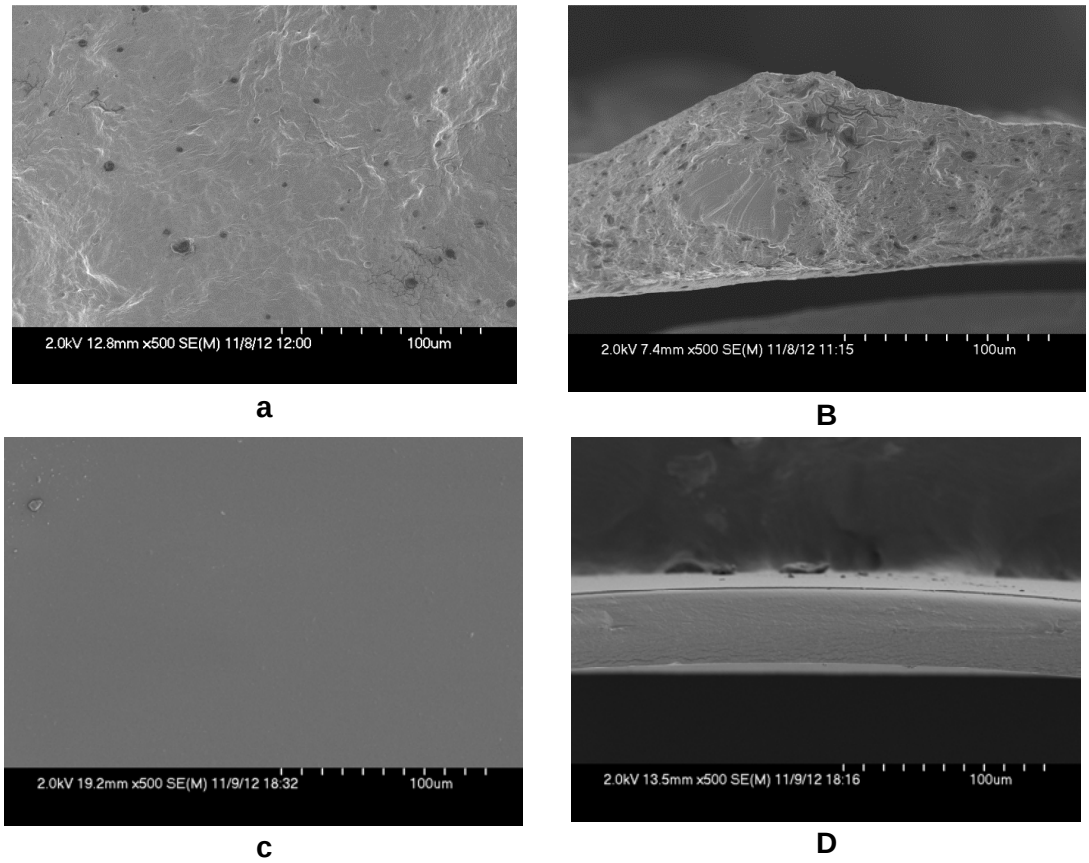

Figure 7. FESEM photomicrograph of açaí edible film, control treatment, (**a** and **b**) and pectin edible film (**c** and **d**).

Similar to our results, Liu, Liu, Fishman, and Hicks (2007) analyzed pectin films by SEM and revealed that the frozen-fractured surface of pectin films had relatively smooth morphology. Moreover, Giancone, Torrieri, Di Pierro, Cavella, Giosafatto, and Masi (2011) indicated that pectin films are characterized by tightly packed clusters. The conditions in the present study allow for the visualization of finer details from sample surfaces than in those from a conventional SEM. Nevertheless, the micrographs are quite similar from the two types of SEM.

Microscopy images allow understanding the differences in the film morphology due to the addition of the antimicrobial components (Bastarrachea, Dhawan, & Sablani, 2011). Açaí puree incorporated with apple skin polyphenols at the highest tested concentration (6.07 % w/w) resulted in a much smoother surface than açaí alone. There was little evidence of clustering and the thickness of the film was much more uniform compared to the control film. However, pits, or voids of all sizes were

apparent in cross section (Figure 8.a, b). The brittleness of this film probably resulted from the presence of these voids in the interior of the film.

Açaí film incorporated with the highest tested concentration of thyme essential oil (6.07 % w/w) had clusters and crater-like pits in its surface. The cross section of this film had a more cracked structure when compared to the control film in combination with the presence of inner pits as a result of the presence of a low concentration (3.10 % w/w) of apple skin polyphenols (Figure 8.c, d).

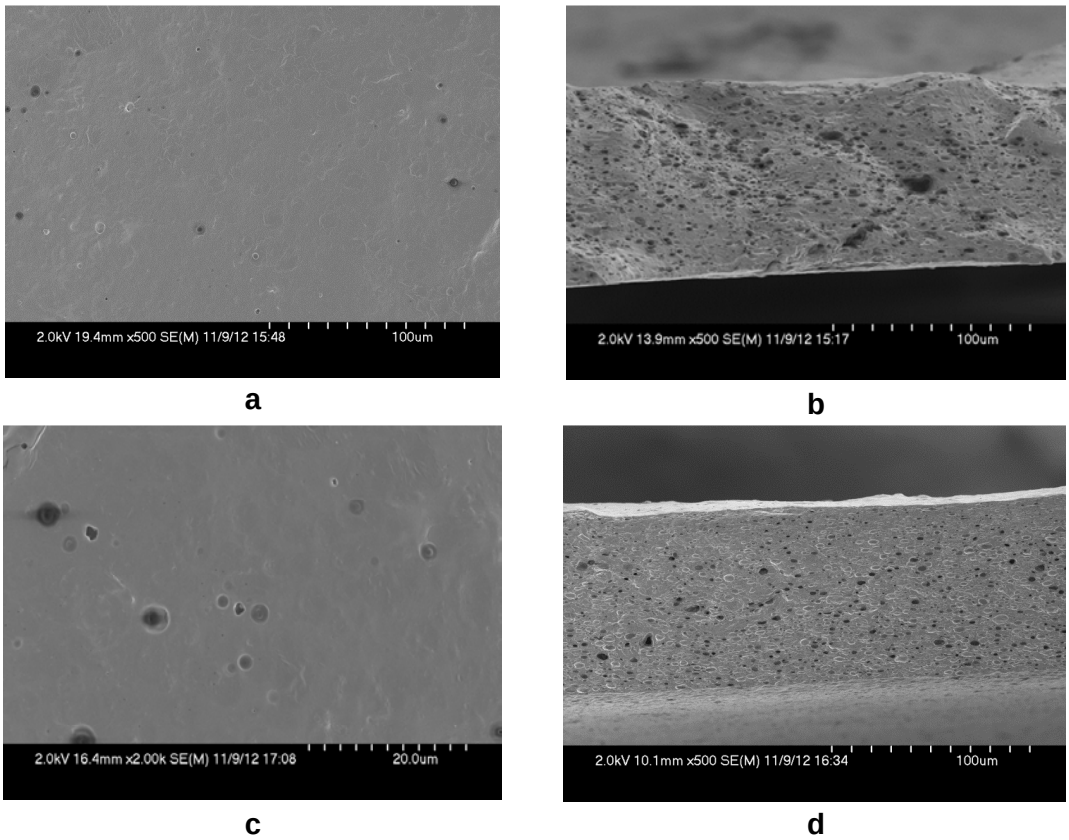

Figure 8. FESEM photomicrograph of surface and cross section of açaí edible film incorporated with 6.07 % apple skin polyphenols and 3.10 % thyme essential oil (**a** and **b**); and 6.07 % thyme essential oil and 3.10 % apple skin polyphenols (**c** and **d).**

Crater-like pits on surfaces of pectin-based films have been previously reported by Murillo-Martínez, Pedroza-Islas, Lobato-Calleros, Martínez-Ferez, and Vernon-Carter (2011) who developed edible film cast from double emulsion, composed of mineral oil and water, stabilized with low-methoxyl pectin-whey protein isolate complex. These scientists indicated that the

oriented microstructure of the films consisted mainly of fibrous-like structures attributed to aggregates of the biopolymers and the presence of voids originally occupied by the relatively large-sized droplets of the emulsion.

3.7 Optimization by the Desirability Function Approach

Optimization of films was performed in order to achieve açaí edible films with good antimicrobial, mechanical and colorimetric properties. Previous researchers have reported the use of multi-response analysis in order to find the optimal process conditions for film elaboration (Aloui, Khwaldia, Slama, & Hamdi, 2011; Espitia, et al., 2013; Pelissari, Andrade-Mahecha, Sobral, & Menegalli, 2013; Tapia-Blácido, do Amaral Sobral, & Menegalli, 2011; Tapia-Blácido, Sobral, & Menegalli, 2013). Selected variables for optimization by the desirability approach were antimicrobial activity, elastic modulus and colorimetric parameters L*, a* and b*. Other responses were not considered in this analysis since they presented no statistical significance according to the RSM.

The desirable condition for açaí edible films was observed at darkest region of the desirability surface (Figure 9).

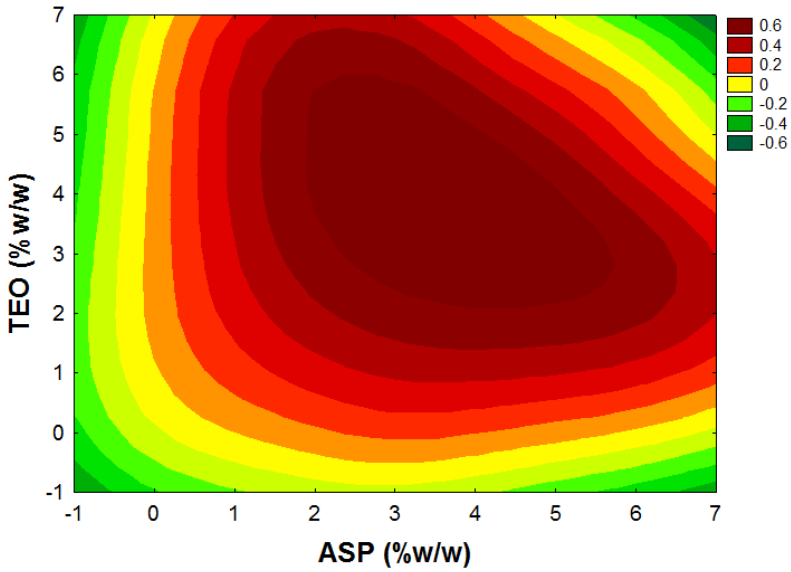

Figure 9. Overall desirability of açaí edible films incorporated with apple skin polyphenols (ASP) and thyme essential oil (TEO). Desirability function varied from zero (undesired condition) to one (desired condition)

Moreover, for the desirability profile the antimicrobial activity was set with a value of one, since a high value of this property was desirable for food preservation. Elastic modulus was set at zero in order to avoid film brittleness. Colorimetric parameters L* was set at one to obtain brighter films, a* was set at one since films with a strong tendency to redness were desired and b* was set at zero in order to obtain films with less tendency to yellowness (Figure 10).

According to our results, açaí edible film with desired characteristics is achieved by incorporating 6.07 % (w/w) of apple skin polyphenols and 3.1 % (w/w) of thyme essential oil into the film (Figure 10).

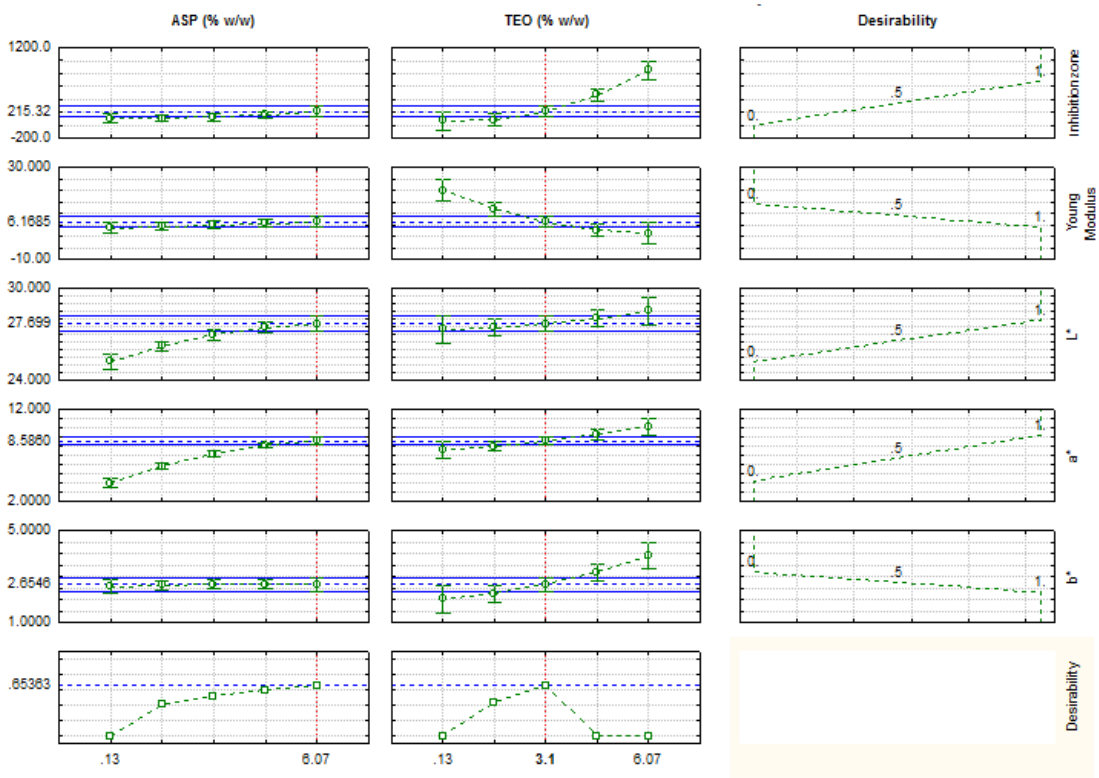

Figure 10. Simultaneous optimization of process conditions for the açaí edible films and desirability profile as function of apple skin polyphenol and thyme essential oil concentrations.

4. CONCLUSIONS

Knowledge of antimicrobial and physical properties of new packaging materials is essential for future industrial food application. In this study, the incorporation of açaí edible films with apple skin polyphenols and thyme

essential oil resulted in antimicrobial activity against *L. monocytogenes*. Significant influence of both compounds was observed in the antimicrobial activity of açaí edible films. Mechanical resistance of açaí edible films was improved by the incorporation of apple skin polyphenols. However, increased concentrations of thyme essential oils reduced this property. Water vapor permeability of açaí edible films was not significantly influenced by any of antimicrobials incorporated. Açaí edible films presented color tones ranging from dark red to yellow, with colorimetric parameters being significantly influenced by the incorporation of antimicrobials and the interaction between the antimicrobials. Increasing concentration of apple skin polyphenols in açaí edible films resulted in enhanced thermal stability. SEM images showed heterogeneous surface of açaí edible films. Incorporation of apple skin polyphenols resulted in smoother surface, while thyme essential oil incorporation resulted in crater-like pits in the açaí edible film surface. Based on the results of the desirability function analysis, optimal concentrations of tested antimicrobials are 6.07 % (w/w) of apple skin polyphenols and 3.1 % (w/w) of thyme essential oil. Therefore, this work showed the antimicrobial synergy of apple skin polyphenols and thyme essential oil when incorporated in açaí edible films, and demonstrated the potential application of these antimicrobial edible films on food preservation due to their antimicrobial activity and good physical-mechanical properties.

ACKNOWLEDGMENTS

The authors thank Mr. Carl Olsen (PFR Unit, USDA/ARS) for providing technical support. Paula Espitia gratefully acknowledges her doctoral scholarship provided by Coordenação de Aperfeiçoamento de Pessoal de Nível Superior (CAPES). The authors gratefully acknowledge Mr. Nicholas J. Walker for providing language help and writing assistance.

5. REFERENCES

Alberto, M. R., Canavosio, M. A. R., & Nadra, M. C. M. d. (2006). Antimicrobial effect of polyphenols from apple skins on human bacterial pathogens. *Electronic Journal of Biotechnology, 9*(3), 205-209.

Aloui, H., Khwaldia, K., Slama, M. B., & Hamdi, M. (2011). Effect of glycerol and coating weight on functional properties of biopolymer-coated paper. *Carbohydrate Polymers, 86*(2), 1063-1072.

Araujo, J. R., Mano, B., Teixeira, G. M., Spinacé, M. A. S., & De Paoli, M.-A. (2010). Biomicrofibrilar composites of high density polyethylene reinforced with curauá fibers: Mechanical, interfacial and morphological properties. *Composites Science and Technology, 70*(11), 1637-1644.

ASTM. (1980). ASTM E96-80. In *Standard test methods for water vapor transmission of materials*). Philadelphia, PA: ASTM International.

Avérous, L., & Le Digabel, F. (2006). Properties of biocomposites based on lignocellulosic fillers. *Carbohydrate Polymers, 66*(4), 480-493.

Azeredo, H. M. C., Mattoso, L. H. C., Wood, D., Williams, T. G., Avena-Bustillos, R. J., & McHugh, T. H. (2009). Nanocomposite edible films from mango puree reinforced with cellulose nanofibers. *Journal of Food Science, 74*(5), N31-N35.

Bastarrachea, L., Dhawan, S., & Sablani, S. (2011). Engineering properties of polymeric-based antimicrobial films for food packaging: A review. *Food Engineering Reviews, 3*(2), 79-93.

Bilbao-Sáinz, C., Avena-Bustillos, R. J., Wood, D. F., Williams, T. G., & McHugh, T. H. (2010). Composite edible films based on hydroxypropyl methylcellulose reinforced with microcrystalline cellulose nanoparticles. *Journal of Agricultural and Food Chemistry, 58*(6), 3753-3760.

Bledzki, A. K., & Faruk, O. (2004). Creep and impact properties of wood fibre–polypropylene composites: influence of temperature and moisture content. *Composites Science and Technology, 64*(5), 693-700.

Bourtoom, T., & Chinnan, M. S. (2008). Preparation and properties of rice starch–chitosan blend biodegradable film. *LWT - Food Science and Technology, 41*(9), 1633-1641.

Box, G. E. P., & Draper, N. R. (1989). *Empirical Model-Building and Response Surfaces*. New York: John Wiley & Sons.

Brereton, R. G. (2003). *Chemometrics: Data Analysis for the Laboratory and Chemical Plant*. Chichester: John Wiley & Sons.

Burt, S. A., & Reinders, R. D. (2003). Antibacterial activity of selected plant essential oils against *Escherichia coli* O157:H7. *Letters in Applied Microbiology, 36*(3), 162-167.

Castro, C. D. P. d. C., Dias, C. G. B. T., & Faria, J. d. A. F. (2010). Production and evaluation of recycled polymers from açaí fibers. *Materials Research, 13*, 159-163.

Derringer, G., & Suich, R. (1980). Simultaneous optimization of several response variables. *Journal of Quality Technology, 12*(4), 214-219.

Du, W. X., Olsen, C. W., Avena-Bustillos, R. J., Friedman, M., & McHugh, T. H. (2011). Physical and antibacterial properties of edible films formulated with apple skin polyphenols. *Journal of Food Science, 76*(2), M149-M155.

Du, W. X., Olsen, C. W., Avena-Bustillos, R. J., McHugh, T. H., Levin, C. E., & Friedman, M. (2008a). Antibacterial activity against *E. coli* O157:H7, physical properties, and storage stability of novel carvacrol-containing edible tomato films. *Journal of Food Science, 73*(7), M378-M383.

Du, W. X., Olsen, C. W., Avena-Bustillos, R. J., McHugh, T. H., Levin, C. E., & Friedman, M. (2008b). Storage stability and antibacterial activity against *Escherichia coli* O157:H7 of carvacrol in edible apple films made by two different casting methods. *Journal of Agricultural and Food Chemistry, 56*(9), 3082-3088.

Du, W. X., Olsen, C. W., Avena-Bustillos, R. J., McHugh, T. H., Levin, C. E., & Friedman, M. (2009). Effects of allspice, cinnamon, and clove bud essential oils in edible apple films on physical properties and antimicrobial activities. *Journal of Food Science, 74*(7), M372-M378.

Espitia, P., Soares, N. F., Coimbra, J. S. R., Andrade, N. J., Cruz, R. S., & Medeiros, E. A. A. (2012). Zinc oxide nanoparticles: Synthesis, antimicrobial activity and food packaging applications. *Food and Bioprocess Technology, 5*(5), 1447-1464.

Espitia, P. J. P., Soares, N. D. F. F., Botti, L. C. M., & Silva, W. A. (2011). Effect of essential oils in the properties of cellulosic active packaging. *Macromolecular Symposia, 299-300*(1), 199-205.

Espitia, P. J. P., Soares, N. d. F. F., Teófilo, R. F., Coimbra, J. S. d. R., Vitor, D. M., Batista, R. A., Ferreira, S. O., de Andrade, N. J., & Medeiros, E. A. A. (2013). Physical-mechanical and antimicrobial properties of nanocomposite films with pediocin and ZnO nanoparticles. *Carbohydrate Polymers,* http://dx.doi.org/10.1016/j.carbpol.2013.01.003.

Espitia, P. J. P., Soares, N. F. F., Botti, L. C. M., Melo, N. R., Pereira, O. L., & Silva, W. A. (2012). Assessment of the efficiency of essential oils in the preservation of postharvest papaya in an antimicrobial packaging system. *Brazilian Journal of Food Technology, 15*, 333-342.

Fratianni, F., Coppola, R., & Nazzaro, F. (2011). Phenolic composition and antimicrobial and antiquorum sensing activity of an ethanolic extract of peels from the apple cultivar Annurca. *Journal of Medicinal Food, 14*(9), 957-963.

Giancone, T., Torrieri, E., Di Pierro, P., Cavella, S., Giosafatto, C. L., & Masi, P. (2011). Effect of surface density on the engineering properties of high methoxyl pectin-based edible films. *Food and Bioprocess Technology, 4*(7), 1228-1236.

Govaris, A., Botsoglou, E., Sergelidis, D., & Chatzopoulou, P. S. (2011). Antibacterial activity of oregano and thyme essential oils against *Listeria monocytogenes* and *Escherichia coli* O157:H7 in feta cheese packaged under modified atmosphere. *LWT - Food Science and Technology, 44*(4), 1240-1244.

Henríquez, C., Speisky, H., Chiffelle, I., Valenzuela, T., Araya, M., Simpson, R., & Almonacid, S. (2010). Development of an ingredient containing

apple peel, as a source of polyphenols and dietary fiber. *Journal of Food Science, 75*(6), H172-H181.

Hosseini, M. H., Razavi, S. H., & Mousavi, M. A. (2009). Antimicrobial, physical and mechanical properties of chitosan-based films incorporated with thyme, clove and cinnamon essential oils. *Journal of Food Processing and Preservation, 33*(6), 727-743.

Ignat, I., Volf, I., & Popa, V. I. (2011). A critical review of methods for characterisation of polyphenolic compounds in fruits and vegetables. *Food Chemistry, 126*(4), 1821-1835.

Kang, J., Thakali, K. M., Xie, C., Kondo, M., Tong, Y., Ou, B., Jensen, G., Medina, M. B., Schauss, A. G., & Wu, X. (2012). Bioactivities of açaí (*Euterpe precatoria* Mart.) fruit pulp, superior antioxidant and anti-inflammatory properties to *Euterpe oleracea* Mart. *Food Chemistry, 133*(3), 671-677.

Kang, J., Xie, C., Li, Z., Nagarajan, S., Schauss, A. G., Wu, T., & Wu, X. (2011). Flavonoids from acai (*Euterpe oleracea* Mart.) pulp and their antioxidant and anti-inflammatory activities. *Food Chemistry, 128*(1), 152-157.

Kiani, H., Ashori, A., & Mozaffari, S. A. (2011). Water resistance and thermal stability of hybrid lignocellulosic filler–PVC composites. *Polymer Bulletin, 66*(6), 797-802.

Leontowicz, M., Gorinstein, S., Leontowicz, H., Krzeminski, R., Lojek, A., Katrich, E., Číž, M., Martin-Belloso, O., Soliva-Fortuny, R., Haruenkit, R., & Trakhtenberg, S. (2003). Apple and pear peel and pulp and their influence on plasma lipids and antioxidant potentials in rats fed cholesterol-containing diets. *Journal of Agricultural and Food Chemistry, 51*(19), 5780-5785.

Liu, L., Liu, C.-K., Fishman, M. L., & Hicks, K. B. (2007). Composite films from pectin and fish skin gelatin or soybean flour protein. *Journal of Agricultural and Food Chemistry, 55*(6), 2349-2355.

López, P., Sánchez, C., Batlle, R., & Nerín, C. (2007). Development of flexible antimicrobial films using essential oils as active agents. *Journal of Agricultural and Food Chemistry, 55*(21), 8814-8824.

Majeed, K., Jawaid, M., Hassan, A., Abu Bakar, A., Abdul Khalil, H. P. S., Salema, A. A., & Inuwa, I. (2013). Potential materials for food packaging from nanoclay/natural fibres filled hybrid composites. *Materials & Design, 46*(0), 391-410.

Martins, M. A., Pessoa, J. D. C., Gonçalves, P. S., Souza, F. I., & Mattoso, L. H. C. (2008). Thermal and mechanical properties of the açaí fiber/natural rubber composites. *Journal of Materials Science, 43*(19), 6531-6538.

McHugh, T. H., Avena-Bustillos, R., & Krochta, J. M. (1993). Hydrophilic edible films: Modified procedure for water vapor permeability and explanation of thickness effects. *Journal of Food Science, 58*(4), 899-903.

Murillo-Martínez, M. M., Pedroza-Islas, R., Lobato-Calleros, C., Martínez-Ferez, A., & Vernon-Carter, E. J. (2011). Designing W1/O/W2 double emulsions stabilized by protein–polysaccharide complexes for producing edible films: Rheological, mechanical and water vapour properties. *Food Hydrocolloids, 25*(4), 577-585.

Okubo, K., Fujii, T., & Thostenson, E. T. (2009). Multi-scale hybrid biocomposite: Processing and mechanical characterization of bamboo fiber reinforced PLA with microfibrillated cellulose. *Composites Part A: Applied Science and Manufacturing, 40*(4), 469-475.

Pelissari, F. M., Andrade-Mahecha, M. M., Sobral, P. J. d. A., & Menegalli, F. C. (2013). Optimization of process conditions for the production of films based on the flour from plantain bananas (Musa paradisiaca). *LWT - Food Science and Technology,* http://dx.doi.org/10.1016/j.lwt.2013.01.011.

Pranoto, Y., Rakshit, S. K., & Salokhe, V. M. (2005). Enhancing antimicrobial activity of chitosan films by incorporating garlic oil, potassium sorbate and nisin. *LWT - Food Science and Technology, 38*(8), 859-865.

Ravishankar, S., Jaroni, D., Zhu, L., Olsen, C., McHugh, T., & Friedman, M. (2012). Inactivation of *Listeria monocytogenes* on ham and bologna using pectin-based apple, carrot, and hibiscus edible films containing

carvacrol and cinnamaldehyde. *Journal of Food Science, 77*(7), M377-M382.

Rojas-Graü, M. A., Avena-Bustillos, R. J., Friedman, M., Henika, P. R., Martín-Belloso, O., & McHugh, T. H. (2006). Mechanical, barrier, and antimicrobial properties of apple puree edible films containing plant essential oils. *Journal of Agricultural and Food Chemistry, 54*(24), 9262-9267.

Rounds, L., Havens, C. M., Feinstein, Y., Friedman, M., & Ravishankar, S. (2012). Plant extracts, spices, and essential oils inactivate *Escherichia coli* O157:H7 and reduce formation of potentially carcinogenic heterocyclic amines in cooked beef patties. *Journal of Agricultural and Food Chemistry, 60*(14), 3792-3799.

Srinivasa, P. C., Ramesh, M. N., Kumar, K. R., & Tharanathan, R. N. (2003). Properties and sorption studies of chitosan–polyvinyl alcohol blend films. *Carbohydrate Polymers, 53*(4), 431-438.

Tapia-Blácido, D. R., do Amaral Sobral, P. J., & Menegalli, F. C. (2011). Optimization of amaranth flour films plasticized with glycerol and sorbitol by multi-response analysis. *LWT - Food Science and Technology, 44*(8), 1731-1738.

Tapia-Blácido, D. R., Sobral, P. J. d. A., & Menegalli, F. C. (2013). Effect of drying conditions and plasticizer type on some physical and mechanical properties of amaranth flour films. *LWT - Food Science and Technology, 50*(2), 392-400.

Teófilo, R. F., & Ferreira, M. M. C. (2006). Quimiometria II: planilhas eletrônicas para cálculos de planejamentos experimentais, um tutorial. *Química Nova, 29*, 338-350.

CONCLUSÃO GERAL

O estudo da dispersão ótima de nanopartículas de ZnO mostrou que a presença do agente dispersante (pirofosfato de sódio) teve efeito significativo sobre o tamanho das nanopartículas. As nanopartículas de ZnO apresentaram tamanho mínimo de 238 nm, produzidas por sonicação a uma potência de 200 W durante 45 minutos, na presença do agente dispersante.

A dispersão ótima das nanopartículas nas concentrações testadas apresentou atividade contra *E. coli, S.* Choleraesuis e *S. aureus*. No entanto, as nanopartículas de ZnO não apresentaram atividade antimicrobiana contra *P. aeruginosa, L. plantarum* e *L. monocytogenes*. A dispersão de nanopartículas de ZnO nas concentrações testadas apresentou atividade antifúngica contra *S. cerevisiae* e *A. niger* por até três dias.

A incorporação de nanopartículas de ZnO e pediocina em filmes de metil celulose permitiu o desenvolvimento de uma nova embalagem antimicrobiana para a preservação de alimentos. As propriedades de cristalografia, alongamento na ruptura, estabilidade térmica e cor dos filmes foram influenciadas pela incorporação dos antimicrobianos. Os filmes apresentaram atividade antimicrobiana contra *L. monocytogenes* e *S. aureus.* Estes resultados indicam o potencial de aplicação dos filmes desenvolvidos para o controle de micro-organismos patogênicos. Entretanto, mais estudos são necessários para testar a sua atividade antimicrobiana em alimentos.

Por outro lado, filmes comestíveis de açaí para uso como embalagem antimicrobiana foram desenvolvidos incorporados com óleo essencial de tomilho e polifenóis de casca de maçã. Os filmes apresentaram atividade antimicrobiana contra *L. monocytogenes*. Propriedades como resistência mecânica, cor e estabilidade térmica dos filmes de açaí foram influenciadas

pela adição dos antimicrobianos utilizados. Mediante a metodologia de superfície de resposta e a função de desejabilidade foram determinadas que as concentrações ótimas dos agentes antimicrobianos testados são 6,07 % (m/m) de polifenóis de casca de maçã e de 3,1 % (m/m) de óleo essencial de tomilho. Portanto, este trabalho demonstrou uma sinergia antimicrobiana entre polifenóis de casca de maçã e óleo essencial de tomilho quando incorporados em filmes comestíveis de açaí. Isto indica o potencial de aplicação destes filmes ativos na conservação de alimentos devido à atividade antimicrobiana e boas propriedades físico-mecânicas obtidas.